**Enhanced Properties of Polymethyl Methacrylate Coated with Atomic Layer Deposited Ceramic Nanofilm**

BY

ELEONORA PENSA
B.S., Politecnico di Milano, Milan, Italy, 2016

THESIS

Submitted as partial fulfillment of the requirements
for the degree of Master of Science in Bioengineering
in the Graduate College of the
University of Illinois at Chicago, 2018

Chicago, Illinois

Defense Committee:
Dr. C.G. Takoudis, Chair and Advisor
Dr. Bin Yang, College of Dentistry
Dr. Stephen Campbell, College of Dentistry
Dr. Roberto Chiesa, Politecnico di Milano

## ACKNOWLEDGEMENTS

First of all, I would like to express my sincere gratitude to my advisor, Prof. Christos Takoudis, for his continuous support of my M.S. study and research project. He is a passionate professor who is always desirous to help his students with his knowledge and experience.

Besides, I want to thank my co-advisor Dr. Bin Yang for her useful suggestions and patient guidance. In addition, I would like to thank my committee member, Dr. Roberto Chiesa for following me in my double-sided thesis collaborated between University of Illinois at Chicago and Politecnico di Milano.

I also want to thank Niloofar Therani, from Dr. Indacochea's laboratory who trained me on the hardness tester, Olivia Thompson, who trained me on the SEM system, Fengyuan Shi for the guidance in XPS analysis and Andrea Donohue, for her useful suggestions on the SE system. Thanks to my group members Arghya Kamal Bishal, Nickolas Anderson, Mina Shahmohammadi and Sarah Hashemiastaneh for their kind help. In addition, thanks to Harshdeep Bhatia of AMRel Lab, who trained me on the ALD system and the main procedures to get started with the whole thesis project. Moreover, thanks to Dr. Wang who assisted me in the main steps of the process.

Lastly, I must express my very profound gratitude to my family members and my friends who provide constant encouragement and unconditional support.

Financial supports from Wach Fund and Restorative department at College of Dentistry and Bio Engineering units (University of Illinois at Chicago) are gratefully acknowledged.

EP

## TABLE OF CONTENTS

**CHAPTER** **PAGE**


**1 INTRODUCTION** ..... 1
1.1 Atomic layer deposition technique ..... 1
1.2 Titanium Dioxide ..... 2
1.3 Zirconium Dioxide ..... 3
1.4 Polymethyl methacrylate ..... 4
1.5 Mixed Oxides coatings by ALD ..... 5
1.6 Objectives and prior studies ..... 7

**2 MATERIALS AND METHODS** ..... 10
2.1 ALD system ..... 10
2.2 Characterization techniques ..... 11
2.2.1 Spectroscopic Ellipsometry ..... 12
2.2.2 Water Contact Angle ..... 14
2.2.3 Thermogravimetric analysis ..... 15
2.2.4 X-ray Photoelectron Spectroscopy ..... 15
2.2.5 Scanning Electron Microscopy ..... 16
2.2.6 Atomic Force Microscopy ..... 17
2.2.7 Microhardness Test ..... 17
2.2.8 Three-Point Bending test ..... 18
2.2.9 Polident Treatment ..... 20
2.3 Samples Preparation ..... 20
2.4 ALD System Impurity ..... 21
2.5 ALD System Inhomogeneity ..... 21
2.6 Titania and Zirconia mean growth rates on silicon ..... 22
2.7 Titania and Zirconia mean growth rates on PMMA ..... 23
2.8 Mixed oxides coating mean growth rate on silicon ..... 23
2.9 Mixed oxides coating mean growth rate on PMMA ..... 24

**3 RESULTS AND DISCUSSION** ..... 28
3.1 Results of system impurity ..... 28
3.2 Results of system inhomogeneity ..... 29
3.3 Results of Titania and Zirconia mean growth rate on silicon ..... 30
3.4 Results of Titania and Zirconia mean growth rates on PMMA ..... 33
3.4.1 Results of Titania mean growth rate on PMMA ..... 33
3.4.2 Results of Zirconia mean growth rate on PMMA ..... 38
3.5 Results of mixed oxides coating mean growth rate on silicon ..... 45
3.6 Results of mixed oxides coating mean growth rate on PMMA ..... 47
3.7 Water Contact Angle results ..... 49
3.8 Thermogravimetric analysis results ..... 51
3.9 X-ray Photoelectron Spectroscopy results ..... 53
3.10 Scanning Electron Microscopy results ..... 59
3.10.1 Scanning Electron Microscopy of separate oxides ..... 59
3.10.2 Scanning Electron Microscopy of mixed oxides ..... 61

**TABLE OF CONTENTS (continued)**

**CHAPTER** **PAGE**


3.11 Atomic Force Microscopy results ..... 62
3.12 Microhardness test results ..... 65
3.13 Three-point bending test results ..... 68
3.14 Conclusions ..... 70

**4 FUTURE WORK** ..... 72

**APPENDICES** ..... 75

**CITED LITERATURE** ..... 84

**VITA** ..... 89

## LIST OF TABLES

**TABLE** **PAGE**

I THICKNESS AND GROWTH RATE OBTAINED FROM THE DEPOSITION OF TITANIA WITH 1 S PULSE OF TDMAT AND 15 S OF PURGE BUT NO OXIDIZER PULSE ON SILICON SAMPLES AT 150°C AND 0,97 TORR AND BUBBLER TEMPERATURE SET TO 70°C (THE STANDARD DEVIATION IS FOR MEASUREMENTS WITHIN THE SAME SAMPLE) ..... 28

II GROWTH RATE IN Å/CYCLE OBTAINED FROM THE DEPOSITIONS AT DIFFERENT TEMPERATURES AND DIFFERENT PULSE TIMES FOR TDMAZ AND $O_3$ ON SILICON SAMPLES (PRESSURE 0,97 TORR AND 0,48 TORR FOR TDMAT AND TDMAZ RESPECTIVELY, NITROGEN PURGE EQUAL TO 15 SECONDS IN EVERY DEPOSITION) ..... 31

III NUMBER OF CYCLES, MEAN THICKNESS AND DIFFERENTIAL GROWTH OF THE TITANIA COATING THICKNESS ON SILICON IN THE SAME CHAMBER WITH THE POLYMER AT 120°C (SAME DEPOSITION CONDITIONS AS FIGURE 8) ..... 36

## LIST OF FIGURES

**FIGURE** **PAGE**


1 Polymethyl Methacrylate chemical formula ..... 4

2 Schematic of the structure of the mixed oxide coating on top of the substrate that can be either silicon or PMMA ..... 6

3 Structure of the reaction chamber of Kurt J. Lesker ALD 150 LE from system manual ..... 10

4 Equilibrium angle at the interface between the liquid, air and the solid phase ($\gamma_{sg}$, $\gamma_{sl}$ and $\gamma_{lg}$ are the energies at the solid-vapor, solid-liquid and liquid-vapor interfaces respectively) .. 15

5 Schematic of three-point bending test: F(N) represents the load applied to sample top surface, L(m) is the distance between two supports and H is the thickness of the specimen (m) ..... 19

6 Theoretical structure of the mixed titania-zirconia coating obtained by ALD at 100°C on PMMA substrate. 6 Supercycles, made of 40 cycles of TDMAT and 20 cycles of TDMAZ each, were performed. Theoretically this ALD recipe should result in the structure shown, with a thickness ratio 5:1. The theoretical thickness of the layers are calculated with the mean growth rate per cycle obtained in the other experiments ..... 26

7 Mean thickness of the silicon samples coated for 300 cycles with ZrO2 at different conditions. Group 1 coated at 150 °C with 1 s and 10 s of TDMAZ pulse and purge and 1,8 s and 15s of ozone pulse and purge, group 2 at 150°C with 1,5 s and 10 s of TDMAZ pulse and purge and 2s and 15s of ozone pulse and purge, group 3 coated at 120°C with 1,5 s and 10 s of TDMAZ pulse and purge and 1,8s and 15s of ozone pulse and purge, group 4 at 120°C with 1,5 s and 10 s of TDMAZ pulse and purge and 1,8s and 15s of ozone pulse and purge with different position in the chamber. After Fix is the group of samples coated with same conditions of group 4 but after the system was fixed. (Pressure constant to 0,48 Torr and bubbler temperature constant at 70°C) ..... 30

8 Mean Growth rate of TiO2 and ZrO2 from TDMAT/TDMAZ and ozone on silicon as a function of ALD cycles at 120°C. Pressure was 0,96 Torr and 0,48 Torr for TDMAT and TDMAZ respectively, bubbler temperature was 70°C for both materials. 1 s and 15 s of pulse and purge of TDMAT and 1,5 s and 10 s of purge of TDMAZ, 1,8 s and 15 s of pulse and purge of ozone for both oxides The number of cycles was the only parameter changed in each deposition, all the other were kept constant. The mean thickness was obtained with spectroscopic ellipsometry, the models used were described in previous sections. The dotted lines are the linear approximations obtained with Excel Software, the $R^2$ value is the correlation coefficient, the closer is to one the better is the fit. ..... 32

**LIST OF FIGURES (continued)**

**FIGURE** **PAGE**


9 Growth rate of TiO2 from TDMAT and ozone on PMMA, on silicon alone and on silicon in the same chamber with PMMA as a function of ALD cycles at 120°C (Same deposition conditions as Fig. 8) The number of cycles was the only parameter changed in each deposition, all the other were kept constant. The mean thickness was obtained with spectroscopic ellipsometry, the models used were described in previous sections. The dotted lines are the linear approximations obtained with Excel Software, the $R^2$ value is the correlation coefficient, the closer is to one the better is the fit. ..... 35

10 Growth rate of TiO2 from TDMAT and ozone on silicon in the same reaction chamber with PMMA as a function of ALD cycles at 120°C with 2 different linear approximations at same conditions as Fig. 8 (blue line and green line) ..... 37

11 Growth rate of TiO2 from TDMAT and ozone on PMMA and on silicon in the same chamber with PMMA as a function of ALD cycles at 120°C for higher cycles (Same deposition conditions as Fig. 8) The number of cycles was the only parameter changed in each deposition, all the other were kept constant. The mean thickness was obtained with spectroscopic ellipsometry, the models used were described in previous sections. The dotted lines are the linear approximations obtained with Excel Software, the $R^2$ value is the correlation coefficient, the closer is to one the better is the fit. ..... 38

12 Growth rate of ZrO2 from TDMAZ and ozone on PMMA, on silicon alone and on silicon in the same chamber with PMMA as a function of ALD cycles at 120°C (Same deposition conditions as Figure 8) The number of cycles was the only parameter changed in each deposition, all the other were kept constant. The mean thickness was obtained with spectroscopic ellipsometry, the models used were described in previous sections. The dotted lines are the linear approximations obtained with Excel Software, the $R^2$ value is the correlation coefficient, the closer is to one the better is the fit. ..... 39

13 Growth rate of $ZrO_2$ from TDMAZ and ozone on PMMA and on silicon in the same chamber with PMMA as a function of ALD cycles at 120°C for higher cycles (Same deposition conditions as Figure 8). Red line is dotted as the ellipsometric fitting was not considered accurate and reliable, the optical constants obtained were not similar to zirconia constants so the measurements acquired were not considered as the actual thickness of the coating. ..... 43

14 Mean Growth rate of mixed oxides coating on silicon at 120°C with respect to ZrO2 percentage when TiO2 is chosen as the first layer on the substrate (Same deposition conditions as Figure 8) ..... 46

15 Mean Growth rate of mixed oxides coating on silicon at 120°C with respect to ZrO2 percentage when ZrO2 is chosen as the first layer on the substrate (Same deposition conditions as Fig. 8) ..... 47

16 Growth rate of the mixed oxides layer deposited at 100°C on top of PMMA (16,7 % corresponds to 360 cycles and ratio 5:1 with expected total thickness 36 nm) as a function of the ZrO2 percentage from SE data when $TiO_2$ is chosen as the first layer (Same pressure and pulse times as Figure 8) ..... 48

**LIST OF FIGURES (continued)**

**FIGURE** **PAGE**


17 Mean contact angle and standard deviation before (0 cycles) and after the depositions of TiO2, ZrO2, and mixed TiO2-ZrO2 films on PMMA at different cycles, before and after Polident treatment (4h) and after 15 days of DI water storage. The PMMA coated with single oxides were deposited at 120°C while the Mixed coated PMMA were deposited at 100°C (Same pressure and pulse times of Figure 8). All the measurements were made right after the deposition if not differently specified. The standard deviation is meant for the measurements of the same sample, so it indicates the uniformity for the samples.. ..... 50

18 Thermogravimetric curve of not coated PMMA between 25°C and 250°C in Nitrogen atmosphere. The green curve represents the weight percentage while the blue curve represents the weight derivative: when the slope of the derivative changes, the weight varies. ..... 52

19 XPS spectra comparison of 3 PMMA samples: (C) one PMMA not coated (control), (A) one PMMA (1mm) coated with 10nm (100 cycles) ZrO2 treated for 4 hours after 2 weeks of DI water storage, (B) one PMMA (1mm) coated with 10nm (100 cycles) ZrO2 after 2 weeks of DI water storage (Same pressure and pulses of Figure 8). The treatment consists in 4 hours of sonication in Polident solution..... 54

20 XPS High resolution spectrum result of Zr-3d peak from the scan of the ZrO2 (10 nm) coated PMMA (1 mm) after 4 hours of Polident sonication and DI water storage for 3 months deposited at 120°C (100 cycles)..... 55

21 XPS High resolution spectrum result of Ti-2p peak from the scan of the 7 nm-TiO2 coated PMMA (1 mm) at 120°C (Same sample as Figure 19)..... 55

22 ZrO2 XPS survey of a thin zirconia film (580nm) deposited by CVD on soda-lime glass substrate (55)..... 56

23 XPS spectra result of mixed $TiO_2$-$ZrO_2$ coated (around 40 nm, ratio 5:1, 6 supercycles, 360 cycles) PMMA (1 mm) after 1 month of DI water storage deposited at 100°C tilted at 0°(A) 20°(B) and 60°(C) (Same pressure and pulses of Figure 8). Sample A and C were treated: the treatment consists in 4 hours of sonication in Polident solution..... 57

24 XPS spectra comparison of (A) mixed TiO2-ZrO2 coated (around 40 nm, ratio 5:1, 6 supercycles, 360 cycles) PMMA (1 mm) after DI water storage for 1 month deposited at 100°C and (B) mixed TiO2-ZrO2 coated (around 15nm, ratio 2:1, 2 supercycles, 140 cycles) PMMA (1 mm) deposited at 100°C (Same deposition conditions as Figure 8) and (C) not coated PMMA as a control..... 58

25 Cross-section SEM image (A) and EDS mapping of the Ti, C, and O element distribution of ALD coated (40 nm, 500 cycles) TiO2-PMMA sample at 100°C (Same deposition conditions as Figure 8)..... 60

26 Cross-section SEM image (A) and EDS mapping of the Zr, C and O element distribution of ALD coated (around 30 nm) ZrO2-PMMA sample at 120°C (350 cycles with deposition conditions same as Figure 8)..... 60

**LIST OF FIGURES (continued)**

**FIGURE** **PAGE**


27 Cross-section SEM image (A) and EDS mapping of Ti, C, and O distribution of ALD coated mixed TiO2-ZrO2 PMMA sample (ratio 5:1, coated at 100°C with 360 cycles and 6 supercycles with the conditions of Figure 8) ..... 62

28 AFM three-dimensional image of the surface morphology of a not coated PMMA sample (spot dimension 10$\mu$m x 10$\mu$m)..... 63

29 AFM three-dimensional image of the surface morphology of a mixed TiO2-ZrO2 coated PMMA sample deposited at 100°C (ratio 5:1, around 40 nm, 360 cycles, 6 supercycles), at same conditions as Figure 8 (spot dimension 10$\mu$m x 10$\mu$m) ..... 64

30 AFM three-dimensional image of the surface morphology of (A) TiO2 coated PMMA deposited at 100°C with 350 cycles and (B) ZrO2 coated PMMA at 100°C with 400 cycles at same conditions as Figure 8 (spot dimension 5$\mu$m x 5$\mu$m) ..... 65

31 Mean Vickers hardness number and standard deviations of the PMMA samples not coated and coated with different thicknesses of zirconia and titania layers (150 cy ZrO2 at 120°C ~9nm, 400cyTiO2 at 120°C ~35nm, 400cyZrO2 at 120°C ~30nm, 360cy mixed TiO2-ZrO2 at 100°C ~40nm with ratio 5:1 and with $TiO_2$ first layer). The treatment mentioned consists in 4 hours of sonication in Polident solution. Blue lines represent the statistical difference between the group of samples. ..... 67

32 Mean flexural strength of ZrO2 coated (25nm, 350 cycles) PMMA(1mm) and Mixed TiO2-ZrO2 coated (40nm, ratio 5:1, 360 cycles and 6 supercycles) PMMA at 100°C (Same pressure and pulse times of Figure 8) ..... 69

33 ALD cycle number vs. mean thickness (Å) of the TiO2 layers on silicon, PMMA, and silicon with PMMA at 90°C and 120°C for 50 and 150 cycles from TDMAT and Ozone (Same pressure and pulses of Figure 8) ..... 77

34 PMMA Lucitone 199 Powder Composition and safety data sheet taken from the Company website……...80

35 FTIR spectra of uncoated PMMA ans 30 nm TiO/ 30 nm ZrO coated PMMA stored in DI water for 3 weeks……...82

## LIST OF ABBREVIATIONS

| | |
|---|---|
| ALD | Atomic Layer Deposition |
| PMMA | Polymethyl Methacrylate |
| CVD | Chemical Vapor Deposition |
| TDMAT | Tetrakis(dimethylamido)titanium |
| TDMAZ | Tetrakis(dimethylamido)zirconium |
| SE | Spectroscopic Ellipsometry |
| XPS | X-ray Photoelectron Spectroscopy |
| SEM | Scanning Electron Microscopy |
| AFM | Atomic Force Microscopy |
| WCA | Water Contact Angle |
| EDS | Energy Dispersive X-Ray Spectroscopy |
| XRR | X-ray Reflectivity |
| XRD | X-ray Diffraction |
| DI | Deionized |
| FTIR | Fourier Transform Infrared |

## SUMMARY

Polymethyl Methacrylate is a polymer used as a denture base material since 1936. PMMA has desirable properties such as good biocompatibility, good aesthetics, ease of processing and low cost but its poor surface properties and wear resistance can lead to fracture, deformation and loss of surface accuracy. Functionalization of this material is needed since studies have proved that 68% of dentures degrade in the first few years of usage. The oral environment is very aggressive; due to fast pH and temperature changes and the presence of different kinds of bacteria, the polymer can undergo biodegradation, discoloration and increase of surface roughness.

Atomic Layer Deposition technique can provide conformal and uniform thin ceramic films made of metal oxides like $TiO_2$, $ZrO_2$ and mixed $TiO_2$-$ZrO_2$ on polymeric substrates that we conjecture would reduce PMMA drawbacks. The process can be performed at low temperature like 90-120°C, which is desirable especially when working with polymers which melt at 160°C, as PMMA. This technique was selected among the other coating technologies because of its high control over composition and thickness at the Ångström scale. A variety of thicknesses and chemical compositions of the coatings, surface characterization, physical and mechanical properties of the coated PMMA were investigated with non-coated PMMA as a control, in order to have a standard for comparison of the results and detect if the properties of the coated polymer are improved or not with respect to the non-coated one. The characterization was challenging as the polymer used is weak, melts at low temperature and it is also non-conductive, which leads to difficulties in using traditional techniques such as electron microscopy. The goal was to obtain a ceramic nano-thin film on the polymer that would improve the surface properties of the substrate while maintaining the desirable bulk properties of the material.

The bonding strength of the nano-thin ALD coating on the polymer was effective since after four hours of aggressive treatment the ceramics were still attached to the polymer: chemical

analyses of the surface showed same results for samples freshly deposited and samples tested with both a chemical and physical treatment in a popular denture cleanser. Our ALD coating proved to be physically and chemically attached to PMMA, in agreement with other related literature results.

All coated surfaces showed increased wettability compared to the uncoated polymers right after the depositions. The contact angle decreased from 80° to 25-35°. Moreover, surface wettability resulted in being stable even after extended treatments such as four hours of sonication in a denture cleanser solution.

In addition to the wettability increase, a 30 nm-thick ceramic coating successfully managed to increase the PMMA surface hardness value by 60%, which can be helpful in facilitating finishing and polishing and in providing resistance to damage during cleaning of prosthodontics. On the other hand, the desirable flexural properties of the bulk material were maintained in the coated samples. Moreover, surface morphology was confirmed not to be affected significantly by the coating: the root mean square roughness value ranged from 45± 0.7nm to 28± 4nm in the best case. The change is not even in the micrometer range, which was anticipated, since ALD is a conformal technique and it covers all the peaks and troughs present on the surface to coat.

# CHAPTER 1

# INTRODUCTION

## 1.1 Atomic layer deposition technique

Atomic layer deposition is a popular layer-by-layer technique used to deposit ultra-thin coatings on various surfaces. Traditionally it has been widely used for microelectronic devices but recently it has been adopted also for doing other kinds of coatings as on particles, porous polymeric materials or fibers. In the last decade devices have been designed in smaller size and structured into complex shapes and, as a consequence, the growing need of ultrathin coatings has increased over the years: ALD is currently applied to microelectronics, to photovoltaic devices as dye sensitized solar cells, to medical devices as orthopedic or dental prosthesis, and to tribology for highly durable coatings (1).

This kind of deposition results in a self-limiting process, meaning that the active sites on the surface to coat are all saturated by the reactants and so no active sites are retained on the surface leading to a continuous and pinhole-free coating (2). The reactants cover all the sites of the surface for any surface geometry, so the ALD is constrained just by the reaction chamber dimensions (2).

The rate of deposition is usually expressed as angstroms or nanometers per cycle. The technique consists of applying sequentially two precursors on the surface of a solid sample, so that the applied reactants chemically react in a self-limiting process. (3). One cycle of an ALD deposition starting from two precursors A and B consists in the exposition to reactant A, some seconds of purging, exposition to reactant B and some seconds of purging. The purging step is used both to remove any kind of non-reacted precursors and to remove any byproduct of the reaction at the surface between the reactants and the active sites on the surface.

In each exposition to the chemical reactants all the active sites of the surface to be coated are saturated so that the rough substrates are coated in all the peaks and troughs (2). Moreover, the ability to control the composition is really useful when working with composite coatings and this

allows to match the properties to the application's requirements (4). A lot of coating properties can be tuned by changing the ratio of the components, for example, roughness, refractive index and band gap (4). High control over the thickness and composition makes ALD a good technique to realize nanostructured surfaces (3).

The specific rate of deposition can be tuned with the temperature, the choice of the precursors and the reactor set up (5). The ALD precursors should be chosen carefully, as they should display some characteristics as volatility, thermal stability for an efficient transport, high vapor pressure and good reactivity to promptly react with all the active sites on the substrate surface (5).

It presents some advantages over other techniques such as Chemical Vapor Deposition or sol-gel method as the fabrication of highly conformal and uniform coatings with precise thickness at the nanometer level. For example, the sol-gel method is usually quick and affordable but it presents the drawback of generating non-homogeneous and rough coatings and moreover there is no easy way to control the thickness as with ALD (6). With this technique, the thickness is highly controllable because it is linearly dependent on the number of cycles which is a really useful feature if the desirable thickness is around the Angstrom level (2). Moreover, it can be performed at low temperature, a very important feature that allows this method to be used with polymeric substrates that usually have a low melting temperature (6). The most widely investigated film deposited on polymers by ALD so far has been alumina ($Al_2O_3$) (5).

One of the main disadvantages is the slow deposition rate that can be attributed to the long cycle times made of the pulse and purge times for each precursor (5).

## 1.2 Titanium Dioxide

Titanium dioxide is a very well-known material in the biomedical field. It is the natural oxide that grows on top of titanium surfaces and it is highly biocompatible and presents a low toxic level when it is in contact with human tissue (7). It is widely used because of its multiple

advantages as excellent biocompatibility, low toxicity, high chemical stability, good corrosion resistance and unique photocatalytic property (7). The photocatalytic property is a particular feature of the semiconductor materials that produce an exciton if they absorb a photon with energy bigger than the characteristic band gap of the material. An exciton is an electron-hole pair and it is produced if the semiconductor absorbs enough energy so that an electron can jump from the valence band to the conductive band, leaving a positive hole behind. The excitons are really reactive and allow oxidation-reduction reactions to happen at the surface of the semiconductors. So, if the material is in an aqueous environment highly oxidative species are created, as $O_2$- or OH radicals, that can kill bacteria and microorganisms. If the photocatalyst is not very efficient the exciton recombines rapidly. This is not desirable for photoactivity so, to improve the exciton lifetime, different approaches have been tried such as using phase heterojunctions, nanoparticles of noble metals or doping with other elements (8).

The traditional biomedical applications of this material are in the orthopedic and dental field but recently, some promising novel applications have been studied as using titania to realize effective antimicrobial devices, photodynamic cancer treatments or new cell imaging techniques (7).

### 1.3 Zirconium Dioxide

Zirconium dioxide is another popular biomaterial in the dental field. It has excellent biocompatibility, low toxicity, high chemical stability, good mechanical properties such as strength and hardness, good corrosion and wear resistance, and also good aesthetic property (9).

Usually this kind of oxide is used as a reinforcement for other ceramic based materials. Si J. et al. confirmed that including zirconium dioxide in composites “significantly improve the toughness and the bonding strength of composite material” (10). In this study Si J. et al. proved that a $TiO_2$/ $ZrO_2$ coating showed an increased shear bond strength, microhardness and bioactivity with respect to $TiO_2$ coating alone on Titanium plates (10).

Scarano et al. in 2004 proved that discs made of zirconia (Y- TZP) placed inside the oral cavity of ten patients for 24 hours showed less early bacterial adhesion than the commercially pure titanium discs, when the devices had equal surface roughness (11). They measured the percentage of the bacterial surface coverage and the lower values on zirconia (19.3% +/- 2.9 for titanium and 12.1% +/- 1.96 for zirconia) were attributed to the lower electrical conductivity and superficial structure of zirconia with respect to titanium (11).

Another interesting study is by Rimondini et al., that analyzed the bacterial adhesion *in vivo* of grade 2 commercially pure titanium and tetragonal zirconium dioxide specimens (Y-ZTP). The comparison showed that the Ti samples had a higher total number of bacteria and a more uniform bacterial coating with respect to zirconia, that showed bacterial clusters, with a prevalence of cocci and the absence of long rods (12).

Due to these interesting properties, ceramic based implants start to appear as a valid alternative to the traditional titanium ones.

### 1.4 Polymethyl methacrylate

Polymethyl methacrylate is a polymer used as a denture base material since 1936. It is a methacrylate ester (Fig. 1) and it has some desirable properties such as good biocompatibility when it is in contact with human tissues, ease of processing and low cost. Moreover, it has good aesthetics which is critical in the dental field: this allows it to be used to match the color of the pink oral tissue and the white teeth (13).

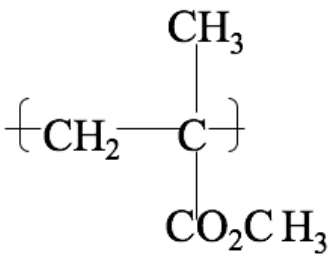


Figure 1: Polymethyl Methacrylate chemical formula

Unfortunately, there are some drawbacks too as poor surface properties and wear resistance that can lead to fracture, deformation or surface volume loss. Studies have proved that 68% of dentures broke in the few years of usage (14). The oral environment is very aggressive due to rapid pH and temperature changes and the presence of different kinds of bacteria. The polymer surface can be easily attacked causing surface roughness increase, fracture or loss of detail.

It is evident that functionalization of this material is needed and different approaches have been studied. Studies have been focused on structural reinforcement of this material even if the most effective approach is not apparent because every attempted solution presents some drawbacks. Firstly, metal wires have been added to PMMA to increase the overall strength of the material but the poor bonding strength between the metal and the polymer did not increase the properties in a desired way (14). Secondly, glass, polyamide and polyethylene fibers were incorporated in the PMMA structure but this method resulted in tissue irritation, problems with polishing and also poor bonding with the polymer chains (14). Lately, nanoparticles or nanofibers have been incorporated as carbon nanotubes or $TiO_2$ or $SiO_2$ nanoparticles but some of these showed decreased mechanical properties (14). The problem with nanofillers seems to be the tendency to form clusters which may lead to inhomogeneity in the structure ending in the creation of weakness points (13). Whereas, the main drawback of fibers reinforcement is the interruption of the polymer homogeneous matrix, caused by the poor combination of resin and fibers, that decreases the mechanical properties of the composite (15).

## 1.5 Mixed Oxides coatings by ALD

Precise control over the thickness and composition makes ALD a good technique to realize nanostructured surfaces (3). A lot of coating properties can be tuned by changing the ratio of the components such as band gap, refractive index and roughness (4). For example, in the study by J. Lopez at al. of 2016 in which silicon was coated by ALD with $Al_2O_3$ and ZnO nanolaminate, the refractive index and the final band gap varied with the thickness of the bilayer (16).

The final structure should be a sequence of alternated zirconia and titania layers and the final composition will be tuned by modifying the ratio of the cycles (4).

Figure 2 shows the final structure of a mixed $TiO_2$-$ZrO_2$ coating deposited by ALD technique. The number of cycles displayed in the image, which is three, is just an example. On top of the polymer or silicon the coating should be a sequence of $TiO_2$ and $ZrO_2$ layers.

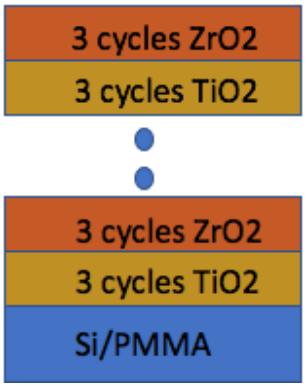


Figure 2: Schematic of the structure of the mixed oxide coating on top of the substrate that can be either silicon or PMMA

To obtain this structure the ALD sequence of opening and closing valves should follow this path: TDMAT pulse, Nitrogen purge, Ozone pulse, Nitrogen purge, repeated for a definite NT number of cycles, then TDMAZ pulse, Nitrogen purge, Ozone pulse, Nitrogen purge, all repeated for a definite number of cycles NZ and then repeat NZ and NT for a total number of cycles.

When mixing two materials with ALD technique a lot of phenomena can arise and modifications in the growth mechanism can happen. Existing studies provide information on ALD deposited mixed coatings: for example, Christensen S. T. et al. in 2009 tried to mix iridium and platinum with ALD to obtain a mixed thin film by tuning the ratio of the iridium cycles with respect to the platinum cycles (3). They claim that inhibited nucleation or some sort of etching of one material with respect to the other one can modify the growth mechanism (3). They also affirm

that mixing layers by ALD is feasible if the "surface chemistries of the different components are mutually compatible and the deposition conditions are similar" (3).

Another interesting study that has the goal of creating nanolaminates of $Y_2O_3$ and $Al_2O_3$ is the one by Lin K. Y. et al. of 2017. Using the results from STEM, XRD and XRR they concluded that for $Al_2O_3$ grown on $Y_2O_3$ and vice versa for $Y_2O_3$ grown on $Al_2O_3$ an incubation period of 1 cycle was to take into consideration when calculating the final growth rate (17). The incubation period is well defined by Choi J.H. et al. in 2013: it is the period needed by the surface to be activated with the desired functional group to allow the half reactions of ALD (18). Benner F. et al. in 2014 deposited nanolaminates of alumina and titania on silicon wafers and they concluded that the growth rate of the ALD cycles changes with respect to the material deposited in the previous cycle (19). For example, they found that titania growth on alumina was delayed by 50% due to the number of the incubation cycles that the material took to start growing on top of the other (19). Moreover, Chang S. et al. in 2018 created mixed tin oxide-titanium oxide coatings on silicon. By varying the ALD cycle ratio they successfully managed to tune the composition and by varying the numbers of ALD subcycles they obtained more alloy or laminate structures (4). They investigated the growth to detect any "etching effects, incomplete ligand elimination, interrupted nucleation and transfer of ligands" but none were detected (4). The different deposition rates were proved to be due to densities variations of the chemisorbed precursors (4).

Crystallinity of the coating, due to the low deposition temperature, is supposed to be amorphous: Mitchell D. R. G. et al. deposited ceramic coatings as $TiO_2$ at different temperatures by ALD and the results showed that the ceramic coatings below 200°C were amorphous, independently from the number of cycles (20). For temperatures between 250°C and 350°C $TiO_2$ was deposited in the anatase phase, after a few hundreds of cycles (20).

## 1.6 Objectives and prior studies

In this study, our intention is to mix titanium and zirconium dioxide, using the ALD technique in order to obtain a ceramic nano film on top of the polymer, and to prove that this novel

functionalization can improve PMMA properties such as surface wear resistance, wettability and hardness effectively while maintaining desirable properties as PMMA flexural strength. The purpose of the study would be to develop and characterize $TiO_2$ and $ZrO_2$ ALD coating deposited on PMMA for dental applications. Before mixing the oxides a characterization of the separate coating materials has to be made and the ALD deposition dynamic has to be investigated and understood. Having two materials instead of one opens up the possibility of tunable properties with different ratios for multiple applications to fulfill different requirements.

The nano-thin coating is expected to enhance some surface properties like wettability, surface wear resistance and surface hardness while retaining the bulk properties of the polymer which are considered suitable for denture applications. Wear is a real issue intraorally with PMMA, that may result in loss of surface volume and loss of accuracy: ALD coating might help in reducing the drawback and enhance polymer stability by increasing the wear resistance.

Moreover, coupling two semiconductors seems to be a novel approach to increase the photocatalytic property of the materials. The study of Lipika Das et al. of 2013 proved that a nanocomposite of zirconia (11,8%)-titania, made by sol-gel method, had the greatest photocatalytic effect compared to titania and zirconia alone and to other ratios of the two materials (8). Photocatalytic property may be useful to kill bacteria on the surface. Titania alone has good properties but it presents easy recombination of the excitons so this novel approach allows a better charge separation and a longer lifetime of the excitons.

Few studies have focused on the deposition of both $TiO_2$ and $ZrO_2$ on PMMA. $TiO_2$ and $Al_2O_3$ have been deposited on different polymers, among them PMMA. In the study by Kemell et al. in 2008 (21), the goal was to understand the adhesion and the ALD nucleation on different polymeric substrates.

Wilson et al. in 2005 deposited $Al_2O_3$ on different polymeric families to analyze the ALD nucleation periods, but no attempts were done with $TiO_2$ or $ZrO_2$ (22).

Kaariainen et al. in 2009 successfully deposited $TiO_2$ layers by low temperature ALD on PMMA to improve the adhesion strength of the sputtered metal on top. 50 nm $TiO_2$ coating proved to strongly increase the adhesion of the film (23).

Although zirconium dioxide nanofiller has successfully improved PMMA fracture toughness and hardness (1.5%, 3%, 5% and 7% concentrations), no study mentions ALD $ZrO_2$ coatings for this purpose (24). In this study, $ZrO_2$ nanofillers powder from Sigma-Aldrich were added during curing of the acrylic resin in different concentrations. 7% nanofiller concentration resulted in the best choice for increasing both toughness and hardness (24).

ALD has been extensively used on polymers, at different temperatures and deposition conditions (2). In the dental field though, the accuracy and the precision of the final dental prostheses play an important role for the satisfaction of the patient. Potentially, there might be some issues related to the ALD process and the elevated temperatures to which the polymer is exposed for three or four hours, which is the time needed for a 30 nm thick coating to be deposited. One first potential problem might be the shrinkage of the PMMA due to additional polymerization from heating and evaporation of the volatile components as non-reacted monomer (25). Deformation may be a second drawback of the processed PMMA at 100-120°C due to release of the residual stress accumulated during PMMA processing but literature confirms that after heating up to 120°C the roughness of PMMA was proved not to vary over 1 nm (26).

# CHAPTER 2

# MATERIALS AND METHODS

## 2.1 ALD system

The system used in this study is the commercial Kurt J. Lesker ALD 150 LE. It presents a perpendicular flow reaction chamber made with a reactant shower head that provides an efficient precursor delivery and purging (Fig. 3). The maximum diameter of the sample that can be used is 150 mm while the height of the chamber is 10 mm. It has a standard vacuum pumping system made of a rotary vane pump. System base pressure is 14 mTorr. The whole system is controlled by a software that is supplied by the manufacturer of the system and it is called eKLipse. This software is used to monitor all the temperatures, pressure values and the sequence of opening and closing of the valves during the deposition.

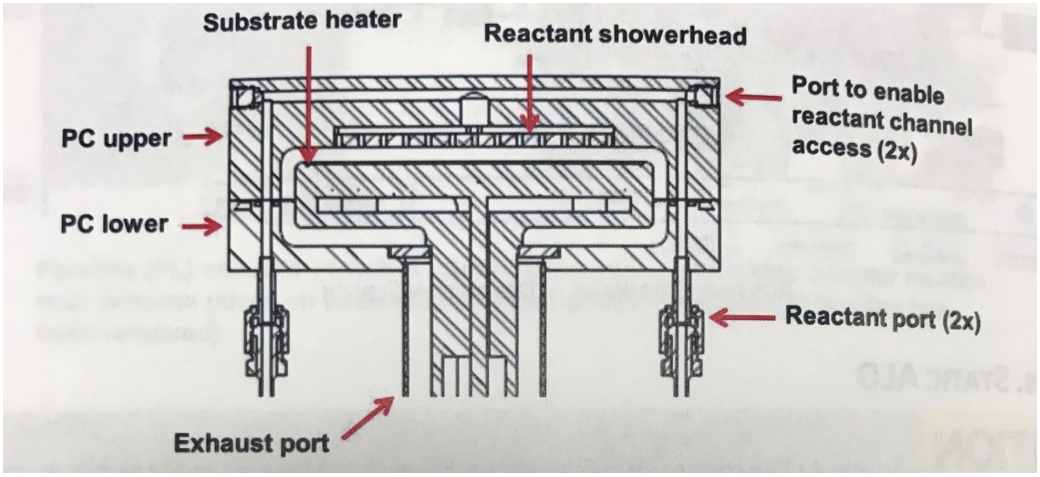


Figure 3: Structure of the reaction chamber of Kurt J. Lesker ALD 150 LE from system manual

The precursors chosen were TDMAT (Tetrakisdimethylamidotitanium) and TDMAZ (Tetrakisdimethylamidozirconium), the oxidizer chosen was ozone and the purging gas was nitrogen. Ozone is produced with an ozone generator made of an oxygen reservoir and a UV lamp.

Different precursors have been used for ALD depositions of $TiO_2$. One of the most popular precursors is $TiCl_4$, that is usually used with water as an oxidant, but it has some drawbacks due to the corrosive by-product HCl and residual $TiCl_4$ (27). Titanium alkoxides are recently studied precursors without corrosive halogen residuals. Isopropoxide and titanium ethoxide undergo decomposition of the reactants that brings an undetermined ALD temperature window. Moreover, for titanium isopropoxide, significant decomposition happens at lower temperature with respect to titanium ethoxide (27).

TDMAT was chosen due to the high reactivity of the metal amides and due to the absence of corrosive byproducts. Ozone was chosen instead of water as, at low temperature such as below 150°C, the water vapor exposure on titania surface requires a long purge. In addition, using water as an oxidant is known to produce impurities, such as hydroxyl groups (–OH) in the coating (27). All the depositions in this study were made by pulsing the precursor one time and then purging with nitrogen right after the pulse of the reactant.

## 2.2 Characterization techniques

All samples were characterized right after the deposition with a spectroscopic ellipsometer to obtain the thickness of the coating and by measuring the water contact angle to obtain the surface wettability. Microhardness test was performed on some polymer samples in order to detect any change in hardness. XPS characterization was performed on some coated and non-coated polymer samples in order to determine the surface chemical composition. AFM tests were performed on some coated and non-coated samples to analyze the surface morphology and roughness. SEM and EDS imaging techniques were used to perform composition mapping of the cross section of some coated PMMA samples. Three-point bending test was made by the Department of Dental Materials, Peking University School and Hospital of Stomatology on our coated PMMA samples to analyze the flexural strength of the coated polymer.

### 2.2.1 Spectroscopic Ellipsometry

At the end of the deposition, the samples were analyzed with a spectroscopic ellipsometer (Model M44, J.A. Woollam Co., Inc.).

This is a nondestructive and sensitive technique that uses polarized light to measure the ratio between the light reflected and transmitted through the bulk material. This is widely used especially for thin films to obtain the optical constants. Traditional ellipsometry measures two parameters associated to the change in polarization of the light when it passes through the sample (28). The thickness and the optical constants are obtained from two measured values: Psi (ψ) related to the amplitude change and Delta (Δ) related to phase change (29). Psi and Delta are obtained from equation 2.1:

$$\frac{r(p)}{r(s)} = \exp(i\Delta) * \tan\psi \qquad (2.1)$$

In equation 2.1 r(p) and r(s) are called Fresnel reflection coefficients and relate to p and s polarizations (29). To traduce Psi and Delta into the desired thickness value the system fits a Cauchy model on the experimental data acquired by minimizing the mean square error, the values of the optical constants and the thickness of the coating are obtained (29). The first step is to build a model and modify the model with a fitting algorithm to minimize the difference between the generated data and the measured ones (29). The parameters fitted are usually n, refractive index, and k, extinction coefficient. The mean square error (MSE) expresses the difference between the experimental data and the values approximated by the model used. Usually a mean square error below 5 is considered to build a good approximation.

The refractive index (n) of a PMMA like layer was calculated by the system using a Cauchy dispersion model showed by equation 2.2 (29).

$$n(\lambda) = \frac{B}{\lambda^2} + \frac{C}{\lambda^4} + A \qquad (2.2)$$

The parameter A, B and C are the constants of the Cauchy dispersion model, n represents the refractive index and $\lambda$ is the wavelength. The thickness of the layer can then be calculated if a set of ellipsometric parameters are acquired ($\Delta, \psi$) and if the refractive index, the angle of incidence and the light wavelength are known.

For each silicon sample the measure was repeated at three different points of the samples, two if the sample was smaller as the PMMA ones. For silicon, the Cauchy model used was already present in the system (WVASE 32) and already evaluated but for the polymer, which is a transparent substrate characterized also by backside reflections, the model was not present. Backside reflections usually happen in thin transparent polished samples in which the surface and back reflections enter simultaneously in the detector (30).

Since different forming methods can result in different polymer properties the model found in the literature did not seem very reliable for our samples. We decided to use the Cauchy model fitted on the data from the acquisitions of our samples by the Woollam Co. Inc.'s staff. This model seemed to be the best one although it has not been confirmed by a different technique. However, we also applied the model on bare polymer, on coated polymer at different cycles, and the data seemed to be the most consistent compared to other models we built and also with the values found in the literature. For each sample, the SE model was obtained by taking some acquisitions of the bare PMMA sample and by fitting sequentially A, B, C parameters of the model provided by Woollam Co. for our samples before the depositions. For example, the parameters used for one PMMA sample were: A= 1.4636, B=-0.0071313, C=0.0012993. A $TiO_2$ or $ZrO_2$ layer was added on top of the obtained substrate, then the acquisitions of the coated samples were taken and the thickness of the oxide was fitted. The optical parameters of the $TiO_2$ and $ZrO_2$ layers were taken from the WVASE32 archive.

### 2.2.2 Water Contact Angle

The water contact angle is an easy method to obtain the surface wettability of a material. When a water drop is placed on top of a surface, the angle formed with the surface is a consequence of how the interfacial energies reach an equilibrium at the interface between air, water and the material (31). Young's equation explains how this happens:

$$\gamma_{sg} - \gamma_{sl} - \gamma_{lg} * \cos\theta = 0 \quad (2.3)$$

Equation 2.3 shows the relationship between the solid-gaseous ($\gamma_{sg}$), solid-liquid ($\gamma_{sl}$) and liquid-gaseous ($\gamma_{lg}$) interfacial energies "$\gamma$" and the cosine of the equilibrium contact angle $\theta$ (31). If the angle is above 90 degrees the material is hydrophobic while if it is below 90 degrees it means it is well spread and so the material is hydrophilic, below 10-5 degrees is considered super hydrophilic.

Equation 2.1 is valuable if we assume that the surface is smooth, homogenous and clean: ideal surfaces are really difficult to obtain in practical engineering conditions so the data obtained needs to be analyzed taking into account that the conditions are not completely fulfilled (31).

The contact angle is highly affected by surface finish and impurities, both in the solid and in the liquid (31). In the biomedical field, surface wettability is an important property to tune because the bacteria and the cell adherence to materials can be affected by the surface wettability.

Right after the samples were characterized with the spectroscopic ellipsometer the samples were cleaned with deionized water (resistivity > 17 M Ω cm), dried with nitrogen and then the contact angle was measured. A water drop of 5 microliters was placed on top of the sample and then a picture was taken with the NRL C.A. Goniometer 100-00 (Ramè-hart inc.) and the eZGrabber software. For each sample, the procedure was repeated twice. Then the images were analyzed with a java software ImageJ that quantifies the angle from the images. The equilibrium angle formed at the interface (Figure 4) equilibrates the interfacial energies and provides the information on the hydrophilicity or hydrophobicity of the material.

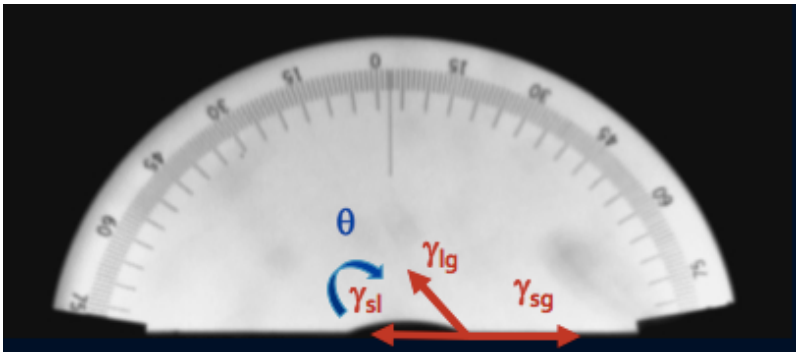


Figure 4: Equilibrium angle at the interface between the liquid, air and the solid phase ($\gamma_{sg}$, $\gamma_{sl}$ and $\gamma_{lg}$ are the energies at the solid-vapor, solid-liquid and liquid-vapor interfaces respectively)

### 2.2.3 Thermogravimetric analysis

Thermogravimetric analysis is a technique used to investigate a change in the weight of an initial quantity of a material. The mass is controlled with respect to temperature or time. The information provided is the evaporation rate as a function of temperature, as it measures the volatile emissions of the sample. It is useful to detect quantitative data on phenomena that determine weight loss during a controlled heating process (15).

In this study, TGA Q5000 was used. An 18 mg PMMA non-coated sample was used for the test. The test was performed in nitrogen atmosphere and the temperatures investigated were 25°C-250°C at a rate of 20°C/min. The most interesting temperature for our depositions was 120°C so we kept the temperature constant at 120°C for 30 minutes and then continued the heating ramp till 250°C.

### 2.2.4 X-ray Photoelectron Spectroscopy

XPS is a technique that uses as ionizing radiation a monochromatic beam of X-rays; usually Al or Mg is used. It is used to detect the chemical elements of the outer surface layers. The elements are detected with 0.1-l % of sensitivity (32). Usually the maximum detectable depth is considered

to be around 10 nm. The spectrum contains the chemical information of the surface atoms and the peak intensities can be easily quantified. Charging problems are not significant so that insulators are simply analyzed. Organic substrates can be studied with no significant damage as the radiative destructive effect is low (32).

Kratos AXIS-165 XPS was the system used to detect the elements of the surface of the coatings by analyzing the electrons energies produced due to the irradiation of X-rays. AXIS 165 features a "standard dual (Mg/Al) anode and monochromatic (Al) X-ray sources, a 15 keV electron gun for AES analysis and Auger or secondary electron imaging, and a 5 keV ion gun for sputter depth profile and sputter deposition" (33). The energy analyzer is a concentric hemispherical analyzer (mean radius 165 mm) with 8 channeltron detectors (33).

The samples were cut into 0.5cm x 0.5cm specimens and cleaned with pure ethanol before XPS by using a gentle brush.

### 2.2.5 Scanning Electron Microscopy

Scanning electron microscopy is widely used in material science (34). It focuses an electron beam on a surface to acquire an image. The electrons focused on the sample interact with the atoms on the surface and create different signals that can be processed to acquire information on the surface morphology and chemical composition. This technique provides high resolution in combination with good depth of field (34). It is different from a conventional microscope as it uses electrons instead of light: as electrons have a much lower wavelength, they can provide better resolution.

The system used was a Hitachi S-3000N variable-pressure SEM. It was used to detect the morphology and the elements present on the surface by using the EDS detector (Energy Dispersive X-ray Spectrometer). The pressure range is 1-270 Pa and the magnification range is 25x to 200,000x. Before the SEM test, the PMMA samples were cut in 1cm x 0.5cm size and were cleaned with ethanol to try to minimize any contamination.

### 2.2.6 Atomic Force Microscopy

This kind of microscopy is an interesting nondestructive 3D-imaging technique that can acquire surface details at the atomic level. It is really useful when working with the morphology of biological materials and other substrates that are not naturally conductive.

The probe is a nano tip that scans the surface of the sample while the system acquires the interatomic forces between the probe and the atoms in the sample. The tip is mounted on a cantilever, that acts as a spring. The small repulsive forces exchanged between the tip and the sample are detected by analyzing the reduced deflections of the cantilever. The back of the spring features a mirror used to reflect the laser beam, whose deviation gives information on the deflection of the spring. This is recorded in the form of an electrical signal from a photodiode that is hit by the laser (35).

In this study, we used a Bruker Dimension Icon system that was installed in a clean room. The AFM was set in the tapping mode meaning that the cantilever is set to vibrate near its resonance frequency, kept constant by the feedback loop. All the samples were scanned in air using a Scanasyst silicon tip. The spring constant of the cantilever was 0.4 N/m and the resonance frequency 70 KHz. The tapping mode was used to scan the samples and the scan rate was around 1 Hz.

### 2.2.7 Microhardness Test

As previously said, PMMA has some disadvantages as low surface hardness and strength: frequently, high masticatory forces or unintended damage can lead to the fragmentation of dentures. Surface hardness, being the ability to resist plastic deformation and indentation, is an important property to be increased that would be helpful in facilitating finishing and polishing and in providing resistance to damage during cleaning of prosthesis (36). If a denture base material has low hardness it may be scratched in the harsh oral environment during brushing or chewing ending with increased surface roughness that will lead to more plaque accumulation, bacteria adhesion

and, in the end, to crack initiation and propagation or loss of accuracy (37). The purpose of hardness testing was to assess the level of abrasiveness of the material as hardness values are frequently used as indicators of surface wear resistance (37).

Microhardness test was performed using a LECO M-400 Hardness Tester. Three samples were tested: one non-coated PMMA sample, one PMMA sample coated with 400 cycles of $TiO_2$ (thickness of films around 20/50 nm) and one PMMA coated with 150 cycles of $ZrO_2$ (around 10 nm thickness). The samples were around 2cm x 2cm and for each sample eight indentation measurements were taken. For each sample, the indentation test consisted in the application of a 300 gram force. The Vickers hardness test uses diamond pyramid indenters. After the indentation areas were imprinted, the samples were then analyzed with a Leica microscope and a picture at 200X magnification was taken for every indentation mark. The pictures were then analyzed with the software ImageJ in which the two diagonals were measured for each indentation area created. The average of the two diagonals was taken as the d value to calculate the Vickers Hardness value for each measurement.

$$\mathrm{HV[Kgf/mm\^2]} = \frac{\mathrm{F}}{\mathrm{A}} = \mathrm{F} * 2 * \frac{\sin\left(\frac{136^\circ}{2}\right)}{\mathrm{d}^2} \approx 1{,}8544 * \frac{\mathrm{F}}{\mathrm{d}^2} \qquad (2.4)$$

Formula 2.4 was used to calculate the Vickers Hardness value for each measurement: F is the force applied to the diamond in Kg, A is the value of the obtained indentation area in $mm^2$, d is the average the diagonals left by the indenter (36).

### 2.2.8 Three-Point Bending test

Three-point bending is a popular method to acquire the flexural strength of materials. It is a quantitative and reproducible method which has some advantages compared to other testing methods such as simple sample preparation and favorable loading device (Fig. 5) (39).

The bending strength was obtained by three-point bending test that was performed in China, by Dr. J. Han from Department of Dental Materials, Peking University School and Hospital of Stomatology.

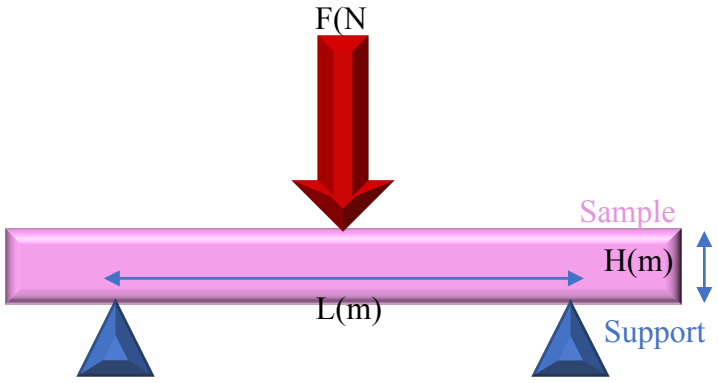


Figure 5: Schematic of three-point bending test: F(N) represents the load applied to sample top surface, L(m) is the distance between two supports and H is the thickness of the specimen (m)

Two groups of samples were tested: $ZrO_2$-coated PMMA with 350 cycles of Zirconium Dioxide with expected thickness around 25nm and mixed $TiO_2$-$ZrO_2$-coated PMMA with a ratio 5:1 and total expected thickness around 40nm (same structure as Figure 6). Both sets of samples were deposited at 100°C with the same pressure and pulse times as Figure 8. Eight specimens for each type of sample were tested. The dimensions of the specimens were: L x B x H= (7±0.1) x (3.1±0.1) x (1.5±0.1) mm.

A universal testing machine was used with a crosshead speed of 5mm/min. All the tests were realized at 22°C.

$$\sigma(\text{MPa}) = \frac{3 \text{ x Fmax x L}}{2 \text{ x B x } H^2} \qquad (2.3)$$

In equation 2.3 (39) $\sigma(\text{MPa})$ represents the flexural strength, $F_{max}$ the maximum force loaded (N), B the width of the sample (m), H the thickness (m) and L is the distance between the supports

(0.005 m). Equation 2.3 was used to calculate the flexural strength for every sample tested, then the mean value and the standard deviation was calculated for every group of specimens.

### 2.2.9 Polident Treatment

After the coating was deposited, some samples were also treated in a Polident solution. Polident is the traditional denture cleanser people use to clean their dentures. We used the "3 minutes tablets" which are supposed to be used to clean the denture in 3 minutes. We placed the samples in the sonication bath with one tablet of Polident and 150 ml of DI water for 1-4 hours and then we repeated the measurement of the thickness, the wettability, and the chemical surface composition to detect any changes.

The ingredients of the 3 minutes tablets of Polident are: "Citric acid, some color additives, polyethylene glycol, potassium monopersulfate, sodium benzoate, sodium bicarbonate, sodium carbonate, sodium lauryl sulfoacetate, sodium percarbonate, tetraacetylethylenediamine, VP/VA copolymer" (40). This treatment is intended to test both physical and chemical durability of the coatings.

## 2.3 Samples Preparation

Silicon samples were cut with a diamond-point cutter, cleaned with DI water and dried with nitrogen before each deposition. The dimensions were around 3 cm x 1 cm for the silicon samples and around 1.5 cm x 1.5 cm for the polymer samples.

PMMA samples (Lucitone 199 by Dentsply) were provided by the College of Dentistry already fabricated. Then the samples were cut with a diamond rotating blade and polished using the Ecomet Polisher with Buehler CarbiMet Special Silicon carbide grinding paper with different grit P800, P1200, P1500, P4000 in order to minimize the surface roughness as much as possible. Then the PMMA samples were cleaned in a 5% in weight NaOH solution for 10 minutes and placed in a sonication bath with DI water for 1 hour. The sonication bath is the Bransonic ultrasonic cleaner 151OR-DTH that has as output 42 KHz ± 6%. After the pretreatment, the samples were

coated in the Lesker system: for each run we used one PMMA sample and one silicon sample to be used as reference.

## 2.4 ALD System Impurity

To characterize the level of impurity inside the reaction chamber the precursor pulse and purge were set to fixed values while the oxygen valve was not opened to prevent any oxidizer particle to reach the reaction chamber. The goal was to try to characterize the oxidizer level inside the reaction chamber when the reservoir valve was not open at all to assess the impurity present in the chamber. If the oxidizer level is almost null, growth rate of the oxide should be null because the substrate would be saturated just with the Titanium precursor and no reaction with oxygen could happen.

We used three silicon samples cleaned with DI water and dried with nitrogen and we ran a deposition with 1 second of TDMAT and 15 seconds of purging nitrogen. Then, after the deposition, we used the spectroscopic ellipsometer to obtain the value of the thickness of the $TiO_2$ layer on the surface of the sample. We expect that, if the reaction chamber is indeed empty of any oxidizer particle, the growth rate of the titania is around zero.

The parameters used for the experiment were the following: the temperature of the bubbler of the Titanium precursor was set to 70°C and the substrate was kept at 150°C, the number of cycles was set to 200 and the pressure was 0.97 Torr. The pulse and purge times of the reactants were 1 second and 15 seconds, respectively, for TDMAT while the pulse time for ozone was 0 seconds. The experiment was not repeated as the results were the ones expected, no deposition of titania occurred.

## 2.5 ALD System Inhomogeneity

Since the system had never been used to deposit $ZrO_2$, we ran multiple depositions to test the system behavior and we observed a significant difference in the final thickness of the coating between the samples in the chamber. We used three samples of silicon for every deposition and

we found that the samples were not uniformly coated inside the chamber as they displayed really different thickness values of the $ZrO_2$ layer. We kept the temperature of the bubbler constant at 70°C for the experiments and we changed the temperature of the substrate from 120°C to 150°C for some experiments, to exclude a temperature dependence. We also varied the pulse times for the precursor and the oxidizer while we kept the same purging times. We ran all the experiments at 300 cycles to better compare the growth rates. The pressure was around 0.62 Torr for every experiment.

The thickness of the coating was measured with the same ellipsometer models right after the deposition had finished with the same procedures. All the thickness values are expressed as Angstroms and the growth rates are always calculated as the mean thickness divided by the number of cycles. For each silicon sample the thickness was evaluated at 3 points and then the mean thickness was obtained. The TDMAZ pulse times were set to 1 or 1.5 seconds and the ozone pulse times were set to 1.8 or 2 seconds. Different temperatures and different times were tested to detect any correlation with other parameters.

## 2.6 Titania and Zirconia mean growth rates on silicon

At first, only silicon substrates were used to tune the machine and to understand the dynamic of the phenomenon. Silicon is more available, it has less variable properties and so the reproducibility is higher, while polymers require a more complicated fabrication, with longer steps and are not as reproducible as the silicon ones. Each silicon sample was cleaned with deionized water and dried with nitrogen right before being inserted into the reaction chamber for the deposition. In each deposition three silicon samples were used and the dimensions were around 3 cm x 1 cm. Different temperatures were tested: 90°C, 120°C, 150°C. We did not test above this because the melting temperature of the polymer is 160°C and the final goal is the deposition on organic substrates. TDMAT ALD saturated window is between 100°C and 250°C so we did not try lower temperatures (27). The precursors were kept in bubblers at 70°C.

After the system was fixed and uniform for both the oxides to deposit we tried to characterize the behavior of the system at 120°C for the two oxides separately on silicon samples. We ran the experiments using two silicon samples pre-cleaned with the same method explained before and we repeated the thickness measurement three times along the samples. We repeated the experiments for different number of cycles by keeping the same bubbler temperature (70°C) and the same pressure (0.97 Torr for $TiO_2$ and 0.48 Torr for $ZrO_2$). The pulse times were 1 second for TDMAT and 1.8 seconds for ozone with 15 seconds purge for both. TDMAZ pulse and purge times were 1.5 and 10 seconds respectively while for ozone were the same as the previous experiment.

## 2.7 Titania and Zirconia mean growth rates on PMMA

After the PMMA samples were fabricated, polished and pre-treated, as described in section 2.3, they were coated in the Lesker system: for each run one PMMA sample and one silicon sample were used. The sample characterization was as previously described. After the deposition, we measured the thickness of the coating with the spectroscopic ellipsometer and the wettability with the water contact angle. The thickness measurement was repeated three times on the silicon samples and two times on the polymer because the samples used were smaller.

The depositions parameters were the same for each experiment, the number of cycles was changed in order to try to understand the behavior of the system on the polymer substrate as we did for the silicon case. The bubbler temperature was fixed at 70°C, the substrate temperature was 120°C. The pulse and the purge times were as in the silicon tests run previously in section 2.6.

## 2.8 Mixed oxides coating mean growth rate on silicon

We tried to deposit one oxide on top of the other using firstly silicon samples as the spectroscopic ellipsometer model for this kind of substrate was already evaluated and so, especially while depositing thin layers of oxides, the results would be much more reliable.

We deposited the layers on one silicon sample per experiment, with the same pre-treatment as explained before, at 120°C, keeping all the parameters unchanged (precursors, pulse and purge times, pressure). When the first layer of material had finished the number of cycles set, the sample was taken out from the chamber and the thickness of the first oxide deposited was obtained by fitting the experimental data with the right SE model ($TiO_2$ or $ZrO_2$ over silicon). Then the sample was loaded again in the chamber and the same procedure was repeated for the deposition of the second oxide. The model used showed 4 layers: silicon at the bottom, 15 Angstroms of silica, the thickness of the first oxide deposited and obtained during the first SE data acquisition and lastly the oxide layer on top.

The structure of these kind of samples resulted, starting from the bottom: silicon, silica, titania and then zirconia (or vice versa). In the SE models already present in WVASE32 software, silica is assumed to be 15 Angstroms, which is the most common thickness for the native oxide on silicon. In order to confirm the effective validity of the assumption we have measured silica thickness on 8 silicon samples and the mean $SiO_2$ thickness obtained was 12.9±0.8 Å.

## 2.9 Mixed oxides coating mean growth rate on PMMA

As the final goal was to try to deposit the two oxides on the polymer substrate we started to apply the two materials sequentially on PMMA by ALD technique. We chose the ratio titania-zirconia 5:1 as it seems the most interesting for dental applications although some attempts were made also for a ratio of 2:1. The desired total thickness of the mixed coating is around 30nm. The goal is to change the surface properties, while minimizing dimensional changes and maintaining the bulk properties constant.

A 20-30nm ceramic coating is confirmed to be the best thickness to be able to keep the maximum polymer flexibility, as ceramics and polymers have different elastic moduli (41). Ceramics are known to be brittle and a lot less flexible than polymers, so a thick ceramic layer on top may delaminate or create cracks and failure during denture bending in the oral environment.

Keeping the coating so thin has also other reasons as thermal expansion coefficients or color-related issues. PMMA change of color may be another concern to choose the right thickness of the ceramic coating for dental applications: $TiO_2$ coatings on PMMA are more studied than $ZrO_2$ coatings in literature. In an interesting study by Mori et al. $TiO_2$ nano-thin uniform coatings were performed by spraying process at 70°C on PMMA samples and both the color and the glossiness were tested: a glossmeter and a reflective colorimeter were used in this study in which non coated and coated acrylic resins were tested (42). The results showed that a nano-thin ceramic coating retains the not coated PMMA color by just increasing the level of glossiness of the surface, which usually has a positive effect on patients' satisfaction (42). This was also detected on our coated samples: by just human observation the coated samples appear glossier and look to be quite pearly after the ceramic depositions, but apparently the color did not look to be changed. Color testing will be performed on our samples too, as it will be explained in the Future Work section.

Lastly, while choosing the ideal coating thickness, also thermal expansion coefficients must be taken into consideration: during heating and cooling the polymer will expand more than the oxide on top as PMMA has a higher thermal expansion coefficient than the ceramic film (43). Lu H. et al. studied the relationship between the thickness of a ZnO film deposited on PMMA and thermal expansion mismatch. Consequently to heating the material at 120°C, an isotropic tensile stress field is produced in the ZnO film and it was proved to depend on the film thickness (43). After the cool down, due to thermal expansion mismatch cracks and wrinkles start to appear on the surface, tested with AFM. A critical thickness of the oxide film for the formation of cracks was detected and it was proved to be around 30nm (43). This study was also taken into consideration to choose the ideal coating thickness: the main goal was to guarantee the precision and the accuracy of the device.

We deposited eight PMMA samples at 100°C that were later stored in DI water. The temperature was lowered to 100°C because there were some concerns that at elevated temperature, such as 120°C, PMMA could be in some way affected. Moreover, previous works had already

proved that oxides were successfully deposited on PMMA at 90°C by ALD (46). We decided to deposit at 100°C because TDMAZ and $O_3$ ALD saturated window is between 100°C and 250°C (27). All the parameters as pulse, purge times and the pressure were kept constant and equal to the other depositions on PMMA described before.

The valves opening sequence was controlled as follows: TDMAT pulse and $N_2$ purge for a defined number of cycles, TDMAZ pulse and $N_2$ purge for a defined number of cycles and repeat. The deposition consisted in a supercycle made of 40 cycles of titania (expected around 5 nm) and 20 cycles of zirconia (expected around 1 nm) and we repeated 6 supercycles. In this way the overall thickness, calculated on the basis of the mean growth rates obtained from the characteristic curves in Fig. 9 and Fig. 12, is expected to be around 36 nm. The coating should start with a 5nm layer of $TiO_2$ and end with a 1nm layer of $ZrO_2$, the structure is displayed in Fig. 6. The 5:1 thickness ratio we speculate the samples should have is a theoretical value, calculated by considering the input cycles for the precursors and the mean growth rates per cycle of the oxides on top of PMMA. So, in this study, when ratio 5:1, 2:1 is mentioned, it is intended in a theoretical sense, by considering what was set as subcycles ratio for the precursors.

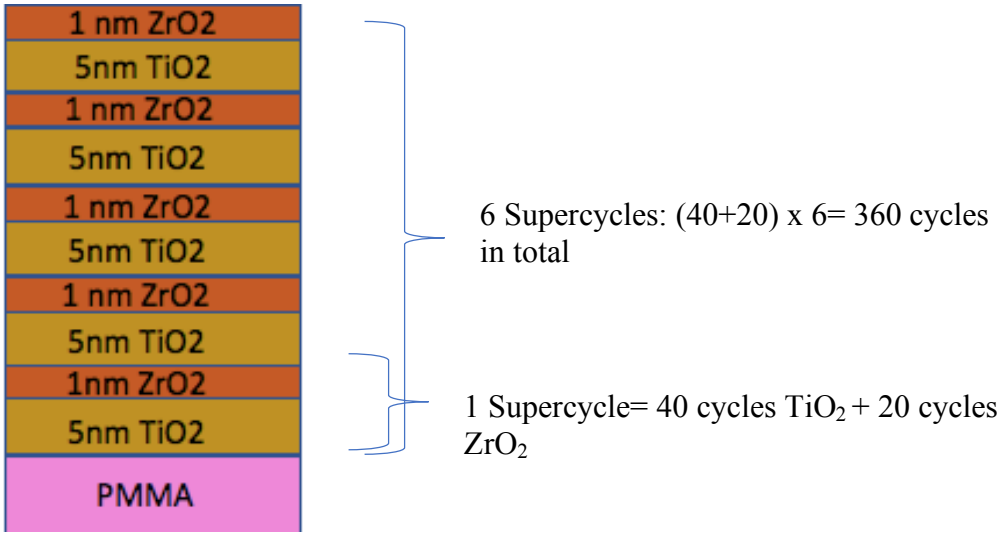


Figure 6: Theoretical structure of the mixed titania-zirconia coating obtained by ALD at 100°C on PMMA substrate. 6 Supercycles, made of 40 cycles of TDMAT and 20 cycles of TDMAZ each, were performed. Theoretically this ALD recipe should result in the structure shown, with a

thickness ratio 5:1. The theoretical thickness of the layers are calculated with the mean growth rate per cycle obtained in the other experiments.

To perform 50 cycles with the pulse and the purge times chosen the system takes around 30 minutes. This means that this mixed coating takes about 4 hours: ALD has multiple advantages, as mentioned previously, but the long times required for the cycles, due to the need of long purge times, was already mentioned as one of the main disadvantages. To shorten the time needed the pulse and purge times may be decreased: too short pulse times may result in a not saturated growth as the precursor must have sufficient time to saturate all the active sites on the surface. On the other hand, too short purge times may not be sufficient to evacuate the not reacted precursor and the reaction byproducts, resulting in not controlled surface reactions.

# CHAPTER 3

# RESULTS AND DISCUSSION

## 3.1 Results of system impurity

To characterize the level of impurity inside the reaction chamber we just used the precursor pulse and purge but we did not open the oxygen valve to prevent any oxidizer particle to reach the reaction chamber. If the level of oxidizer is almost null we should not see any growth rate of the oxide because the substrate would be saturated just with the titanium precursor and no reaction with oxygen could happen. The parameters used in the experiment were displayed in section 2.4 and the results are shown in Table I. The SE model that was used was already present in WVASE 32 software: we used a model made of silicon, silica and a $TiO_2$ layer on top. We fitted the acquisitions to detect a hypothetic $TiO_2$ layer on top.

The results were as expected because the growth rate resulted to be almost zero and one can deduce that the chamber was almost empty of any oxidizer. The growth rate is always obtained as the mean thickness divided by the number of cycles performed. All the thicknesses are displayed in Angstroms (Å). The mean growth rate is calculated as the mean thickness divided by the number of cycles performed. The standard deviation is calculated for measurements within the same sample so it represents the uniformity of the value.

TABLE I: THICKNESS AND GROWTH RATE OBTAINED FROM THE DEPOSITION OF TITANIA WITH 1 S PULSE OF TDMAT AND 15 S OF PURGE BUT NO OXIDIZER PULSE ON SILICON SAMPLES AT 150°C AND 0.97 TORR AND BUBBLER TEMPERATURE SET TO 70°C (THE STANDARD DEVIATION IS FOR MEASUREMENTS WITHIN THE SAME SAMPLE)

| | Mean thickness (Å) | St. Dev. | Mean Growth rate(Å/cy) |
|---|---|---|---|
| Sample 1 | 7.81 | 0.6 | 0.04 |
| Sample 2 | 10.1 | 1.2 | 0.05 |
| Sample 3 | 6.00 | 0.3 | 0.03 |

## 3.2 Results of system inhomogeneity

We ran multiple depositions of $ZrO_2$ and we observed a difference in the final thickness of the coating between the samples inside the chamber. All the parameters used were listed in section 2.5.

We can see from the depositions performed how the deposition is not homogeneous at all on the samples: it is really evident the difference in thickness between the three samples of the different groups displayed in Figure 7. Moreover, for some samples the standard deviation was really high because the coating was not homogeneous even on the same sample. Since high inhomogeneity was detected for the $ZrO_2$ depositions, the heater jacket of the bubbler containing the zirconium precursor was changed because it was assumed not to heat the precursor in a homogeneous way through all the bulk. Secondly, the dose of the carrier gas was changed too because it was assumed not to allow a sufficient concentration of the reactant in the flow coming into the chamber. So, to fix this issue a new program for the software controlling the sequence of the reservoirs valves reducing the carrier gas flow at the 55% was installed (27 sccm).

After the system was fixed we proved that zirconia deposition became uniform. From Figure 7 it is evident how all the three samples were homogenously coated as the mean thickness values and growth rates are really similar for every sample. The standard deviation is calculated for measurements within the same sample so it represents the uniformity of the value.

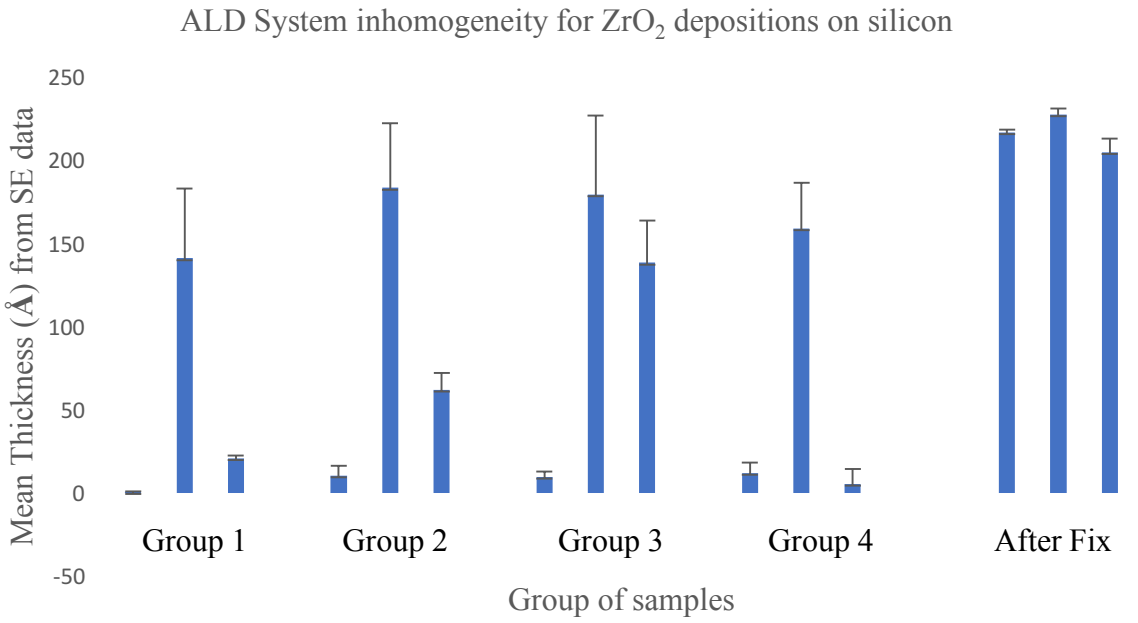


Figure 7: Mean thickness of the silicon samples coated for 300 cycles with $ZrO_2$ at different conditions. Group 1 coated at 150 °C with 1 s and 10 s of TDMAZ pulse and purge and 1.8 s and 15s of ozone pulse and purge, group 2 at 150°C with 1.5 s and 10 s of TDMAZ pulse and purge and 2s and 15s of ozone pulse and purge, group 3 coated at 120°C with 1.5 s and 10 s of TDMAZ pulse and purge and 1.8s and 15s of ozone pulse and purge, group 4 at 120°C with 1.5 s and 10 s of TDMAZ pulse and purge and 1.8s and 15s of ozone pulse and purge with different position in the chamber. After Fix is the group of samples coated with same conditions of group 4 but after the system was fixed. (Pressure constant to 0.48 Torr and bubbler temperature constant at 70°C)

### 3.3 Results of Titania and Zirconia mean growth rate on silicon

The first depositions were used to calibrate the system. The results at the different temperatures and different pulse times are displayed in Table II. Titania deposition was already evaluated and optimized in previous studies (46). In contrast, the system had never been used to deposit zirconia so the behavior was not known and more tests had to be run.

Different pulse times were tested to tune the zirconia deposition and for 0.5 and 1 second of pulse the growth rate turned out lower, 0.25 Å/cycles and 0.47 Å/cycles respectively, instead of 0.6 Å/cycles. The lower deposition rates for the lower pulse times may be attributed to an insufficient precursor pulse time that is not able to saturate all the active sites of the substrate surface leading to a decreased oxide growth. After the system was fixed and uniform for both the

oxides to deposit we tried to characterize the behavior of the system at 120°C for the two oxides separately on silicon samples.

TABLE II: GROWTH RATE IN Å/CYCLE OBTAINED FROM THE DEPOSITIONS AT DIFFERENT TEMPERATURES AND DIFFERENT PULSE TIMES FOR TDMAZ AND $O_3$ ON SILICON SAMPLES (PRESSURE 0.97 TORR AND 0.48 TORR FOR TDMAT AND TDMAZ RESPECTIVELY, NITROGEN PURGE EQUAL TO 15 SECONDS IN EVERY DEPOSITION)

| Temp.(°C) | $ZrO_2$ (1s) $O_3$ (1.8s) | $ZrO_2$ (1s) $O_3$ (1.8s) | $ZrO_2$ (1.5s) $O_3$ (2s) | $ZrO_2$ (1.5s) $O_3$ (1.8s) | $ZrO_2$ (0.5s) $O_3$ (1.5s) |
|---|---|---|---|---|---|
| 90 | 0.413 | | | | |
| 110 | 0.435 | | | | |
| 120 | 0.415 | | | 0.597 | 0.250 |
| 150 | | 0.469 | 0.611 | | |

The results obtained from the ellipsometric acquisitions are all displayed in Figure 8, which shows how titania and zirconia coating's mean thickness changes by changing only the number of cycles keeping all the other parameters constant. The equations of the dotted lines are obtained by doing a linear approximation of the data on Excel software. $R^2$ is the correlation coefficient, the closer it is to 1 the better the fit. The standard deviation is calculated for measurements between the three samples tested in each run.

The mean growth rate for titanium dioxide is 0.41 Angstrom/cycle and it is quite consistent with the values found in literature: the study by Yong-Wan Kim et al. of 2012 confirmed that the $TiO_2$ growth rate found was 0.48 Angstrom/cycle (47). They used a shower head reactor with a vertical flow and the precursors were the same we used. The bubblers were kept at 30°C and the delivery lines at 60°C, the pressure was 0.8 Torr. The growth rate was slightly affected by changing the temperature from 150°C to 225°C and they used X-ray reflectivity (XRR) to measure the thickness (47). Another study by Jin C. et al. in 2015 confirmed that, in the ALD saturated growth

window for TDMAT and ozone, which is 100°C-250°C, the constant growth rate on silicon is 0.46 Å/cycle (27).

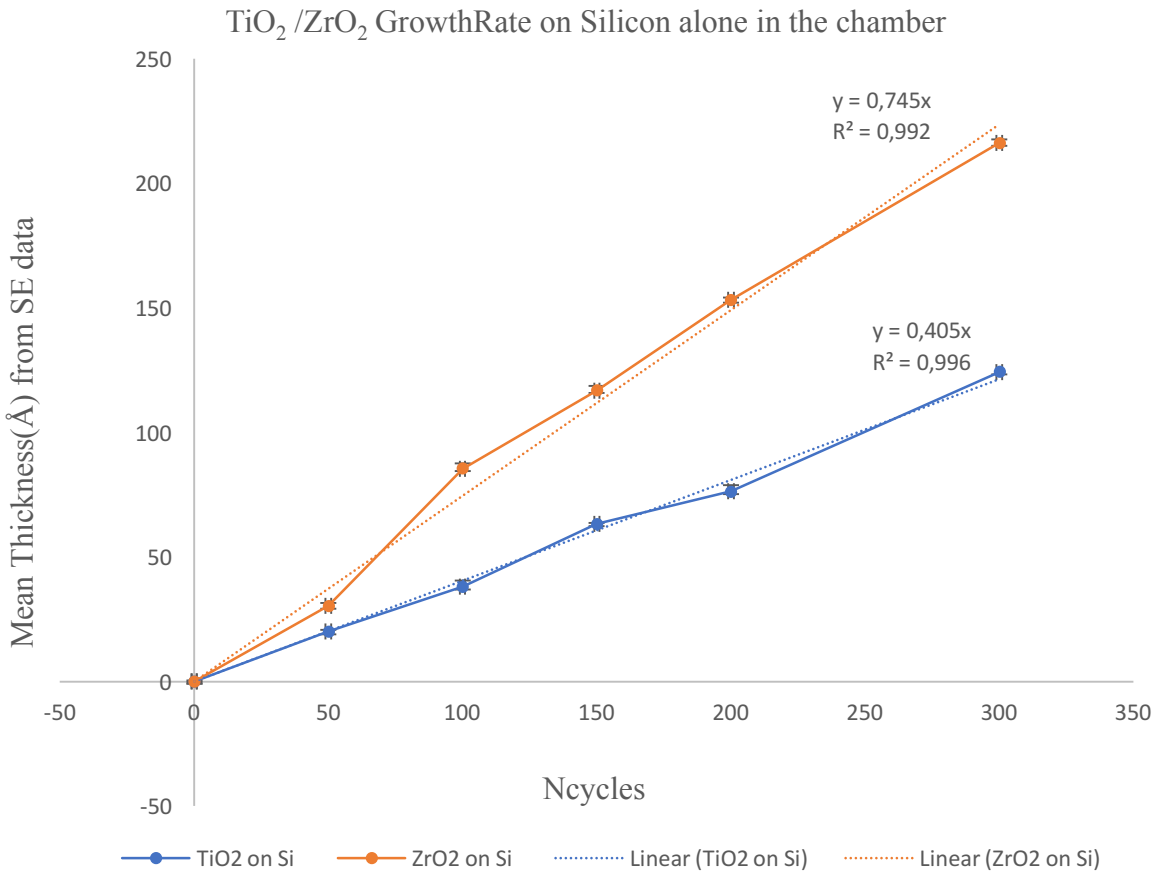


Figure 8: Mean Growth rate of $TiO_2$ and $ZrO_2$ from TDMAT/TDMAZ and ozone on silicon as a function of ALD cycles at 120°C. Pressure was 0.96 Torr and 0.48 Torr for TDMAT and TDMAZ respectively, bubbler temperature was 70°C for both materials. 1 s and 15 s of pulse and purge of TDMAT and 1.5 s and 10 s of purge of TDMAZ, 1.8 s and 15 s of pulse and purge of ozone for both oxides. The number of cycles was the only parameter changed in each deposition, all the other were kept constant. The mean thickness was obtained with spectroscopic ellipsometry, the models used were described in previous sections. The dotted lines are the linear approximations obtained with Excel Software, the $R^2$ value is the correlation coefficient, the closer is to one the better is the fit.

The linear approximation for $ZrO_2$ depositions is 0.75 Angstrom/cycles. For TDMAZ precursor, there are a few studies that can help understanding our results, although almost no study with ozone as oxidizer was found. One study from Qiuyue Yang et al. of 2017 used a commercial

ALD reactor to deposit $ZrO_2$ from TDMAZ but the oxidizer was water (14). The bubbler temperature was 150°C and they deposited at 250°C performing 100, 200, 300 and 400 cycles. The mean growth rate resulted to be 0.97 Angstrom/cycle, slightly higher than ours but they used SEM to measure the thickness (14). Usually electron microscopy and ellipsometry present different thickness values with a difference of about 1-3 nm (40). Another study by Joon Hyung Shim et al. of 2007 used the same precursors as the previous study, TDMAZ and DI water, to deposit yttria stabilized zirconia films (48). The characterization was made with XPS, AFM and XRD. The bubbler temperature was 100°C and the deposition temperature was 250°C. The pressure was around 0.2-0.3 Torr (48). They presented a zirconia growth rate of 1.5 Angstrom/cycle, which is higher than 0.75 and also higher than the previous study that used the same temperature and precursors. It is evident how the growth depends on multiple factors among which bubbler and deposition temperatures, choice of precursors but also type of reactor, pressure and times.

The result was as expected as ALD depositions usually have coating thickness linearly dependent on the number of cycles. Both ZrO2 and $TiO_2$ depositions on silicon substrates showed this behavior.

## 3.4 Results of Titania and Zirconia mean growth rates on PMMA

After the samples were fabricated and pre-treated as explained in section 2.3, they were coated with $TiO_2$ and $ZrO_2$ separately in the Lesker system: for each run we used one PMMA sample and one silicon sample to be used as reference. The coating thickness measurement was repeated three times on the silicon samples and two times on the polymer because the samples used were smaller.

### 3.4.1 Results of Titania mean growth rate on PMMA

The results of the $TiO_2$ depositions on the polymer, on silicon alone and on silicon in the same chamber with the polymer are shown in the tables and in the graphs displayed in Figure 9. The SE data for PMMA and silicon samples were obtained following the same procedure, the only

change is in the Cauchy model used to fit the ellipsometer data. The model for the silicon sample was already evaluated but the model for the polymer was newly built so one of the first things to do is to compare these data with the thickness values coming from another characterization method as, for example, electron microscopy. Cross-section SEM was attempted, but the sample is not conductive and this produced no reliable data due to the high charging of the material. TEM could be a solution but the procedure to cut the samples used would be destructive on a coating with such a thin thickness. Some other technique had to be taken into consideration to measure the nano-film thickness on such a non-conductive and relatively weak polymer. The data produced though, look to be quite consistent with the silicon acquisitions, leading to linear correlation between the cycles and the thickness, which is expected for ALD depositions. For each sample, the SE model was obtained by taking some acquisitions of the bare PMMA sample and by fitting sequentially A, B, C parameters of the model provided by Woollam Co. for our samples before the depositions, as described previously.

Figure 9 shows how $TiO_2$ mean thickness of the coating changes on the different substrates by changing only the number of cycles keeping all the other parameters constant. The equations of the dotted lines are obtained by doing a linear approximation of the data using Excel software. The growth rate of the line is expressed as Angstrom/cycle. $R^2$ is the correlation coefficient, the closer is to 1 the better the fit. The standard deviation is calculated for measurements within the same sample so it represents the uniformity of the value. The linear approximation of the experimental data on PMMA is quite accurate as you can see from the correlation coefficient and it shows that the mean growth rate of Titanium Dioxide on PMMA is around 1.52 Angstrom/cycle.

The linear dependence of the thickness from the number of cycles, was expected as it is one of the features of ALD depositions. This value is dramatically higher than the growth rate obtained for titania on silicon, which is around 0.41 Angstrom/cycle. PMMA in fact, is a totally different substrate from silicon and might have a completely different chemistry that can modify

the growth mechanism of the oxide on top of the surface. The ALD growth of a material strongly depends on the substrate on which the first cycle is deposited (19).

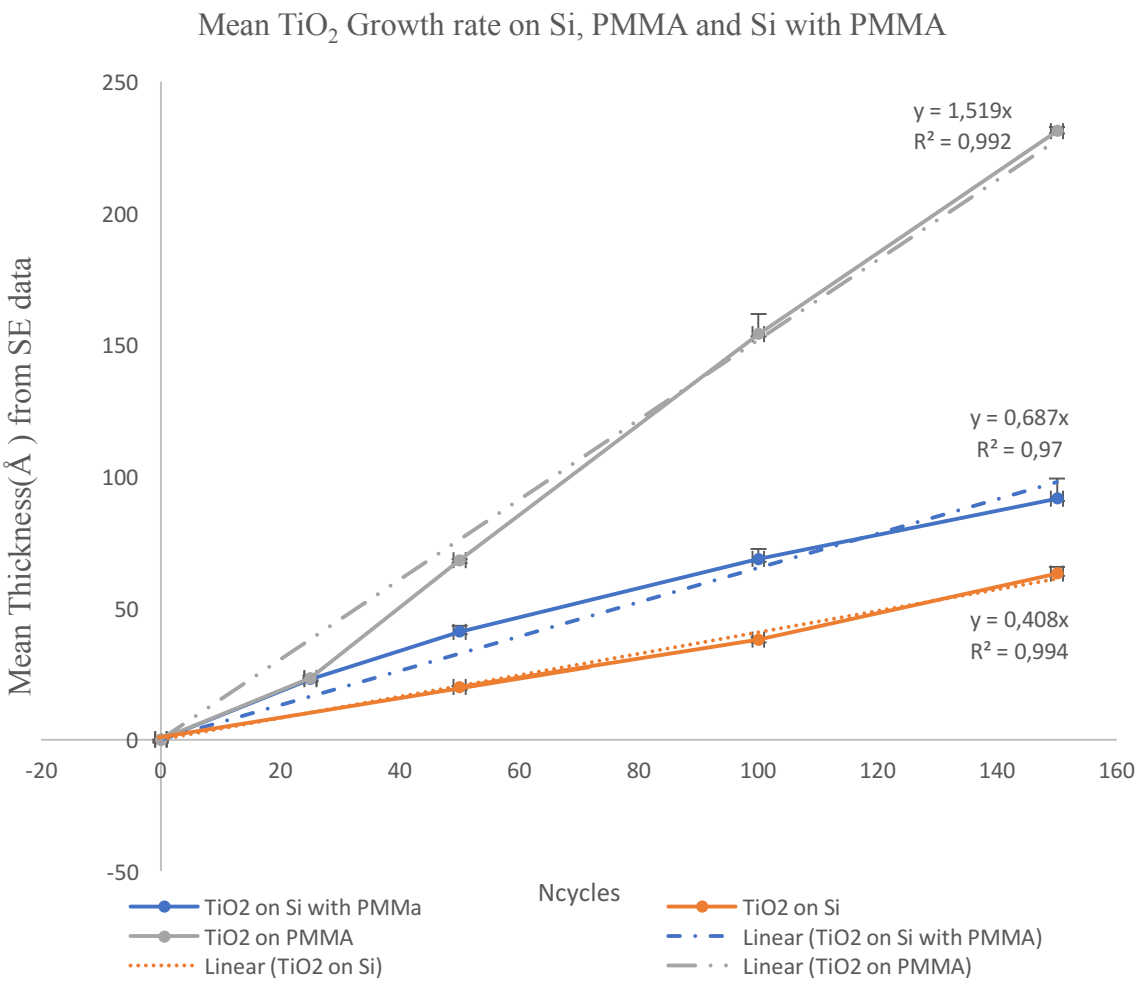


Figure 9: Growth rate of $TiO_2$ from TDMAT and ozone on PMMA, on silicon alone and on silicon in the same chamber with PMMA as a function of ALD cycles at 120°C (Same deposition conditions as Fig. 8). The number of cycles was the only parameter changed in each deposition, all the other were kept constant. The mean thickness was obtained with spectroscopic ellipsometry, the models used were described in previous sections. The dotted lines are the linear approximations obtained with Excel Software, the $R^2$ value is the correlation coefficient, the closer is to one the better is the fit.

The linear approximation of the experimental data shows that the mean growth rate of Titanium Dioxide on silicon in the same conditions is lower for silicon alone than silicon in the same chamber together with PMMA. The differential growth increase displayed in Table III is

obtained by doing the difference between one thickness value and the successive one and by dividing by the difference of the associated number of cycles. The standard deviation is calculated for measurements within the same sample so it represents the uniformity of the value. It is evident that the growth rate is increased a lot in the first 25, 50 cycles and then it returns 0.4 Angstrom/cycle which is the one calculated in the case of silicon alone in the reaction chamber.

TABLE III: NUMBER OF CYCLES, MEAN THICKNESS AND DIFFERENTIAL GROWTH OF THE TITANIA COATING THICKNESS ON SILICON IN THE SAME CHAMBER WITH THE POLYMER AT 120°C (SAME DEPOSITION CONDITIONS AS FIGURE 8)

| Cycles | Mean thickness $TiO_2$ on Si with PMMA(Å) | St.Dev. | Differenntial Growth Rate (Å/cy) |
|---|---|---|---|
| 0 | 0 | 0 | 0 |
| 25 | 23 | 0.4 | 0.9 |
| 50 | 41 | 2.3 | 0.7 |
| 100 | 68.6 | 3.9 | 0.6 |
| 150 | 91.67 | 7.6 | 0.5 |
| 350 | 161.8 | 2.1 | 0.4 |
| 500 | 236.1 | 6 | 0.5 |

This behavior is also shown in Figure 9: the curve has a higher slope in the first part and then over 100 cycles the slope drops down. The linear approximation is less accurate in this case, as you can see from the R^2 value which is less than the previous cases (0.97). As the curve seems to have two different slopes, one from 0 cycles to 50 cycles and one from 50 to 150 cycles we tried to approximate separately the two segments (Fig. 10): from 0 to 50 cycles (red line) you can see the slope is 1.03Å/cy, almost three times the normal growth on silicon, while from 50 to 150 cycles (green line) the slope is 0.40Å/cy, equal to the growth of titania on just silicon found before. The higher R square value indicates that the two lines fit the curve better than the dotted line with slope 0.69Å/cy found before. This suggests PMMA interferes with the growth on silicon in the first cycles and then it stops, as the growth rate of $TiO_2$ on silicon for higher cycles returns the one

found when just silicon was in the chamber. This behavior is well displayed in Figure 11, where the growth rate is shown also for higher cycles: on both substrates, the oxide growth is increased in the first cycles and then drops down for higher cycles. The depositions at higher cycles were repeated twice. So, from the SE data one can conclude that the average growth rate for titania on both substrates in the same runs seems to decrease with the number of cycles.

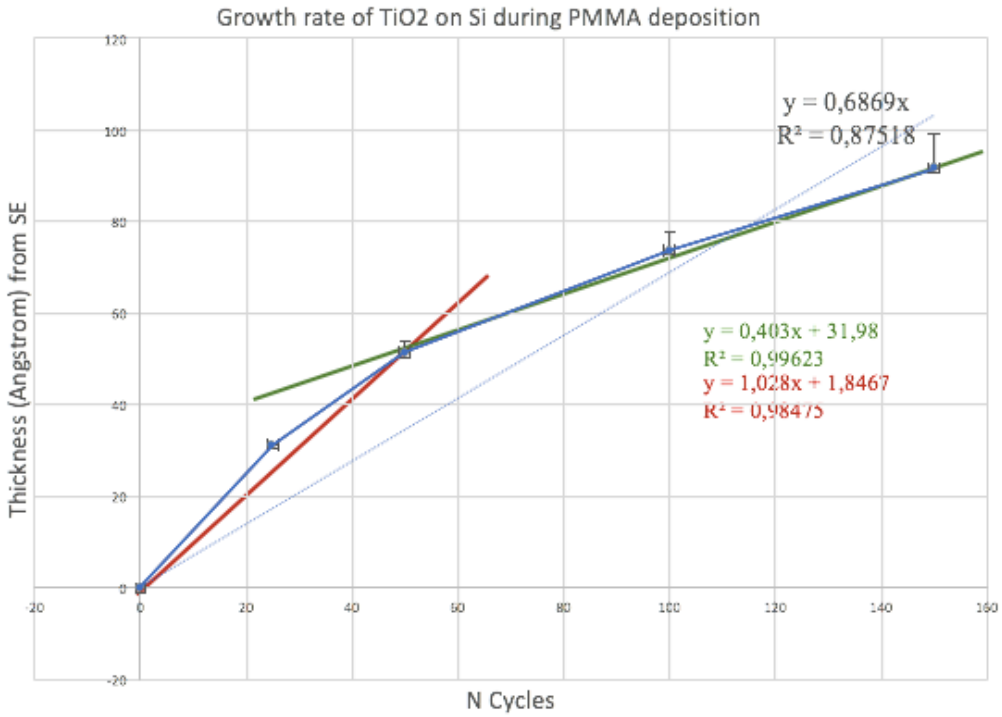


Figure 10: Growth rate of $TiO_2$ from TDMAT and ozone on silicon in the same reaction chamber with PMMA as a function of ALD cycles at 120°C with 2 different linear approximations at same conditions as Fig. 8 (blue line and green line)

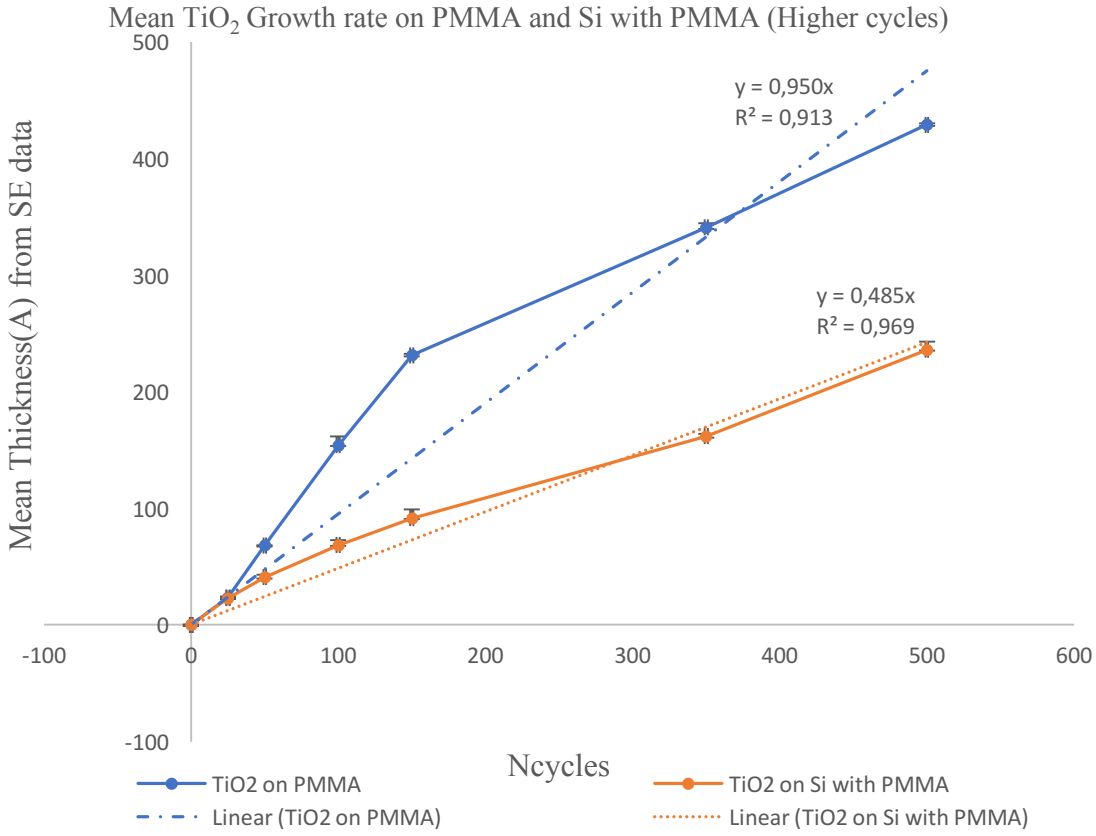


Figure 11: Growth rate of $TiO_2$ from TDMAT and ozone on PMMA and on silicon in the same chamber with PMMA as a function of ALD cycles at 120°C for higher cycles (Same deposition conditions as Fig. 8) The number of cycles was the only parameter changed in each deposition, all the other were kept constant. The mean thickness was obtained with spectroscopic ellipsometry, the models used were described in previous sections. The dotted lines are the linear approximations obtained with Excel Software, the $R^2$ value is the correlation coefficient, the closer is to one the better is the fit.

### 3.4.2 Results of Zirconia mean growth rate on PMMA

The same experiments were run for the Zirconium dioxide on polymer samples and the results of the $ZrO_2$ deposition on the different substrates at the same conditions are showed in Figure 12. The equations of the linear approximations are obtained by processing the data using Excel software. The standard deviation is calculated for measurements within the same sample so it represents the uniformity of the value. The SE mode used was the same described in the previous section in wich the substrate optical paramters were fitted for every non coated sample; the only difference was that the added layer on top was $ZrO_2$.

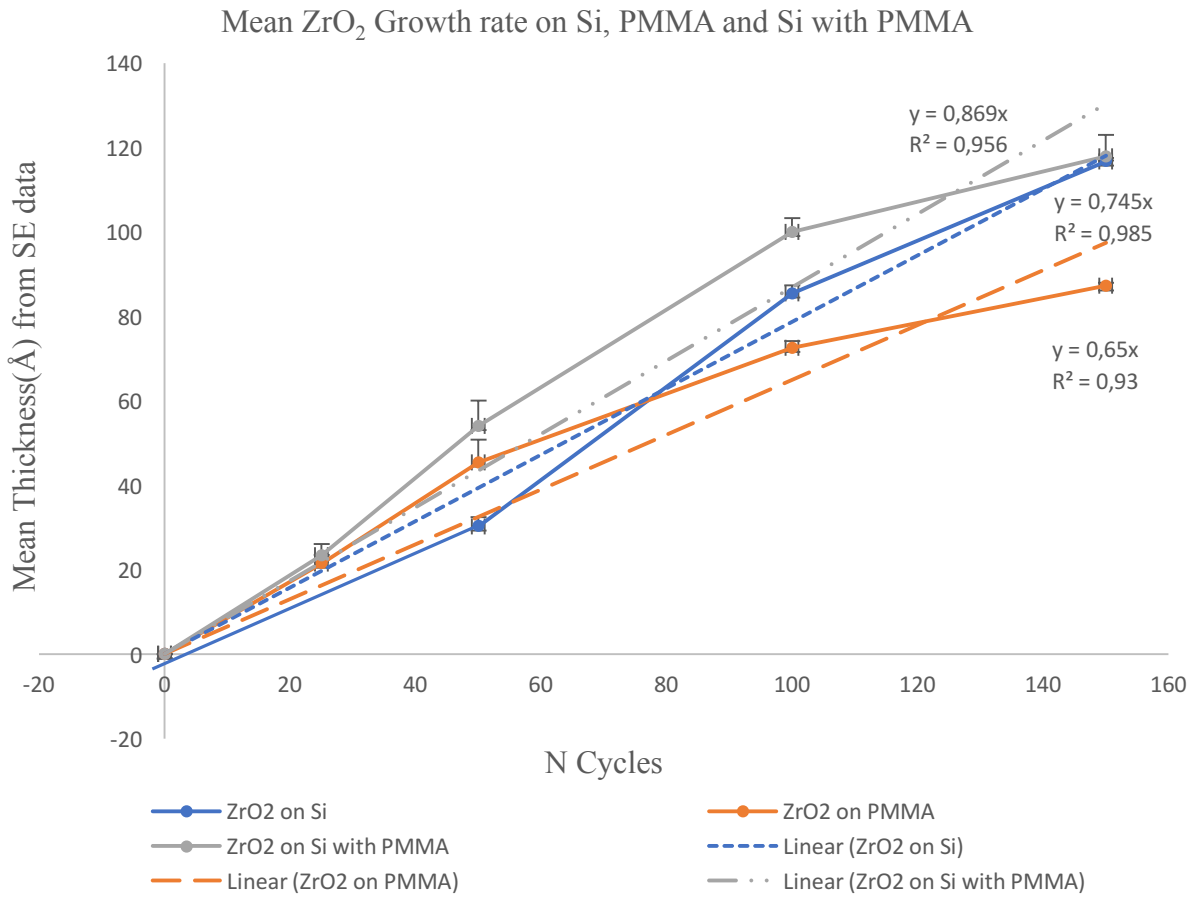


Figure 12: Growth rate of $ZrO_2$ from TDMAZ and ozone on PMMA, on silicon alone and on silicon in the same chamber with PMMA as a function of ALD cycles at 120°C (Same deposition conditions as Figure 8). The number of cycles was the only parameter changed in each deposition, all the other were kept constant. The mean thickness was obtained with spectroscopic ellipsometry, the models used were described in previous sections. The dotted lines are the linear approximations obtained with Excel Software, the $R^2$ value is the correlation coefficient, the closer is to one the better is the fit.

The linear approximation of the experimental data shows that the mean growth rate of Zirconium Dioxide on the different substrates is not so different as for $TiO_2$ deposition. The values differentiate of 0.1-0.2 Å/cy, that is consistent with other studies' results claiming that the deposition rate of different oxides on polymeric substrates and silicon were very similar (21, 22). In particular, one paper by Wilson et al. of 2005 studied the ALD of alumina on PMMA substrates: the precursors used were trimethylaluminum (TMA) and water at 85°C using a viscous flow reactor (22). The pulse and purge times were 1-29-1-29 seconds and the substrates were traditional

silicon compared with silicon spin coated with PS, PMMA, PE and PVC (0.1-0.5 μm). The characterization they used consisted of a quartz crystal microbalance, in order to register the mass changes during each ALD cycle and surface profilometry for the final thickness. The final growth rate they report is consistently 1.2 Å/cy on silicon and it is similar on each polymer, as for our results with zirconia (22).

Another interesting study of ALD on PMMA is the one by Kemell et al. in 2008 that deposited both alumina and titania on PMMA substrates at different temperatures using a flow type reactor with silicon samples spin coated with PMMA, PEEK, PTFE and ETFE (0.1 μm, 500 μm) (21). The characterization was made by FESEM and EDS for the thickness. The results showed growth rates close to silicon reference, which agrees again with our results of zirconia, confirming that it seems that the different chemistry of the two substrates does not affect the growth of the oxide layer (21).

As you can see for silicon with PMMA the relationship thickness/number of cycles is really linear, as expected for ALD, and the approximation seems to be very accurate.

For both the oxides, the deposition rate is higher for silicon deposited with the polymer. This behavior was the same observed by Kaariainien T.O. et al., who found on silicon together with PMMA the same growth rate we calculated (23). In this study, titania was deposited on PMMA at 65°C with TDMAT and $O_3$ and they also used the same polymer pre-treatment with 5% NaOH. They performed 120, 320 and 820 cycles and then they measured the thickness with a SE by J.A. Woollam SE on silicon as reference. They measured 0.6 Å/cy, which is the same titania growth rate we found on silicon when deposited together with the polymer. They confirmed that they observed higher growth rates of titania on silicon while it was in the same reaction chamber with polymers (23). Unfortunately, they did not measure the thickness on the polymer sample, so we cannot compare the growth rates on PMMA.

Both oxides present a higher growth for the first cycles that seems to decrease for higher cycles is observed for both the oxides on both PMMA and silicon with PMMA. The average $ZrO_2$ growth rate shows that for 150 cycles the deposition of $ZrO_2$ on silicon and on silicon with PMMA converges to the same thickness. The decrease of the deposition rate for higher cycles does not look to be present when silicon is alone in the chamber so it is to be attributed to a phenomenon coming from the polymer chemistry. Polymers are particular substrates, made of long repetitive chains of hydrocarbons. When PMMA is heated above 60°C-100°C unreacted monomers and other species as CO, CHO, methanol and monomers without the ester group may gain sufficient energy to move, come to the surface and evaporate (25, 49). At around 100-120°C almost the 10% of the bulk material evaporates. They explained this with a higher mobility inside the film that may cause fragments to reach the surface and evaporate; simultaneously chain scissions happen which may cause cross-linking inside the PMMA (25). These species are reactive and contain a lot of oxygen that may be used to increase the oxygen amount in the chamber available for reactions with the precursor to form more oxide.

Kashiwagi T. et al. confirmed an early reduced weight loss of PMMA for lower temperatures and then rapid weight loss due to degradation. The early small weight loss was attributed to "volatilization of unreacted monomer in the sample" (49). They also confirmed that the purified samples (with no unreacted monomer) were more stable at low temperatures and this can be due to the removal of unreacted monomer.

Evaporation of the volatile species, that takes place when the polymer is first heated to 100-120°C in the reaction chamber, may be responsible of the higher growth rate in the first cycles on silicon when it is in the same chamber by providing more reactive oxygen species. This also explains the higher deposition rate on silicon when it is coated with polymers mentioned previously. Polymer evaporation at 120°C was confirmed by TGA test we performed on our samples.

In addition to this, the higher growth at lower cycles on PMMA, which was detected in both oxides may be attributed not only to the initial evaporation of PMMA but also to the particular mechanism of oxides growth on polymers. Both Kemell et al. and Wilson et al. reported a large uptake of precursor on PMMA, PE and PP during the first exposures to reactants (21, 22). During the first ALD cycles a large amount of precursor is adsorbed and absorbed not only on the surface but also through the bulk of the polymer. Then, as the cycles are increased the oxide clusters start to form a film acting as a barrier for the diffusion of the reactants inside the polymer (22). This is also confirmed in EDS mapping of the cross-section of the ALD coated PMMA samples (in section 3.11, Fig. 25-26) in which both titanium and zirconium look to be uniformly distributed through the bulk material and not only on the surface. Permeability in polymers is controlled by solubility and diffusion: at first the large uptake is due to the high diffusion rate because of the high porosity and free volume, which is then impeded after the first cycles because the film acts as a diffusion barrier (22).

The dynamics of the process appear to be the same for both oxides even if in $ZrO_2$ case the behavior for PMMA is different for higher cycles. In Figure 13, the rate on PMMA does not seem to be decreased for higher cycles, as it happened for all the previous cases. SE data for thicker $ZrO_2$ coatings did not look to be reliable though. The depositions for higher cycles were repeated twice, as the behavior was not as expected.

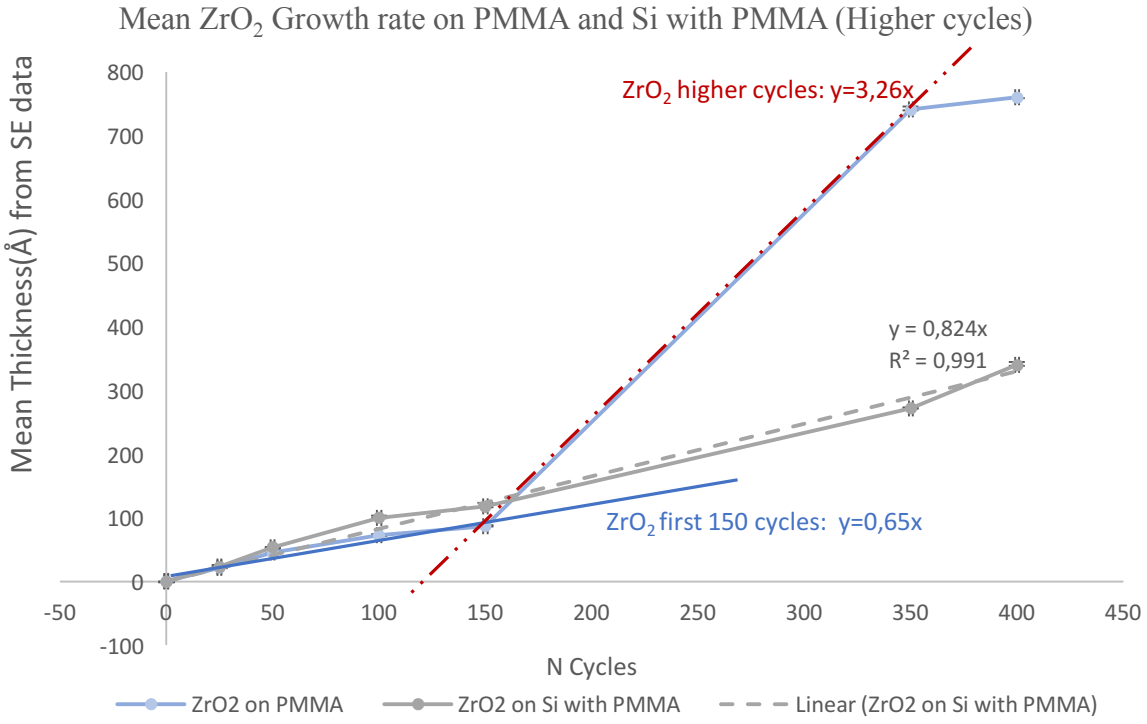


Figure 13: Growth rate of $ZrO_2$ from TDMAZ and ozone on PMMA and on silicon in the same chamber with PMMA as a function of ALD cycles at 120°C for higher cycles (Same deposition conditions as Figure 8). Red line is dotted as the ellipsometric fitting was not considered accurate and reliable, the optical constants obtained were not similar to zirconia constants so the measurements acquired were not considered as the actual thickness of the coating.

For coatings thicker than 20nm, the model to fit the ellipsometer data is different: below 20 nm the sensitivity to the optical constants of the coating is really low so usually the constants present in the database are to be used and only the thickness is fitted while over 20 nm thickness, the sensitivity is higher and the coating constants are to be fitted as well to obtain a more accurate approximation.

For $ZrO_2$ the behavior is not as expected, the thickness obtained is around 70 nm and it is a lot higher than the one expected, which was around 30 nm. The optical constants for zirconia were around 1.5 which is not feasible as the optical constant of this ceramic is around 2, as the acquisitions on the silicon samples confirm. Optically the film appears as a thicker layer, twice the value expected, made of a lower index material than normal zirconia. Zirconia should present a higher index, as the data on silicon confirm. In order to try to explain the data obtained from the

measurements, one can speculate that the long time in the reaction chamber at high temperature makes the polymer interfere in some way with zirconia formation, maybe degrading or changing also itself and modifying the zirconia optical properties. This does not seem to occur with titania deposition though, as the index for titania is almost the same on the polymer and on silicon and coincides with the known index for this oxide. This difference was not expected as the polymer is in the same condition in both cases: heated at high temperature in the same atmosphere for almost 4-5 hours in the same reaction chamber. The chemistry of the two precursors, TDMAT and TDMAZ should not be as different as these results seem to suggest as the structure is quite the same. As ellipsometry relies on the optical differences between the fraction of light reflected and shot through the sample and since the procedure seems to affect the optical properties of the final zirconia coating, a different kind of characterization method seems to be required. Other research groups' studies on zirconia deposited on PMMA are really difficult to find as it does not seem a coating layer interesting for other purposes. This behavior at higher cycles, in which the optical indices seem to change, would require further investigation with different methodology.

The main difference with the $TiO_2$ results is that the growth was higher on PMMA while for $ZrO_2$ the growth seems to be higher on silicon. $TiO_2$ growth on the polymer seems to be twice the value on silicon. First of all, we can speculate about the accuracy of the ellipsometric model used: it is widely known that this technique has a limited accuracy for transparent substrate as the polymer we have used, because of the direction-dependent optical properties. We built a new model that resulted to be consistent within itself but it may work differently for the two oxides, as the two ceramics have different optical properties and behaviors. So, the model may work differently for the two materials and the titania one may present an offset in the measurement that would increase the values detected. In the literature, there are very few studies that observed different deposition rates for polymers and silicon, as the majority found really similar results, as we detected for zirconia. Observing that in the study by Wilson et al. the PMMA presented a very similar behavior to PE, the study by Ferguson et al. of 2004 can be considered interesting to try to

understand the dynamic of the depositions on polymer substrates (22, 41). The study focused on ALD deposition of alumina on Polyethylene particles (diameter 2 μm) from TMA and water precursors. The temperature of the reaction was 77°C and they used a vacuum apparatus to perform an in-situ Fourier Transform Infrared Spectroscopy (FTIR) to monitor the surface chemistry during initiation and growth of the oxide. Transmission electron microscopy (TEM) was also used to characterize the final layer. The interesting results for us is that the expected growth rate was 1.1 Å/cy while the obtained one was 3.3-4.5 Å/cy, which is three times the one expected and this behavior agrees with the results presented for titania growth on PMMA (41). They attributed this phenomenon to the presence of hydrogen bonded water on the $Al_2O_3$ surface that can react with $Al(CH_3)_3$ to deposit additional alumina by Chemical Vapor Deposition (CVD). The hydrogen bonded water was found by analyzing a scissor mode from the FTIR data. The growth of alumina in the CVD technique was confirmed to be 3.3 Å/cy (41). So, CVD can be responsible for increasing the deposition rate by 2 or 3 factors.

### 3.5 Results of mixed oxides coating mean growth rate on silicon

The structure the coating deposited on silicon resulted to be composed by silicon, silica, zirconia and then titania, or viceversa. We repeated this sequential deposition for three samples, changing only the number of cycles for both oxides. From these experiments in which the oxides were deposited on top of each other, we can see the correlation between the growth rate and the previous ALD cycle deposited, as reported in the studies presented before (19).

The percentage shown in Fig. 14 and 15 is the thickness percentage of zirconia in the total thickness of the layer. All the thickness data are obtained from the SE acquisitions as explained before. The first and the last bar show the mean growth rate of titania and zirconia respectively, as calculated before. The standard deviation is calculated for measurements within the same sample so it represents the uniformity of the value. The bars in between show the growth for mixed coatings as the percentage of $ZrO_2$ increases: when $ZrO_2$ is the first layer from the 60% of zirconia the growth is basically the one for only zirconia. On the other hand, when $TiO_2$ is the first layer

on silicon the growth for 57% ZrO2 is 0.5 A/cy, still closer to the titania one. This may suggest that ZrO2 growth is quite retarded on top of $TiO_2$ due to the presence of some incubation cycles that we mentioned before, that basically are needed by the surface to be activated with the desired functional group to allow the half reactions of ALD (18).

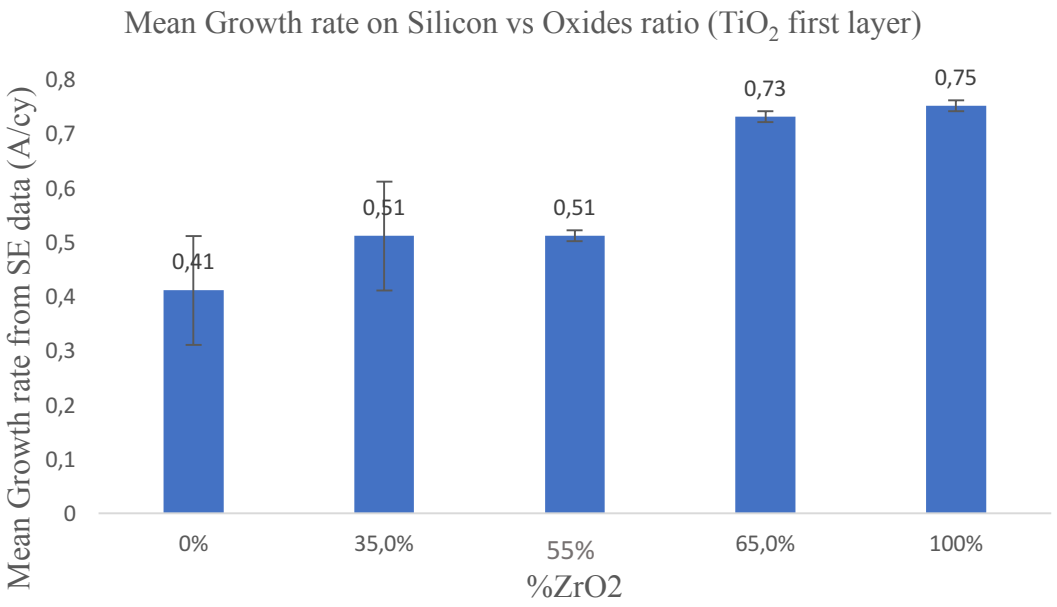


Figure 14: Mean Growth rate of mixed oxides coating on silicon at 120°C with respect to $ZrO_2$ percentage when $TiO_2$ is chosen as the first layer on the substrate (Same deposition conditions as Figure 8)

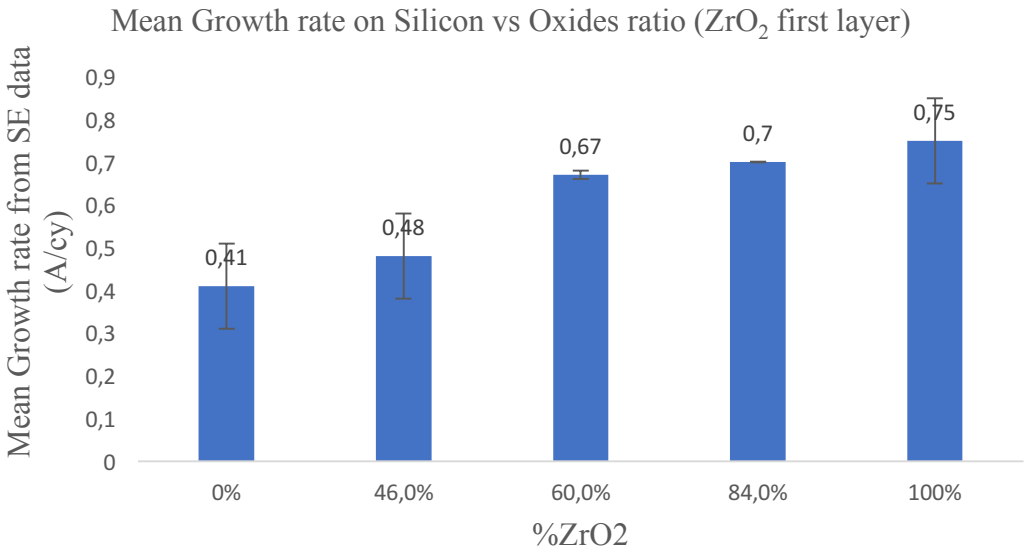


Figure 15: Mean Growth rate of mixed oxides coating on silicon at 120°C with respect to $ZrO_2$ percentage when $ZrO_2$ is chosen as the first layer on the substrate (Same deposition conditions as Fig. 8).

### 3.6 Results of mixed oxides coating mean growth rate on PMMA

The deposition process for the mixed $TiO_2$-$ZrO_2$ coating was described in section 2.9. The temperature of the deposition was changed to 100°C due to concerns about the degradation of the polymer, as it was explained previously. After the depositions, the samples were tested with the ellipsometer but, since ellipsometry with transparent substrates is not an accurate method to be used, due to backside reflections etc., and since the layers we have deposited are really thin, we acquired the thickness data pretending that the whole coating was either titania or zirconia. The model used was created by starting from a layer made of a Cauchy material, which is already present in the WVASE 32 software, with the optical parameters fitted on our samples before the depositions, and then adding the oxide layer on top, titania or zirconia, and by fitting the data for the thickness. Pretending that the whole layer on top of PMMA was $TiO_2$ or $ZrO_2$ produced really similar values. The thickness obtained is not so different from the expected total one, which was around 36nm.

In Figure 16 the growth rate of the mixed oxides coating on the polymer obtained from the ellipsometry data is displayed with respect to the $ZrO_2$ percentage of the total thickness of the coating. The standard deviation is calculated for measurements within the same sample so it represents the uniformity of the value. The values for the 16.7% of zirconia are the values obtained from the mixed layer (thickness ratio 5:1, expected total thickness around 36 nm, 6 supercycles) when fitted pretending the coating is only titania or only zirconia. By pretending the layer on top was titania or zirconia we obtained really similar values (40 nm) and both similar to the one expected, which was 36 nm.The first and the last bar are the linear approximation values for the growth rate of 100% $TiO_2$ and 100% $ZrO_2$, respectively. The mixed $TiO_2$-$ZrO_2$ coatings have a mean growth rate which is in between the two extreme values, as expected.

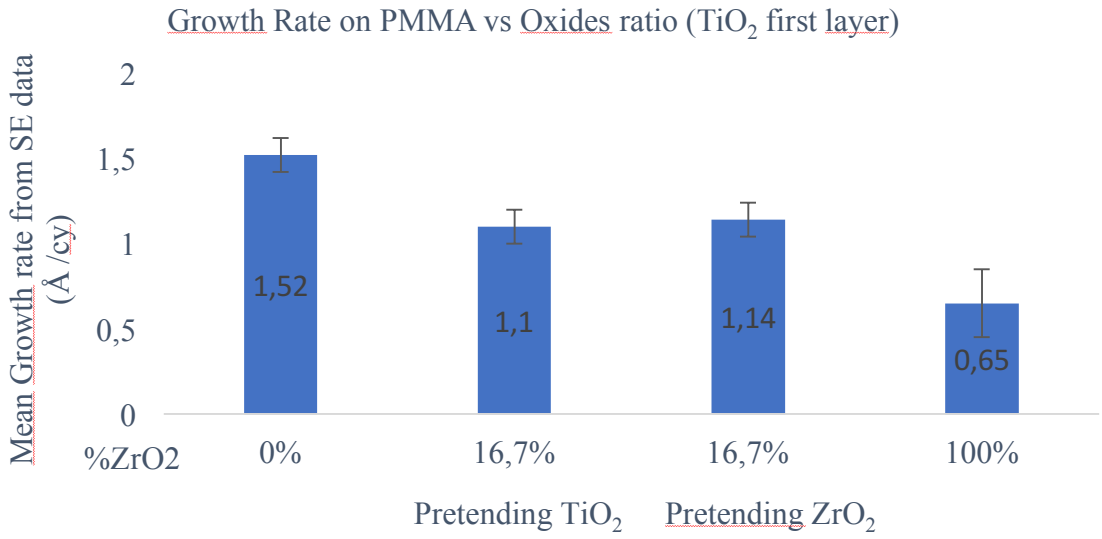


Figure 16: Growth rate of the mixed oxides layer deposited at 100°C on top of PMMA (16,7 % corresponds to 360 cycles and ratio 5:1 with expected total thickness 36 nm) as a function of the $ZrO_2$ percentage from SE data when $TiO_2$ is chosen as the first layer (Same pressure and pulse times as Figure 8)

## 3.7 Water Contact Angle results

The water contact angle was measured right after the ALD deposition by taking a picture of the sample after having deposited a 5 μl of DI water on top of the surface with a syringe. For each PMMA sample two pictures were taken and the mean WCA was calculated before and after the depositions. Some measurements were repeated after 15 days of water storage.

Figure 17 shows the WCA of the coated and non-coated PMMA samples before and after the ALD depositions. The standard deviation is calculated for measurements within the same sample so it represents the uniformity of the value. The angle after the depositions is always decreased meaning that the wettability increased so the substrate became more hydrophilic. Statistical analysis confirmed that there is a significant difference between the mean angle of the coated and not coated specimens ($p < 0.05$). Moreover, after 5-15 days of DI water storage, the WCA was measured again and the angle was not significantly different from the first one meaning that the surface seems to be quite stable after 15 days of water storage (Fig. 17). In addition to this, after the Polident treatment the substrate is still hydrophilic, as the angle is still 39°.

All the coated surfaces showed increased wettability: all the contact angles of the polymeric surfaces passed from 84°, before the deposition, to 25-35°, after the coating. Only the 25 cycles depositions show a higher angle, because the coating may be too thin to change the wettability. Same behavior was observed by Kemell et al. in 2008, who deposited alumina and titania at different conditions on PMMA at 100°C: the angle passed from 72° to 50° (21). Surface wettability depends on different parameters and between these both surface chemistry and roughness. The coating has changed the chemistry of the surface of the polymer, as ceramics like titania and zirconia have a higher surface wettability than PMMA (50, 51). The coating could have also changed the surface roughness, as rough surfaces usually show higher hydrophobicity than less rough surfaces of the same material (21) but this point will be examined in depth in the AFM test section.

Hydrophilic substrates are usually more desired for different reasons in the biomedical field among which there is also lower bacterial attachment. One study from Azuma et al. in 2012 confirmed that by increasing the hydrophilicity of the surface the bacterial adherence decreases. The coated denture base substrates with silica and tested the adherence of the bacteria C. Albicans (52).

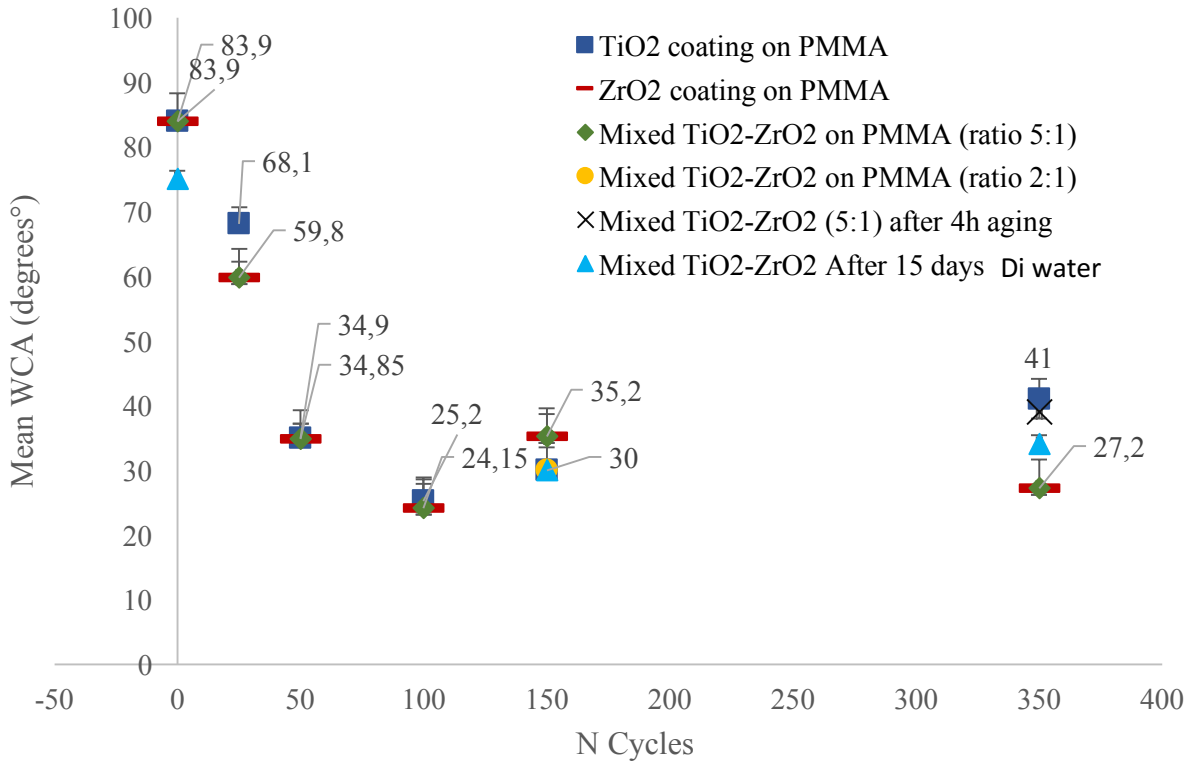


Figure 17: Mean contact angle and standard deviation before (0 cycles, which is the control PMMA not coated) and after the depositions of $TiO_2$, $ZrO_2$, and mixed $TiO_2$-$ZrO_2$ films on PMMA at different cycles, before and after Polident treatment (4h) and after 15 days of DI water storage. The PMMA coated with single oxides were deposited at 120°C while the Mixed coated PMMA were deposited at 100°C (Same pressure and pulse times of Figure 8). All the measurements were made right after the deposition if not differently specified. The standard deviation is meant for the measurements of the same sample, so it indicates the uniformity for the samples.

Same measurements were performed in our laboratory for 30nm-$TiO_2$ coated PMMA samples. The coating was performed with a different system, a custom-made ALD reactor, the

temperature of the depositions was 90°C and the precursors were different: TDEAT and ozone (46). WCA values were different: not coated sample showed a 67° angle and the coated one showed a 5° angle (46). Both the values for the not coated and coated samples were different. The conditions were very similar, apart from the deposition temperature which was 30°C less. Because of the difference also in the not coated PMMA we can hypothesize that the substrate itself might present some changes: polymers are not very reproducible and the properties may change a lot with respect to minor changes in the chemistry. Water contact angle is known to be very sensitive to surface chemistry and roughness (31). With respect to the powder/liquid ratio used and the curing conditions the degree of polymerization inside the polymer may change: the hydrocarbon chains may result in different lengths. Moreover, the degree of polishing plays an important in determining the roughness level of the sample: as the samples are polished manually and they came from College of Dentistry also the operator related conditions may play a role in these differences. In addition to this, the contact angle measurements have to be considered by taking into account that they are highly affected by surface finish and impurities, both in the liquid and in the solid surface (31). The individual set of conditions mentioned may all play a role in determining those differences for the same materials tested.

### 3.8 Thermogravimetric analysis results

The TGA scan obtained from the test is shown in Figure 18. It can be observed that almost no weight loss occurred till temperature reaches ≈ 110-120°C. After this temperature, a decrease in weight was observed, and at ≈ 200-250°C the final degradation seemed to happen fast. PMMA was confirmed not to be thermally stable in the range tested because a mass change was detected. It is clearly evident that at 120°C, which coincides with our deposition temperature, evaporation of the polymer seems to happen, leading to the weight loss detected by the TGA system (green line in Fig. 18).

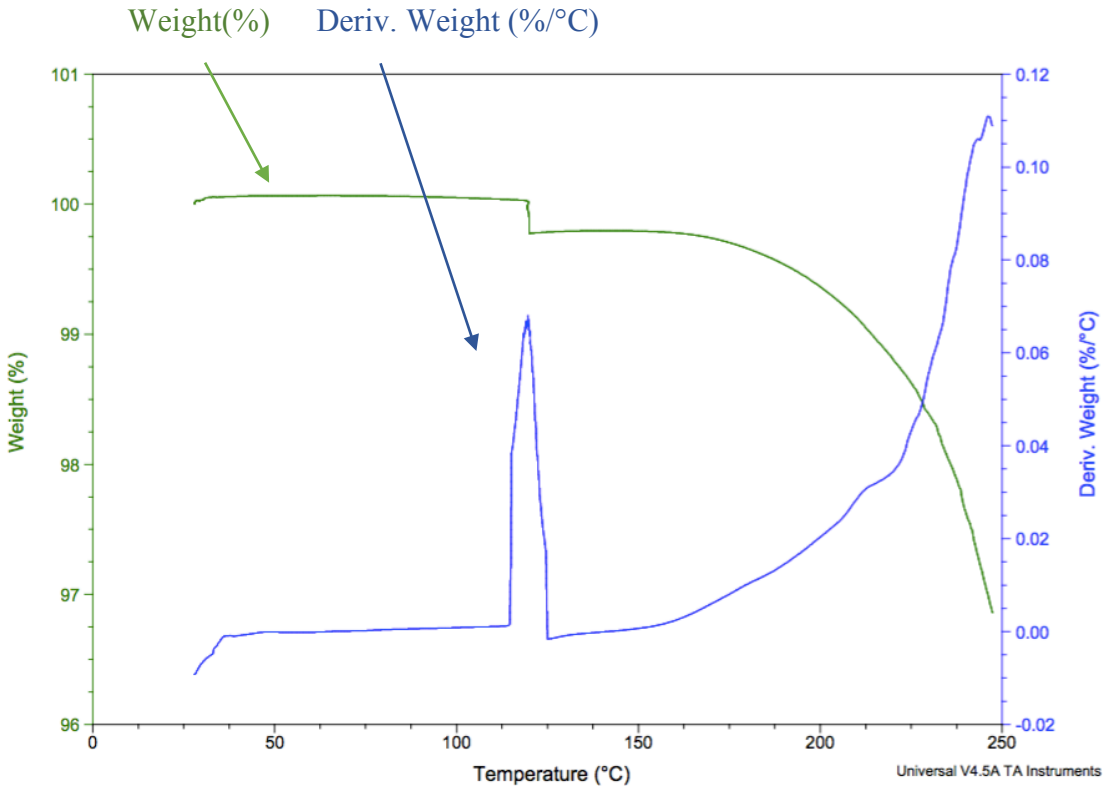


Figure 18: Thermogravimetric curve of not coated PMMA between 25°C and 250°C in Nitrogen atmosphere. The green curve represents the weight percentage while the blue curve represents the weight derivative: when the slope of the derivative changes, the weight varies.

The blue line represents the weight derivative: it has a peak around 120°C meaning that at this temperature the slope of the derivative changes and the weight varies.

This confirms the hypothesis proposed previously that at high deposition temperatures, as the one we used to coat PMMA by ALD, the polymer substrates undergo evaporation and weight loss of the volatile elements. These species may be involved in the higher oxide growth rate detected at 120°C both on PMMA and on silicon while it is in the same reaction chamber of the polymer, mentioned in section 3.4.2. The degradation may be attributed to the existence of vinyl end groups in the PMMA chains that have really low stability and manage to unfold the polymer chains radically through a chain transfer process (15). Compared to the polymer chains, the end groups show weaker bonding and start to decompose at lower temperature with respect to the melting point (15).

### 3.9 X-ray Photoelectron Spectroscopy results

For the $ZrO_2$ coated samples three specimens were tested: one PMMA not coated, one PMMA coated with 10nm $ZrO_2$ treated for 4 hours after 2 weeks of DI water storage and one PMMA coated with 10nm $ZrO_2$ after 2 weeks of DI water storage. The comparison of the XPS spectra is displayed in Figure 19.

From the XPS spectra of all the $ZrO_2$ coated sample you can see Carbon and Oxygen peaks, which were expected as the substrate is a polymer. There is a clear Zirconium peak detected in all the coated samples, also in the sample that was treated for 4 hours. The expected Zirconium-3d peak, which was detected in the HR spectrum, is displayed below (Fig. 20). The Zirconium 3d peak was detected around 180-186 eV, as literature confirms (Fig. 22) (53). Titanium though, is not detectable in any of the non-coated specimens tested even if in the composition of Lucitone 199 (Dentsply Sirona Pty Ltd) $TiO_2$ is incorporated to strengthen the material (weight %<0,05). A 7 nm $TiO_2$ coated PMMA sample was also tested with XPS and the high-resolution scan we did around the titanium binding energy clarified the chemical binding state of Titanium peak that resulted in almost only Ti-2p (464-458 eV) (Fig. 21), which coincides with the peaks found in literature around 459 eV (54). This confirms that the film produced is fully oxidized.

Also, the PMMA samples are not homogeneously formed, as some non-coated samples (Fig. 19-23) had Calcium in it but others, non-coated samples had no Calcium peak for 350 eV. So, we can conclude that the composition of the polymer is not constant and repetitive.

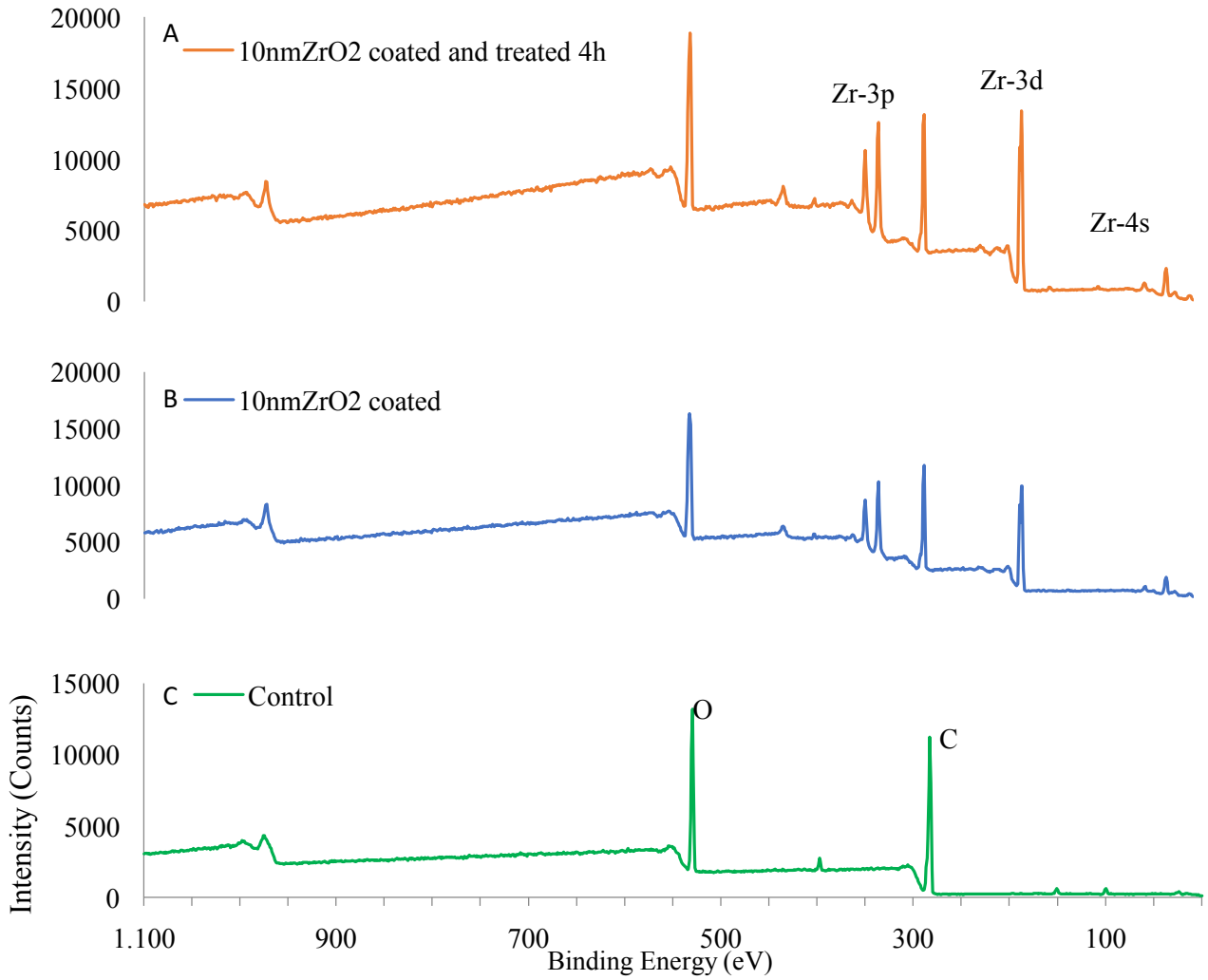


Figure 19: XPS spectra comparison of 3 PMMA samples: (C) one PMMA not coated (control), (A) one PMMA (1mm) coated with 10nm (100 cycles) $ZrO_2$ treated for 4 hours after 2 weeks of DI water storage, (B) one PMMA (1mm) coated with 10nm (100 cycles) $ZrO_2$ after 2 weeks of DI water storage (Same pressure and pulses of Figure 8). The treatment consists in 4 hours of sonication in Polident solution.

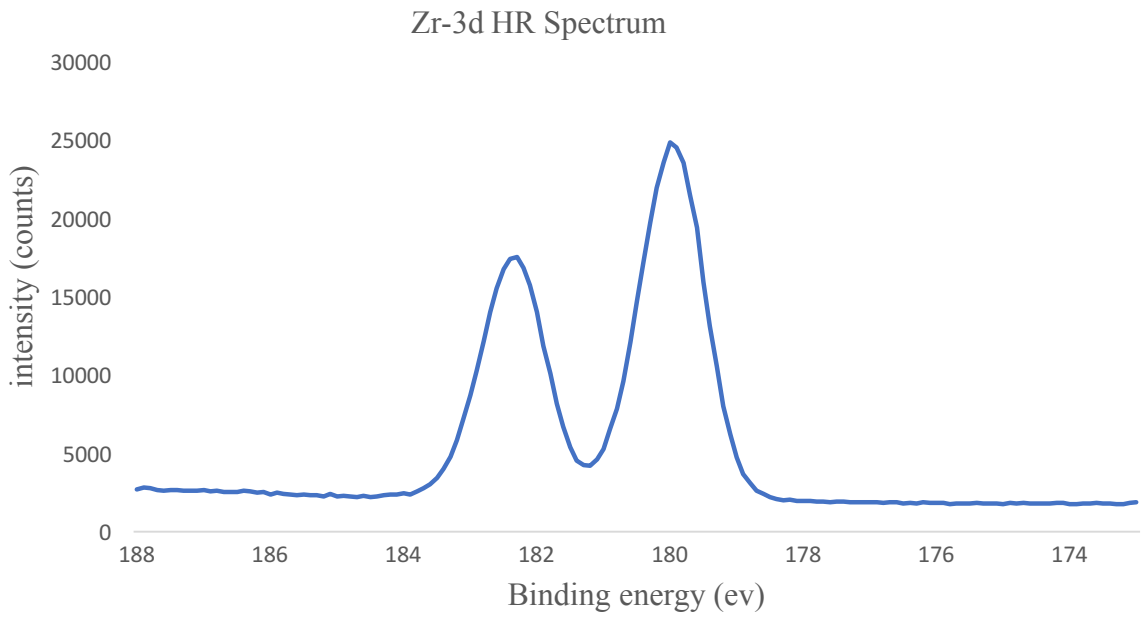


Figure 20: XPS High resolution spectrum result of Zr-3d peak from the scan of the $ZrO_2$ (10 nm) coated PMMA (1 mm) after 4 hours of Polident sonication and DI water storage for 3 months deposited at 120°C (100 cycles)

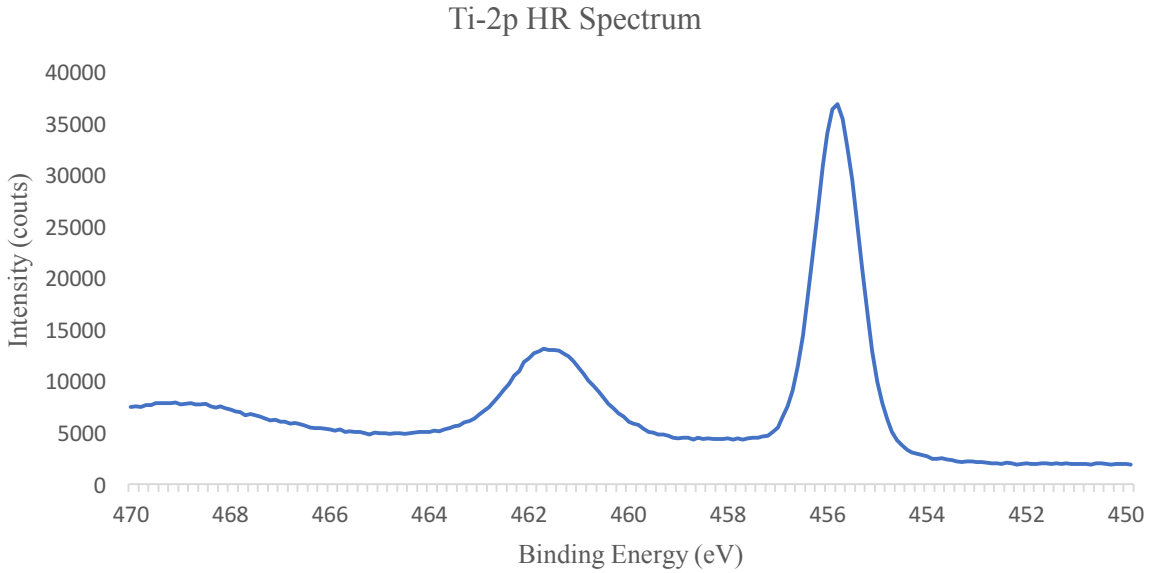


Figure 21: XPS High resolution spectrum result of Ti-2p peak from the scan of the 7 nm-$TiO_2$ coated PMMA (1 mm) at 120°C (Same sample as Figure 19)

As conventional XPS on the mixed $TiO_2$-$ZrO_2$ coated samples (ratio 5:1) showed only Ti peaks and no Zr peaks (Fig. 23) we tried to tilt the stage of the samples holder so that the X-ray

beam would have more surface to analyze, in order to increase the surface of $ZrO_2$ on top of the sample (1nm layer) detected by the system. The total amount the X-ray beam can detect should be around 2 nm that may be too low to be detected as the Zr-3d peaks overlaps with the Calcium peak at about 350 eV. We tried to tilt from 0° to 60°. We tried one control sample not coated and two mixed coated PMMA (ratio 5:1, total thickness around 40nm), one treated for 4 hours and one not treated. The same results were obtained: Ti peaks are strong and clear but the Zr peaks are not easily detectable (Fig. 23). Moreover, the spectra of the non treated and treated samples are completely superimposable.

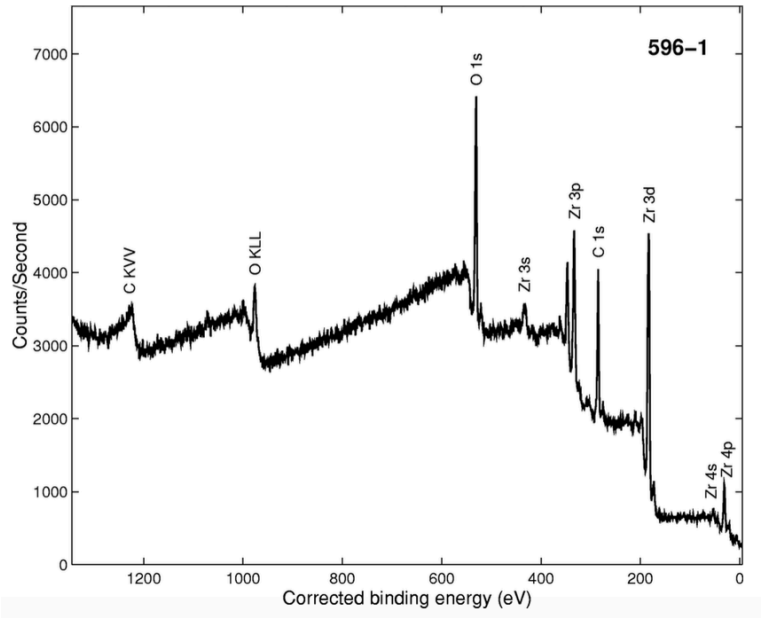


Figure 22: $ZrO_2$ XPS survey of a thin zirconia film (580nm) deposited by CVD on soda-lime glass substrate (55)

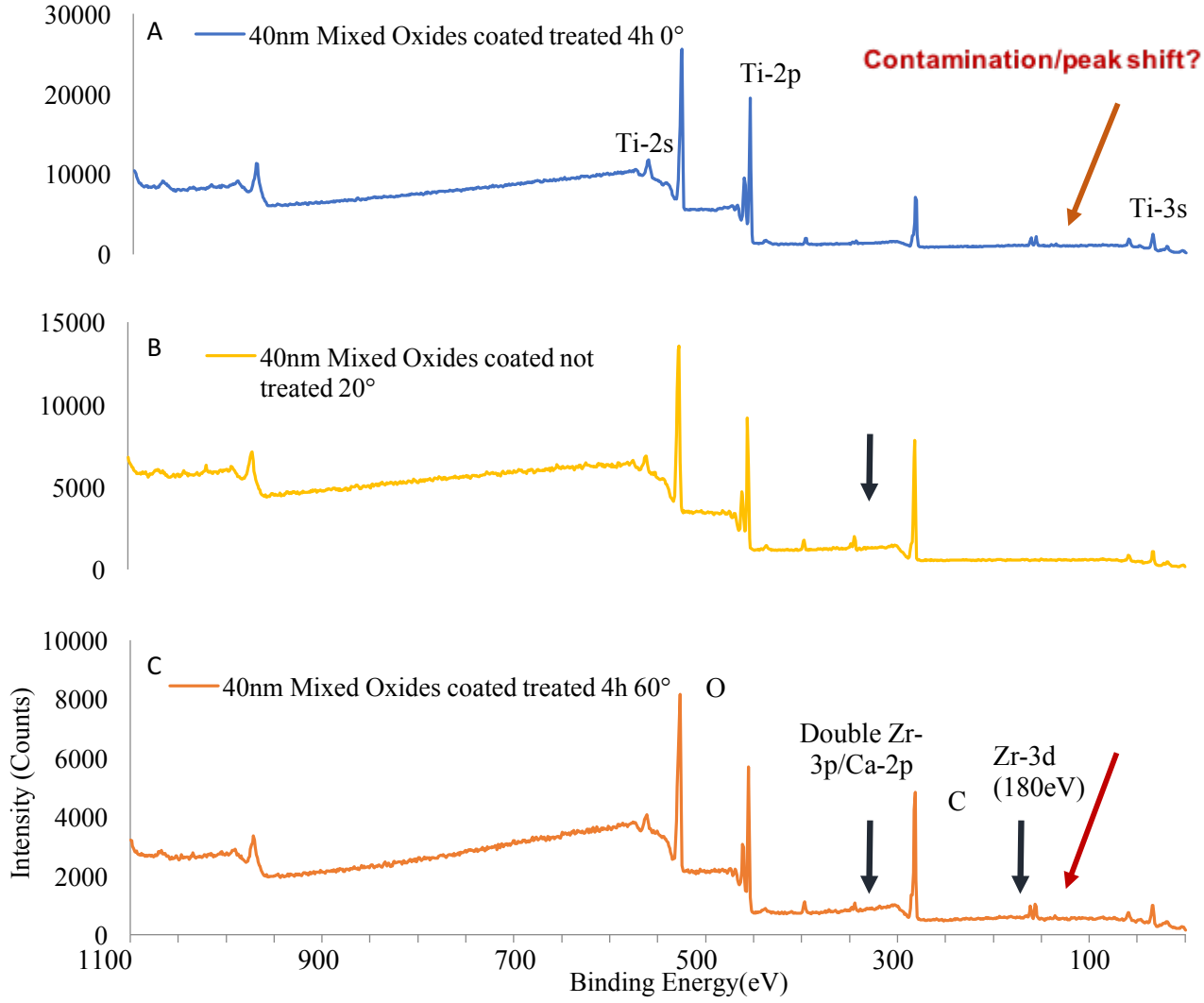


Figure 23: XPS spectra result of mixed $TiO_2$-$ZrO_2$ coated (around 40 nm, ratio 5:1, 6 supercycles, 360 cycles) PMMA (1 mm) after 1 month of DI water storage deposited at 100°C tilted at 0°(A) 20°(B) and 60°(C) (Same pressure and pulses of Figure 8). Sample A and C were treated: the treatment consists in 4 hours of sonication in Polident solution.

Zr peak is still not clearly detectable: in the tilted XPS spectra in Fig. 23 Zr-3s and Zr-3p, overlapped with Ca at 350 eV, are weakly present. The Zr-3d peak, which is supposed to be at around 180 eV (Fig. 22) is still not detectable. The new peak seen in the tilted spectra is around 160-170 eV but Zr-3d is supposed to be at 180 eV. We can attribute the new peak at 160-170 eV to some kind of contamination in the sample or to some sort of peak shift. In fact, the reference

peaks refer usually to pure elements while in our case Zr, being bonded to different species, may be treated as a composite, that is one of the reason peak shifts can happen.

In Figure 24 the ratio of the mixed $TiO_2$ –$ZrO_2$ coating was increased to 2:1: sequentially, 70 cycles of $TiO_2$ (around 10nm) and 70 cycles of $ZrO_2$ (around 5 nm) were performed.

In the spectrum, the Zr peaks are very clear and detectable but the Ti peak is missing. This may result from the high uniformity of the top $ZrO_2$ layer, that manages to shadow the Ti signal underneath.

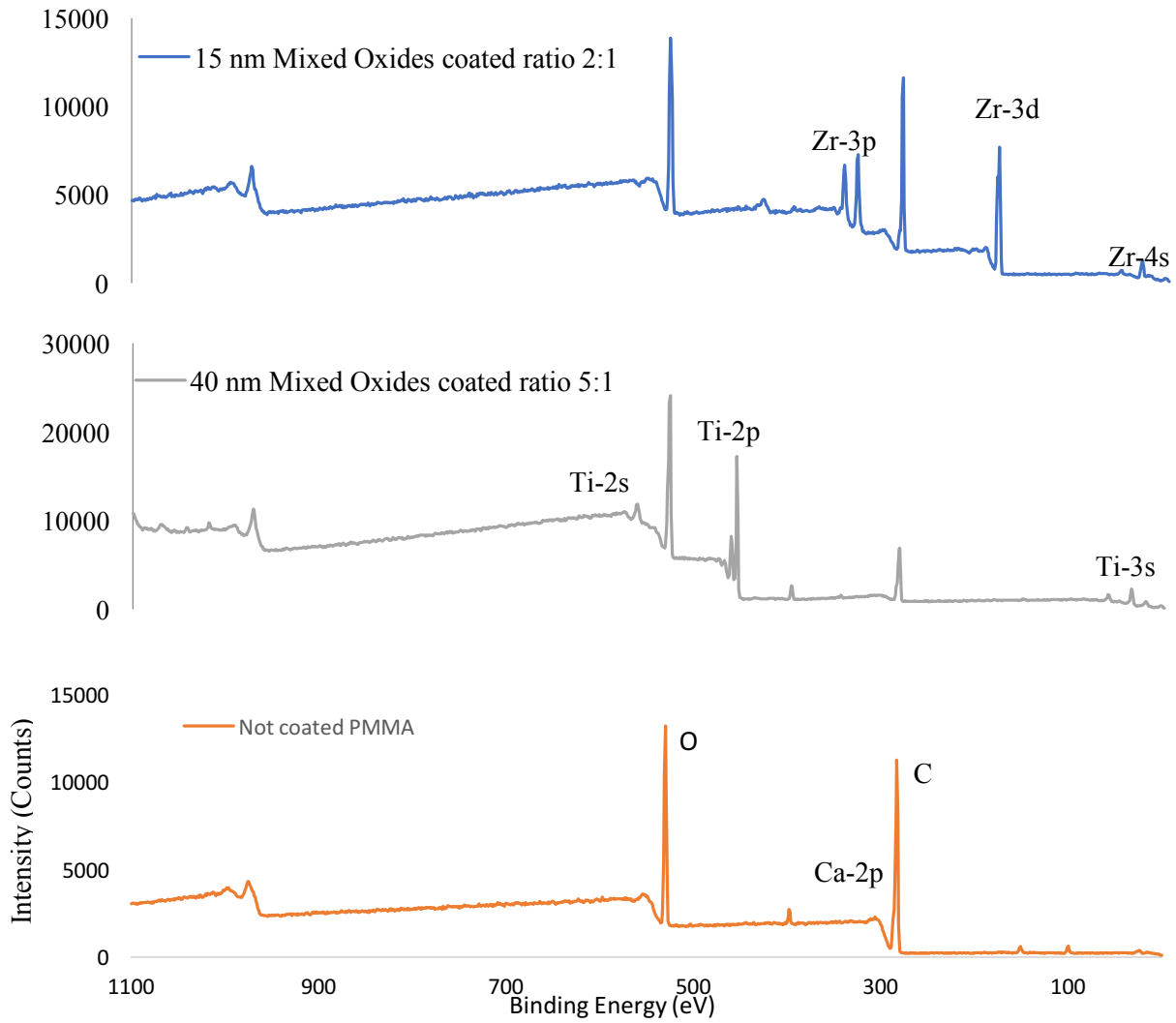


Figure 24: XPS spectra comparison of (A) mixed $TiO_2$-$ZrO_2$ coated (around 40 nm, ratio 5:1, 6 supercycles, 360 cycles) PMMA (1 mm) after DI water storage for 1 month deposited at 100°C and (B) mixed $TiO_2$-$ZrO_2$ coated (around 15nm, ratio 2:1, 2 supercycles, 140 cycles) PMMA (1

mm) deposited at 100°C (Same deposition conditions as Figure 8) and (C) not coated PMMA as a control.

In conclusion, XPS results suggest that the treatment does not affect the ceramic coating layer on top of the polymer, because the ceramics are still on top after the sonication and so the nanometric coating manages to improve the surface wearing resistance to both physical and chemical attack. In fact, ALD is supposed to provide both a physical and chemical attachment between PMMA and the deposited layer.

The presence of separately deposited $TiO_2$ and $ZrO_2$ on PMMA was proved by the XPS spectra and also the presence of $TiO_2$ in the mixed coated samples. $ZrO_2$ on top of $TiO_2$ layers was detected only for higher ratio: in the mixed coated samples with ratio 5:1 Zr was not clearly present, probably due to the small percentage present in the coated samples.

### 3.10 Scanning Electron Microscopy results

Three samples were tested with SEM technique: one PMMA coated with mixed $TiO_2$ – $ZrO_2$ layer (ratio 5:1, approximately 40 nm thick), one PMMA coated with approximately 30nm of $ZrO_2$ and one PMMA coated with approximately 40nm of $TiO_2$. EDS mapping was performed on all the cross sections of the three samples. The electron beam energy was set to 10 kV and the magnification was 80-90. The working distance was set to 15mm.

#### 3.10.1 Scanning Electron Microscopy of separate oxides

From Figure 25 and 26 you can see the chemical composition of the cross section of the ALD coated $TiO_2$-PMMA sample (thickness of coating around 40nm, 500 cycles) and $ZrO_2$-PMMA sample (thickness of coating around 30nm, 350 cycles). As XPS data also confirmed, C, O and Ti are present in the sample and from these data we obtain the presence of the elements also in the cross-section (XPS was performed on the top surface).

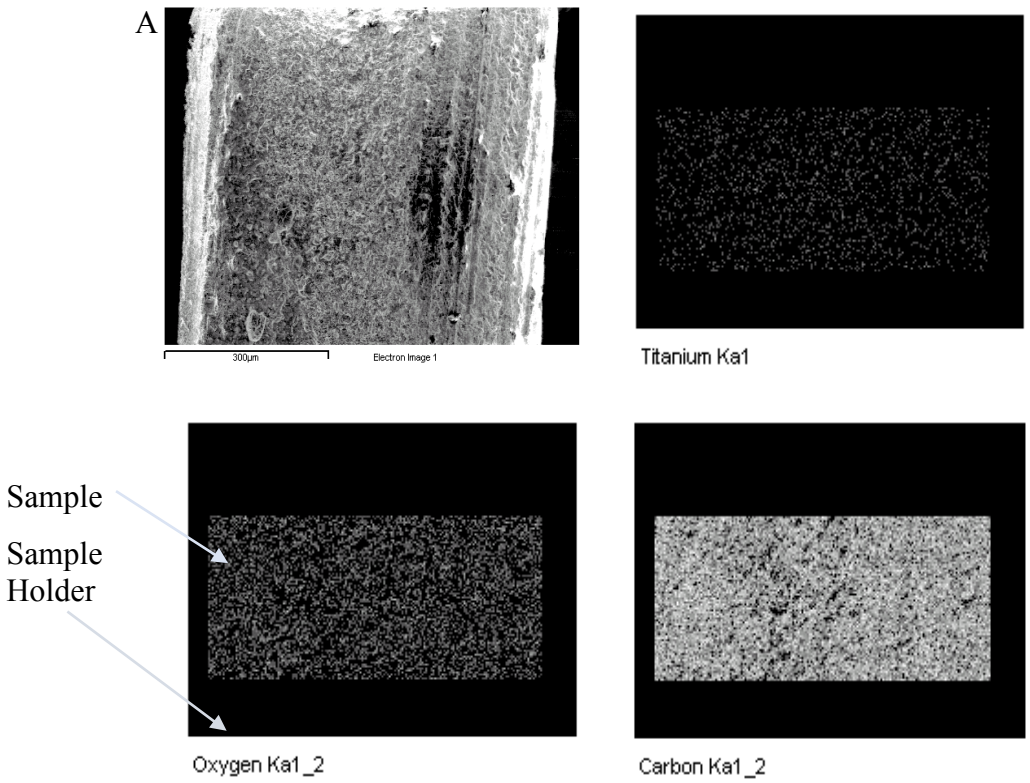


Figure 25: Cross-section SEM image (A) and EDS mapping of the Ti, C, and O element distribution of ALD coated (40 nm, 500 cycles) $TiO_2$ -PMMA sample at 100°C (Same deposition conditions as Figure 8)

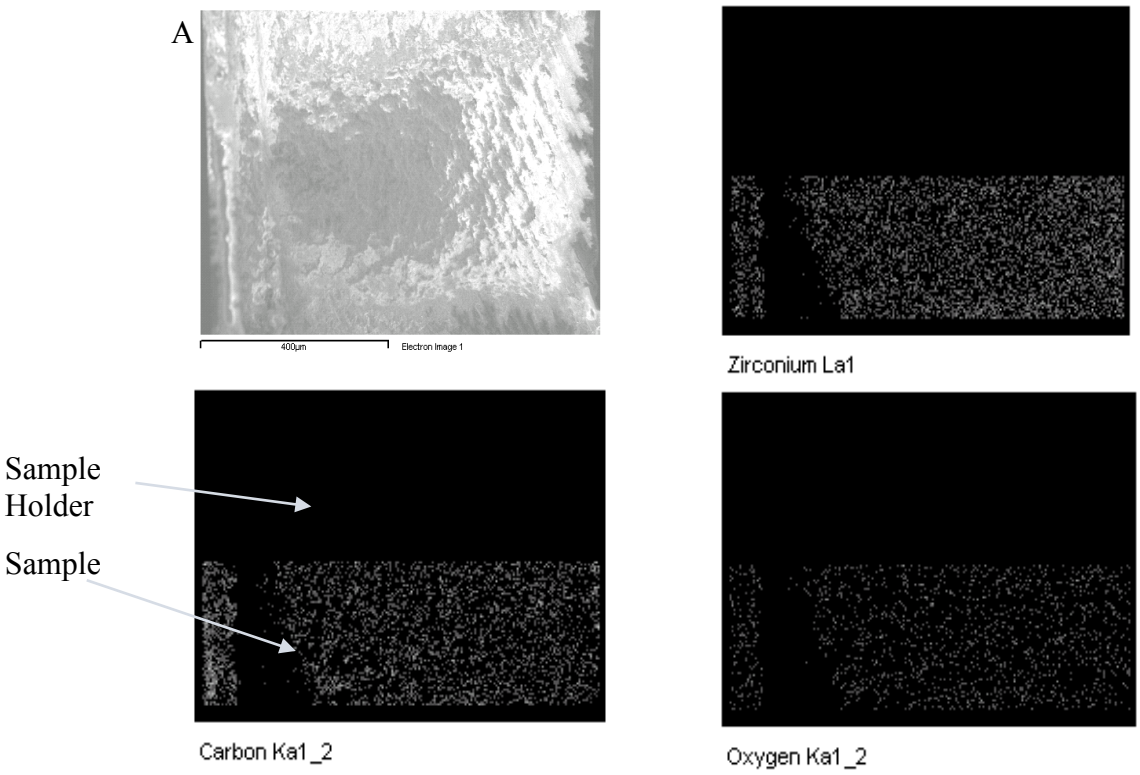


Figure 26: Cross-section SEM image (A) and EDS mapping of the Zr, C and O element distribution of ALD coated (around 30 nm) $ZrO_2$ -PMMA sample at 120°C (350 cycles with deposition conditions same as Figure 8)

Titanium and Zirconium look to be very uniform in the sample, and not just present at the surface layer, where the coating is supposed to be, but also at the bottom of the sample. C and O are uniformly distributed too, as expected as they form the bulk material.

In conclusion both Ti and Zr are uniformly distributed through all the thickness of the PMMA sample. This can be a proof that the ALD deposition can reach the bottom of the PMMA because TiO2 is added in small amounts during PMMA forming but there is no trace of Zr in PMMA composition (Lucitone 199 by Dentsply). Due to the high conformality of ALD and the high porosity of the polymer the precursor might be able to reach the bottom of the sample thanks to the high absorption rate that usually happens during the ALD depositions of oxides onto polymers (22).

### 3.10.2 Scanning Electron Microscopy of mixed oxides

From Figure 27 you can see the chemical composition of the cross section of the ALD coated mixed $TiO_2$ –$ZrO_2$ PMMA sample (thickness of coating around 40nm, ratio 5:1). From the EDS mapping Titanium is shown to be very uniform in the sample as in the other samples coated with titania presented before in Fig. 25. Zr is not present in the spectrum even if it was deposited together with TiO2 layers: the absence of Zr peak was detected also in the XPS analysis of the same samples. We speculate that the 1nm thickness of the Zr layer is too thin and provides too few counts to be detected with certainty.

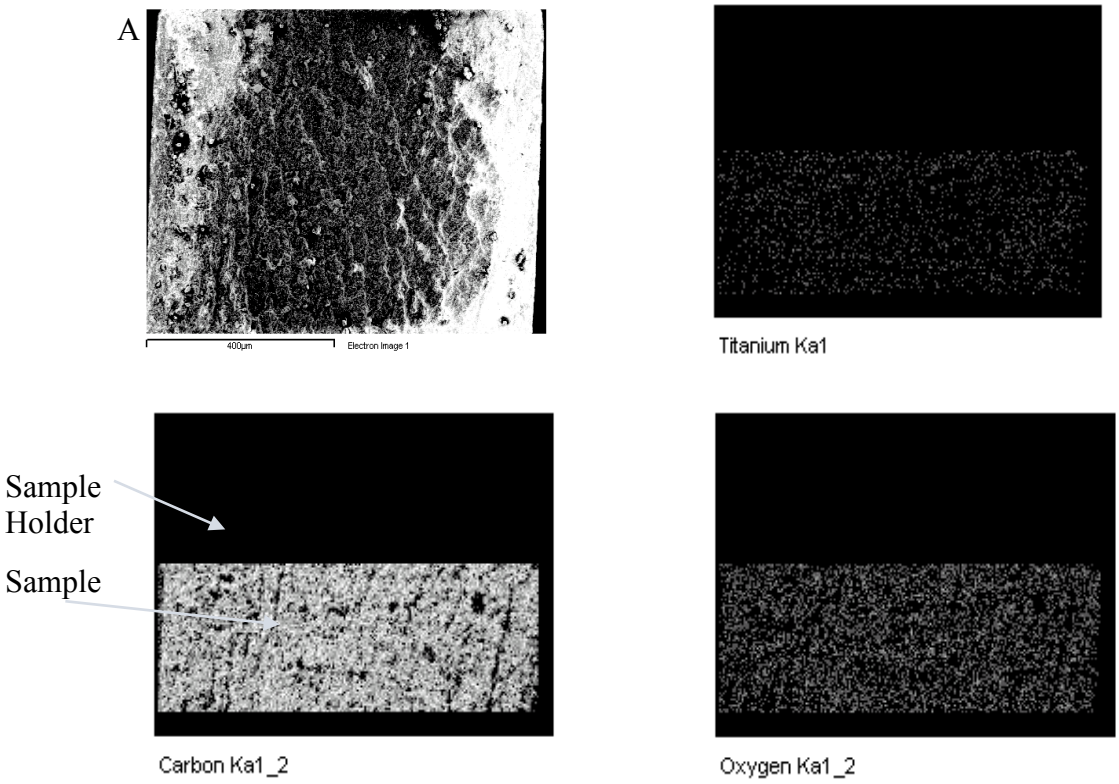


Figure 27: Cross-section SEM image (A) and EDS mapping of Ti, C, and O distribution of ALD coated mixed $TiO_2$ –$ZrO_2$ PMMA sample (ratio 5:1, coated at 100°C with 360 cycles and 6 supercycles with the conditions of Figure 8)

### 3.11 Atomic Force Microscopy results

Figures 28, 29 and 30 are presented in a three-dimensional representation (the brighter the color, the higher the spot). The morphology does not seem to be significantly changed by the coating, although XPS and SEM results show indeed the presence of the ceramic on top of the polymer and throughout the bulk. Since ALD is a conformal technique, meaning that all the active sites of the surface would be saturated by the precursors, it covers all the peaks and troughs of the surface following the morphology of the sample. The root mean square roughness value passed from 45± 0.7nm to 28± 4nm in the best case. The change is not even in the micrometer range which was expected, as ALD is a conformal technique and it covers all the peaks and troughs present on the surface to coat.

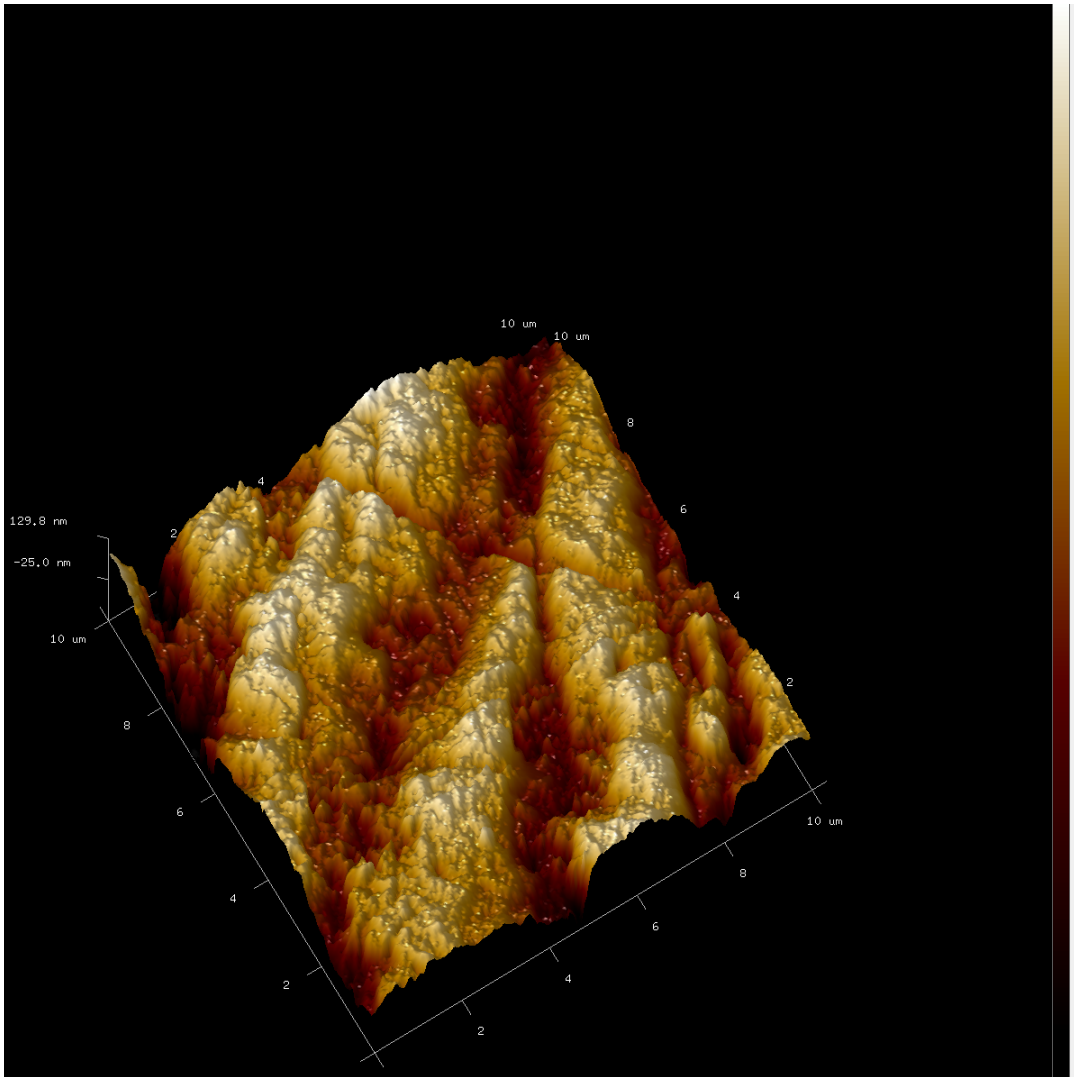


Figure 28: AFM three-dimensional image of the surface morphology of a not coated PMMA sample (spot dimension 10μm x 10μm)

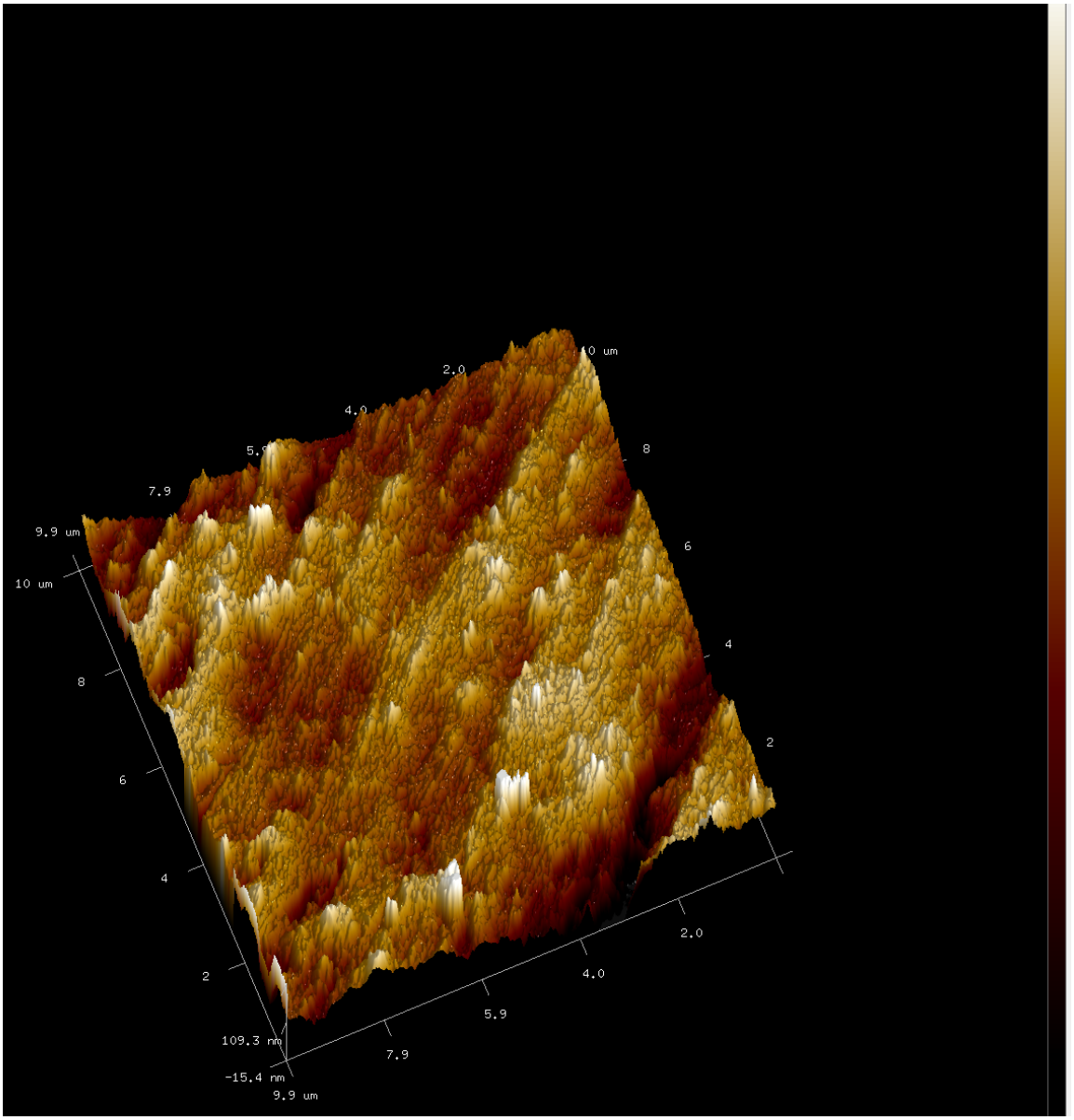


Figure 29: AFM three-dimensional image of the surface morphology of a mixed $TiO_2$ –$ZrO_2$ coated PMMA sample deposited at 100°C (ratio 5:1, around 40 nm, 360 cycles, 6 supercycles), at same conditions as Figure 8 (spot dimension 10μm x 10μm)

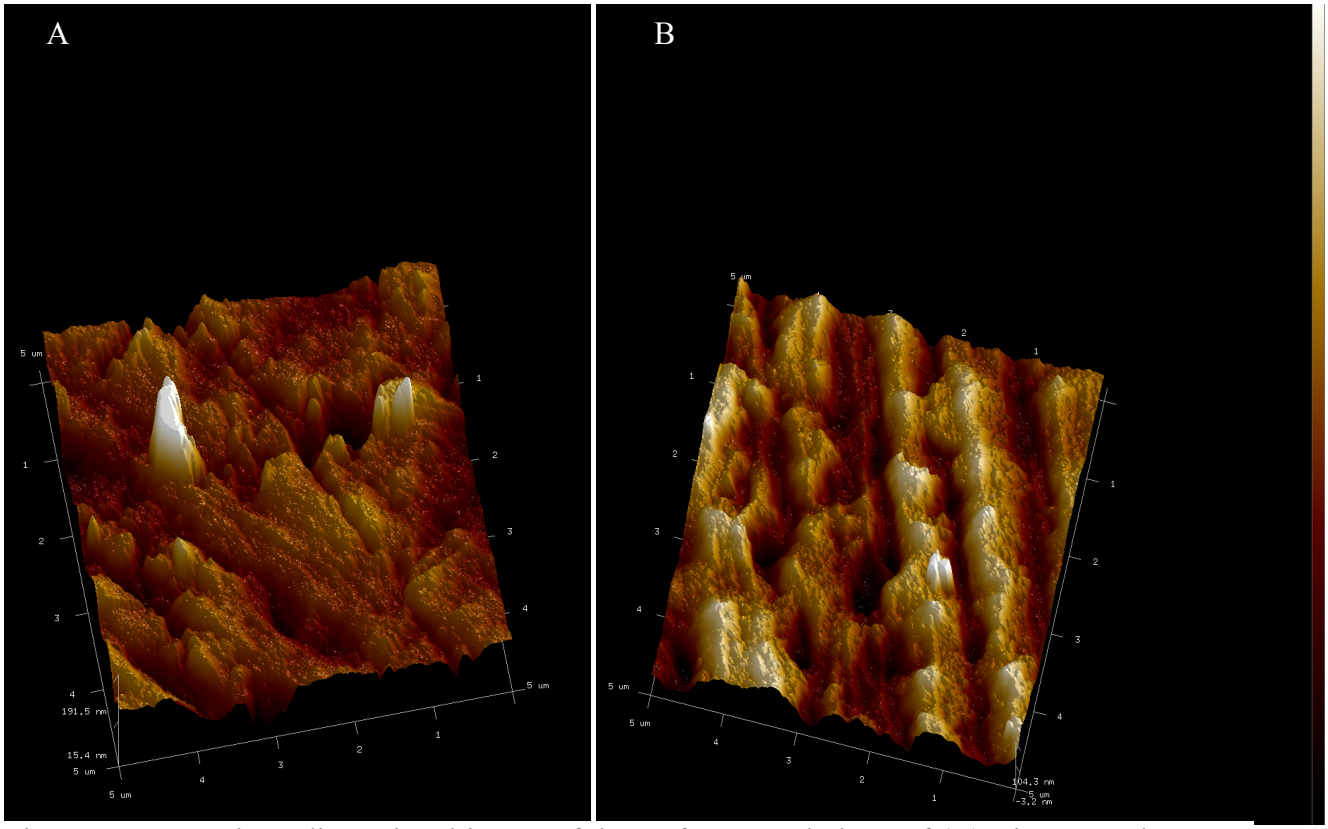


Figure 30: AFM three-dimensional image of the surface morphology of (A) $TiO_2$ coated PMMA deposited at 100°C with 350 cycles and (B) $ZrO_2$ coated PMMA at 100°C with 400 cycles at same conditions as Figure 8 (spot dimension 5µm x 5µm)

## 3.12 Microhardness test results

Surface hardness, being the ability to resist plastic deformation, is another important property to be increased in a dental material that would be helpful in facilitating polishing and in providing resistance to damage during cleaning of prosthesis, so the coated PMMA samples were tested to detect any improvement of surface hardness (36).

Microhardness test was performed using a LECO M-400 Hardness Tester and all the details of the testing method were explained in section 2.2.7.

Three samples coated with one oxide were tested: one not coated PMMA sample, one PMMA sample coated with 400 cycles of $TiO_2$ (thickness of films around 30 nm) and one PMMA coated with 150 cycles of $ZrO_2$ (around 10 nm thickness). In addition, two PMMA samples coated

with the mixed $TiO_2$-$ZrO_2$ layer (ratio 5:1, expected thickness 40nm, 6 superycles) at 100°C by ALD, one not treated and one sonicated for 4 hours in Polident solution were tested too. The standard deviation represents the uniformity in the samples, as it is calculated for the measurements obtained with the same samples.

As you can see from Fig. 31, the non-coated polymer has the lowest hardness, that increases as the coating becomes thicker. A statistic t-student test was performed on the data and the results show that there is a significant difference for $p<0,05$ between the average values of the hardness of the not coated and all the coated samples (blue lines in Fig. 31). This means that there is a probability of <5% that the difference between the hardness values of the non-coated and the coated, either with $TiO_2$ or $ZrO_2$, is not due to occurrence. In addition, there is a statistical difference also between the average values of the hardness of the 150cy $ZrO_2$ coated sample and the thicker coatings of $TiO_2$ and $ZrO_2$. This may suggest that the thickness of the ceramic layer plays a role in enhancing the hardness property of the substrate. On the other hand, there is no significant difference between the hardness of the thicker coatings (400 cy of $TiO_2$ and $ZrO_2$). The thick ceramic layer, around 30-40 nm, seems to follow the same behavior for the two different oxides. Moreover, there is no statistical difference between the treated and not treated specimens, as expected.

In the study by Mathew M. et al. of 2014 they tried to increase PMMA surface hardness by reinforcing it with Silane treated E glass fiber varying the weight percentage and aspect ratio of glass fiber (37). The control samples were around 19.9 VH while the sample with the highest percentage of glass fibers was around 33 VH (37). With the 35-40 nm ceramic coating we managed to obtain the same increase of around 13-14 VH the group of Mathew M. obtained with the highest ratio of incorporated glass fibers.

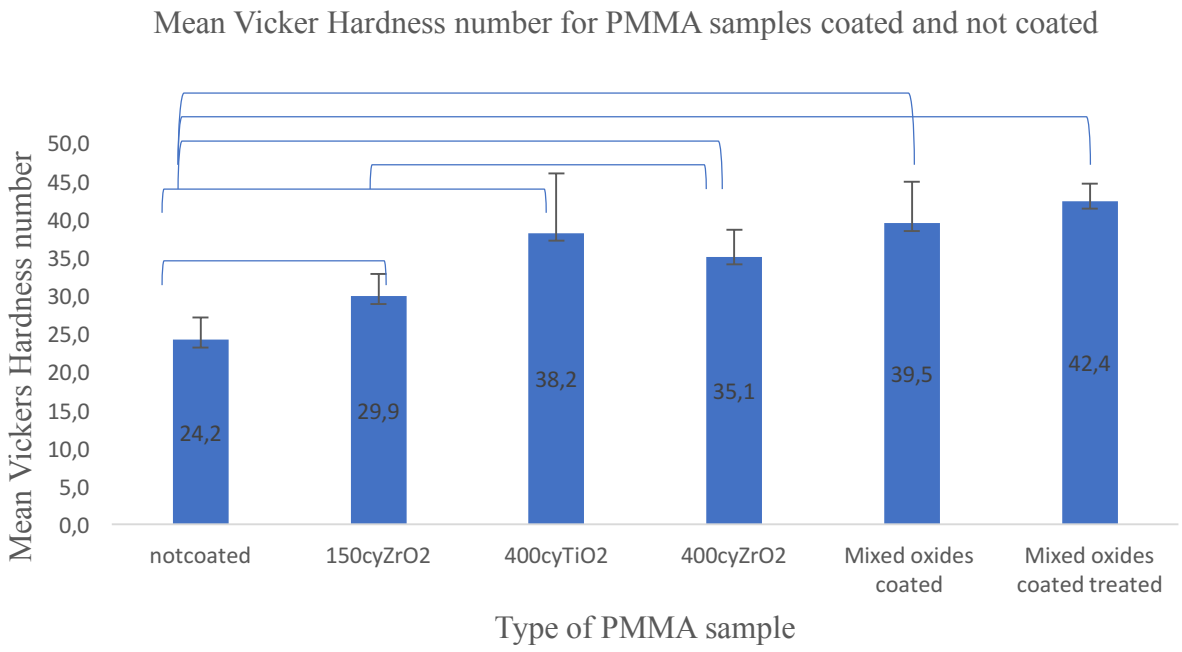


Figure 31: Mean Vickers hardness number and standard deviations of the PMMA samples not coated and coated with different thicknesses of zirconia and titania layers (150 cy $ZrO_2$ at 120°C ~9nm, 400cy$TiO_2$ at 120°C ~35nm, 400cy$ZrO_2$ at 120°C ~30nm, 360cy mixed $TiO_2$ –$ZrO_2$ at 100°C ~40nm with ratio 5:1 with $TiO_2$ first layer). The treatment mentioned consists in 4 hours of sonication in Polident solution. Blue lines represent the statistical difference between the group of samples.

Glass fibers are a good way to increase some mechanical properties of polymers but the most dangerous drawback is that they tend to make the composite brittle, which is not a good characteristic for dental and more in general, biomedical application.

Titania and Zirconia being two ceramics are proven to be harder than the polymer and, even if they are nano-thin films, they manage to increase the surface hardness of the material of the 60%, considering the 30nm thick coatings. Surface hardness increases should provide resistance to scratches in the harsh oral environment during brushing or chewing avoiding, an increase in surface roughness and loss of material that will lead to more plaque accumulation and

bacteria adhesion. In conclusion, the coating should be able to increase PMMA durability and stability in the oral environment.

The increase of surface hydrophilicity and surface hardness should provide less cell and bacterial attachment.

A 30nm deposition takes about 3 hours, in which PMMA is exposed to such high temperatures as 100°C-120°C: polymers are very sensitive to temperature, which may cause changes in the chemical structure of the plastics, as for example change in the chain structure, and in the side groups, leading to an increase of the cross-linking level (44). In literature, few studies tested non-coated PMMA samples hardness after 3 hours at 85°C: the results were consistent and agreed that the change in hardness was about 13%-14.5% for the three hours heating (44, 45). Such high hardness increase of 60% was not detected even for long heating cycles so one can conclude that the ceramic coating might effectively increase the surface hardness of the polymer, with better result than just heating the substrate for hours.

### 3.13 Three-point bending test results

Since previous studies confirmed that 30nm $TiO_2$ ALD coated PMMA retains the flexural properties of the bulk material, we tested 25 nm $ZrO_2$ and 40 nm mixed $TiO_2$-$ZrO_2$ coated PMMA samples (46). The values of PMMA flexural strengths are displayed in Figure 32. The standard deviation is calculated between the values obtained for the eight samples tested for each group.

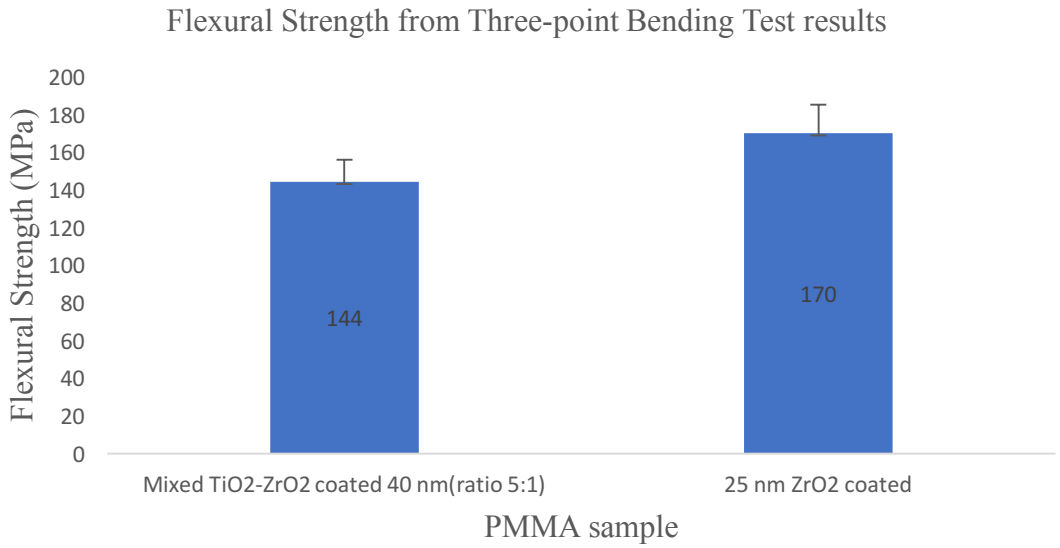


Figure 32: Mean flexural strength of $ZrO_2$ coated (25nm, 350 cycles) PMMA(1mm) and Mixed $TiO_2$-$ZrO_2$ coated (40nm, ratio 5:1, 360 cycles and 6 supercycles) PMMA at 100°C (Same pressure and pulse times of Figure 8)

The values are consistent with the results of the study by Arioli Filho J.N. et al. in 2011, who tested 15 samples of the same type of PMMA (Lucitone 199) non-treated with a three-point bending test (39). He used the same conditions of load and crosshead speed. The mean flexural strength of untreated PMMA was 156.05 MPa, which is consistent with the results presented in Fig. 32 (39).

These results can be used to prove that the nanoceramic coating does not seem to change the bulk mechanical properties of the bulk material in a significant way. In fact, statistical analysis reveals that both ALD $ZrO_2$ and mixed $TiO_2$-$ZrO_2$ coated PMMA samples compared to bare PMMA samples (Lucitone 199) by Arioli Filho J.N. et al. showed no significant difference in mean flexural strength for $p<0,05$. Preliminary analysis of data sets did not show a normal distribution and so the Kruskal-Wallis non-parametric test was used to find the statistical differences ($p<0,05$). All the statistical analysis was conducted with IBM SPSS software.

The 30nm-$TiO_2$ coated samples were tested with the same measurements by previous

studies. The results were similar, meaning that the results were proved to be consistent with the values for not coated PMMA (38). PMMA flexural strength detected was around 139 MPa, with no statistical difference between the coated and not coated samples (46).

PMMA surface reinforcement by ALD deposited conformal nano-thin ceramic coating proved to maintain the desired flexural properties of the denture base bulk material and, at the same time, to successfully improve the surface hardness and the wettability, as demonstrated in previous tests.

## 3.14 Conclusions

This study has investigated the ALD deposition mechanism both on silicon and PMMA substrates and the characterization of the mechanical, chemical and surface properties of the coated polymeric substrates.

The nano ceramic films made of $TiO_2$, $ZrO_2$ and mixed $TiO_2$-$ZrO_2$ were successfully deposited at 100°C-120°C from TDMAT, TDMAZ and ozone on silicon and PMMA substrates and an attempt to explain the ALD film deposition rate on different substrates was made. On silicon alone, the relationship between ALD cycles and thickness of the coating was confirmed to be linear and consistent with the literature values in the same conditions. Regarding the growth of $TiO_2$ on silicon in the same reaction chamber with PMMA, it seemed twice the value on silicon alone, especially for lower number of cycles. In addition, the oxides growth was detected to be higher for lower number of cycles on PMMA also, as after 150-200 cycles the growth rate drops to half the initial value. Phenomena found in literature as polymer evaporation and high initial absorption of the ALD reactants in the polymeric porosity were hypothesized to affect the growth of the oxides on Silicon with PMMA in the chamber and on PMMA respectively.

The bonding strength of the nano-thin ALD coating on the polymer was effective since following four hours of aggressive treatment with the denture cleanser the ceramics were still attached to the polymer: chemical analysis of the surface showed same results for samples freshly

deposited and samples tested with both a chemical and physical treatment in Polident cleanser. ALD coating proved to be physically and chemically attached to PMMA, corroborating other literature results.

All coated surfaces showed increased wettability compared to the uncoated polymers following ALD. The contact angle was found to decrease from 84° to 25°-35° in the coated acrylic samples. Moreover, surface wettability was proved to be stable as after the Polident treatment and DI water storage for two weeks, contact angles were similar. Hydrophilic substrates are usually more desirable for different reasons in the biomedical field among which lower bacterial attachment is one of them.

In addition to this, titania and zirconia, being two ceramics, managed to increase the surface hardness of the material. For 30-40 nm thick coatings, the Vickers hardness number was increased by about 60% with respect to the mean value for untreated PMMA. A surface hardness increase should provide to the denture base material resistance to scratches in the harsh oral environment and improved properties, like resistance to loss of material and volume, thereby improving the stability and accuracy.

Lastly, surface morphology was not significantly changed by the coating, although XPS and SEM results show the effective presence of the ceramic on top of the polymer and through the bulk: the root mean square roughness value was between 45± 0.7nm and 28± 4nm in the best case. This change is not even in the micrometer range, which was expected, since ALD is a conformal technique and it covers all peaks and troughs present on the surface to coat.

Indeed, ALD deposited conformal nano ceramic coatings proved to improve PMMA surface properties like hardness and wettability while maintaining the desired flexural properties of the denture base bulk material.

# CHAPTER 4

# FUTURE WORK

First of all, the new SE model used to fit the data of the oxides thickness on the polymer should be validated in order to confirm the film growth behavior detected. Cross-section SEM was attempted, but the polymer is not conductive and this produced no reliable data due to the high charging of the material. TEM could be a solution but the procedure to cut the samples used would be destructive on a nano-thin coating. Other techniques should be taken into consideration to measure the coating thickness on such a non-conductive and relatively weak polymer.

The mixed $TiO_2$-$ZrO_2$ coatings were tested with XPS but the thickness of the top layer was either too thin to be detected or too thick and uniform to detect the underneath material. Both titanium and zirconium peaks were not detected in the same spectra of the mixed coatings. A different technique should be used to prove the presence of both elements on the surface.

The improvement of wettability and surface hardness is known to provide less cell and bacterial attachment, so antibacterial and antifungi tests should also be conducted. Moreover, the ease of removing the biofilm and bacteria from the surface may also be increased with the photocatalytic property of $TiO_2$, which can be a really useful feature to disinfect the prostheses.

Brushing tests simulating aging on the PMMA samples are currently being run in Peking University School and Hospital of Stomatology in the Department of Dental Materials. We sent two groups of samples for aging test: 25 nm $ZrO_2$-coated PMMA and 40 nm mixed $TiO_2$-$ZrO_2$ coated (theoretical ratio 5:1). XPS results after the brushing can reveal interesting data on the surface wear resistance of the coated samples, as the adhesion of the coating would be tested during the real tooth brushing stress. Wear resistance may also give useful information on the possible loss of surface material, as coating delamination and loss of integrity of the whole denture.

The structure of the six superlayers was theoretically hypothesized starting from the ALD input subcycles and the mean growth rate per cycle obtained for the oxides on top of PMMA. This structure was never tested to be exactly as expected so some characterization regarding this aspect might be useful: for example, X-Ray Reflectivity might be a good choice as usually it is used to find the thickness of nanolaminates. If the polymer substrate is too challenging to test because of the weak properties and non-conductiveness, the same structure can be replicated on silicon substrates that present less problems regarding characterization.

Another important point to focus on would be the nature of the organic-inorganic interface between the polymer and the nano-film deposited on top: in this study, we just concentrated on the presence of the coating on the surface also after some physical and chemical stresses. It would be a good point to understand whether at the interface a chemical and physical bond is truly present and how the two materials bind one to the other. TEM may be a useful tool in this context. The thermal coefficients of the two layers would also be of interest in future studies as the stability of the interface must be kept also with temperature modulation, because fast temperature changes happen often in the oral environment.

Also, some studies on the deformations and changes that temperatures around 100°C-120°C may cause in the polymer would be useful to understand what modifications the substrate may undergo during the depositions. A 30nm deposition takes about 3 hours, in which PMMA is exposed to such high temperatures: polymers are very sensitive to temperature, which may cause changes in the chemical structure of the plastics, as for example increasing the cross-linking level. Color and optical properties may be changed too and this is the reason why a study focused on the color change of PMMA during this kind of ALD depositions is currently being run by College of Dentistry: we deposited 30 nm $TiO_2$ on top of 30 PMMA samples with three different colors at 100°C. Color-based tests will be performed before and after the depositions in order to detect any change in color or optical properties. Lower temperature depositions around 50°C-60°C should be studied in order to try to avoid any deformation or change in the polymer: the quality and control

of growth rate should be studied and characterized properly because outside the ALD saturated temperature window the deposition rate and the quality of the film may vary. The heating cycle through 100°C-120°C can also be a factor affecting some of the properties as the bulk flexural strength and surface hardness: some heated PMMA and not heated PMMA samples may be tested for these properties together with coated samples too.

The penetration of the ALD precursors into the volume of the samples, proved by the EDS mapping showed previously, may be a factor to analyze as it may affect the resistance to degradation and strengthen the material.

Lastly, in the near future the novel coated material is going to be tested in vivo at the UIC College of Dentistry, to detect the actual behavior of the polymer in a real oral environment. Three groups of 13 samples will be tested: 30 nm $TiO_2$-coated, 25 nm $ZrO_2$-coated and 40 nm mixed $TiO_2$-$ZrO_2$ coated (theoretical ratio 5:1). The samples should be characterized before and after the in vivo testing in order to understand if the material durability in a real oral environment is truly improved.

# APPENDICES

# Appendix A

## ALD DEPOSITIONS AT 90°C ON PMMA

In order to understand if there is a kind of correlation between the high growth rate of titania on PMMA at a high temperature such as 120°C we tried to deposit samples also at 90°C. We did not repeat the experiment for zirconia as titania was the oxide with the huge increase in growth rate on the polymer. We kept the same parameters (precursors, pulse and purge times, bubbler temperature and pressure of Figure 8) and changed just the substrate temperature from 120°C to 90°C. We deposited 50 and 150 cycles (Fig. 33). For the silicon deposition, just one sample was pretreated as described before and placed into the chamber while for the PMMA experiment we placed in the chamber a PMMA sample pretreated as described before and one silicon sample. The thickness was measured two times on the polymer sample and four times on the silicon ones.

The results obtained showed the same growth rates for PMMA and Silicon samples deposited at 120°C, so we can conclude that there is no correlation between the increase in growth rate and the high temperature. The only difference seems to be for 50 cycles on silicon with PMMA in the same chamber, even if it does not seem significant. The result was expected as Kaarianianen et al. (23) deposited at 65°C and the growth rate on silicon was already increased. If this phenomenon is to be attributed to the evaporation of volatile species rich in oxygen, both this paper and the one by Fuchs B. confirmed the process starts before 60°C (42).

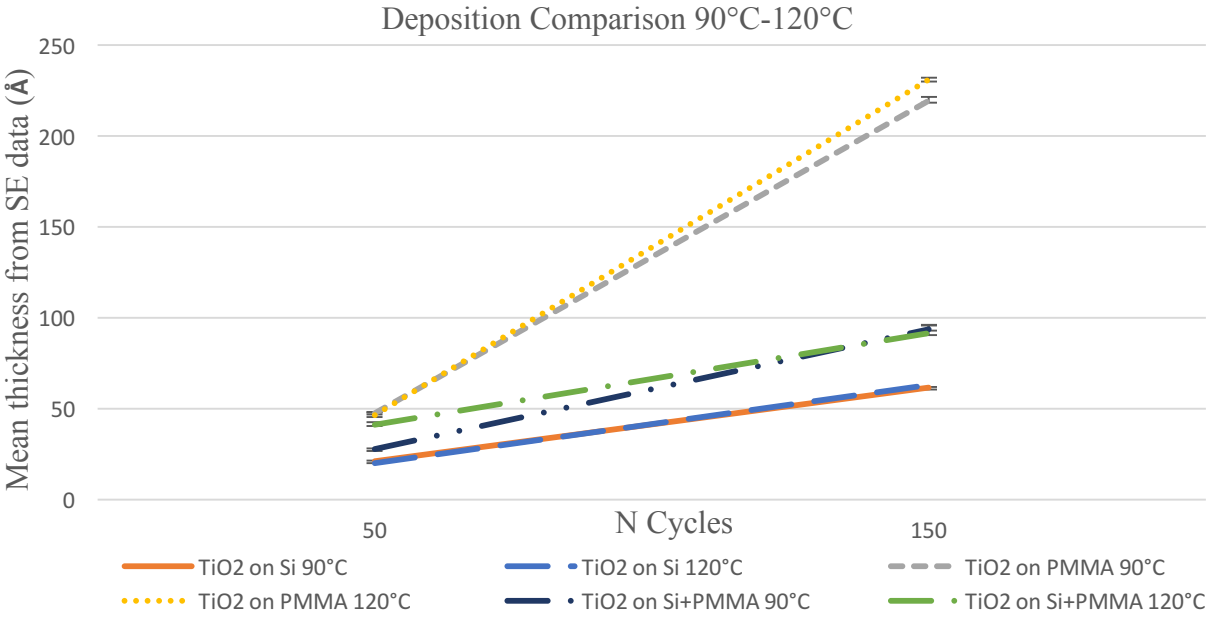


Figure 33: ALD cycle number vs. mean thickness (Å) of the $TiO_2$ layers on silicon, PMMA, and silicon with PMMA at 90°C and 120°C for 50 and 150 cycles from TDMAT and Ozone (Same pressure and pulses of Figure 8)

More depositions increasing the number of cycles should be attempted and $ZrO_2$ depositions at 90°C should be analyzed too in order to understand if the evaporation of the polymer at high temperature can really be involved in the higher growth rate observed both on silicon and PMMA in the same chamber.

# Appendix B

04.12.2018

Davide Barreca
Università degli studi di Padova
Dipartimento di Scienze chimiche
Via Marzolo 1, 35131 Padova, ITALY

I am writing to request the permission to use the following material from your publication ("Zirconium Dioxide Thin Films Characterized by XPS" Davide Barreca, Giovanni A. Battiston, Rosalba Gerbasi, Eugenio Tondello, and Pierino Zanella, Surface Science Spectra 7, No. 4, 2000, pages 303-309) in my thesis. The material will appear as originally published. Unless you request otherwise, I will use the conventional style of the Graduate College of the University of Illinois at Chicago as acknowledgement.

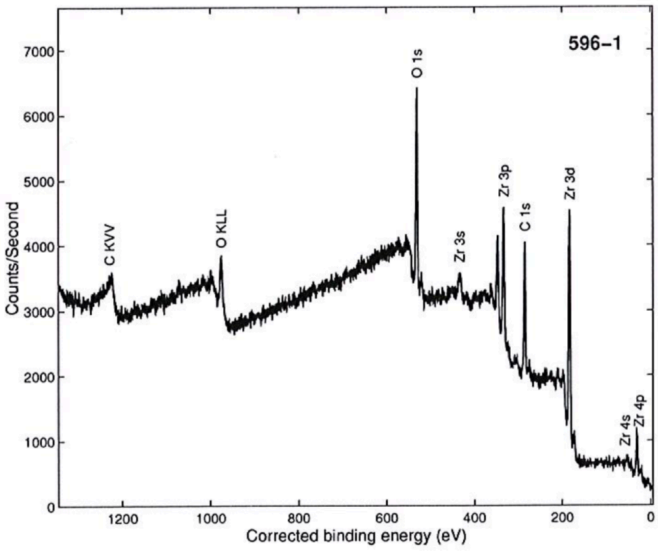


A copy of this letter is included for your records. Thank you for the kind consideration of this request.
Sincerely

Eleonora Pensa
809 S Damen Avenue, Chicago, IL 60612, USA

The above request is approved.

Approved by: Nancy Schuettein Date: 4/13/18
Upon full credit given for re-use as noted above.

# Appendix C

## PMMA LUCITONE 199 COMPOSITION

Figure 34 shows the detailed composition of PMMA Lucitone 199 by Dentsply Sirona Pty Ltd (51):

**Dentsply Lucitone 199 Powder**

**Dentsply Sirona Pty Ltd**

Chemwatch Hazard Alert Code: **2**

Chemwatch: **4993-48**
Version No: **3.1.1.1**
Safety Data Sheet according to WHS and ADG requirements

Issue Date: **27/06/2017**
Print Date: **09/01/2018**
S.GHS.AUS.EN

### SECTION 1 IDENTIFICATION OF THE SUBSTANCE / MIXTURE AND OF THE COMPANY / UNDERTAKING

**Product Identifier**

| | |
|---|---|
| **Product name** | Dentsply Lucitone 199 Powder |
| **Synonyms** | ? |
| **Other means of identification** | Not Available |

**Relevant identified uses of the substance or mixture and uses advised against**

| | |
|---|---|
| **Relevant identified uses** | Denture acrylic resin. |

**Details of the supplier of the safety data sheet**

| | |
|---|---|
| **Registered company name** | **Dentsply Sirona Pty Ltd** |
| **Address** | 11-21 Gilby Road Mount Waverley VIC 3149 Australia |
| **Telephone** | 1300 55 29 29 |
| **Fax** | 1300 55 31 31 |
| **Website** | www.dentsply.com.au |
| **Email** | clientservices@dentsplysirona.com |

**Emergency telephone number**

| | |
|---|---|
| **Association / Organisation** | **Not Available** |
| **Emergency telephone numbers** | 1300 55 29 29 |
| **Other emergency telephone numbers** | Not Available |

### SECTION 2 HAZARDS IDENTIFICATION

**Classification of the substance or mixture**

**NON-HAZARDOUS CHEMICAL. NON-DANGEROUS GOODS. According to the WHS Regulations and the ADG Code.**

**CHEMWATCH HAZARD RATINGS**

| | | Min | Max |
|---|---|---|---|
| Flammability | 1 | | |
| Toxicity | 0 | | |
| Body Contact | 2 | | |
| Reactivity | 1 | | |
| Chronic | 0 | | |

0 = Minimum
1 = Low
2 = Moderate
3 = High
4 = Extreme

| | |
|---|---|
| **Poisons Schedule** | Not Applicable |
| **Classification** | Not Applicable |

**Label elements**

| | |
|---|---|
| **Hazard pictogram(s)** | Not Applicable |
| **SIGNAL WORD** | **NOT APPLICABLE** |

**Hazard statement(s)**

Not Applicable

**Precautionary statement(s) Prevention**

Not Applicable

**Precautionary statement(s) Response**

Not Applicable

**Precautionary statement(s) Storage**

Not Applicable

**Precautionary statement(s) Disposal**

Not Applicable

## SECTION 3 COMPOSITION / INFORMATION ON INGREDIENTS

### Substances

See section below for composition of Mixtures

### Mixtures

| CAS No | %[weight] | Name |
|---|---|---|
| 94-36-0 | <0.2 | dibenzoyl peroxide |
| 13463-67-7 | <0.05 | titanium dioxide |

## SECTION 4 FIRST AID MEASURES

### Description of first aid measures

| | |
|---|---|
| **Eye Contact** | If this product comes in contact with the eyes:<br>• Immediately hold eyelids apart and flush the eye continuously with running water.<br>• Ensure complete irrigation of the eye by keeping eyelids apart and away from eye and moving the eyelids by occasionally lifting the upper and lower lids.<br>• Continue flushing until advised to stop by the Poisons Information Centre or a doctor, or for at least 15 minutes.<br>• Transport to hospital or doctor without delay.<br>• Removal of contact lenses after an eye injury should only be undertaken by skilled personnel. |
| **Skin Contact** | If skin contact occurs:<br>• Immediately remove all contaminated clothing, including footwear.<br>• Flush skin and hair with running water (and soap if available).<br>• Seek medical attention in event of irritation. |
| **Inhalation** | • If fumes or combustion products are inhaled remove from contaminated area.<br>• Lay patient down. Keep warm and rested.<br>• Prostheses such as false teeth, which may block airway, should be removed, where possible, prior to initiating first aid procedures.<br>• Apply artificial respiration if not breathing, preferably with a demand valve resuscitator, bag-valve mask device, or pocket mask as trained. Perform CPR if necessary.<br>• Transport to hospital, or doctor. |
| **Ingestion** | • For advice, contact a Poisons Information Centre or a doctor at once.<br>• Urgent hospital treatment is likely to be needed.<br>• If swallowed do **NOT** induce vomiting.<br>• If vomiting occurs, lean patient forward or place on left side (head-down position, if possible) to maintain open airway and prevent aspiration.<br>• Observe the patient carefully.<br>• Never give liquid to a person showing signs of being sleepy or with reduced awareness; i.e. becoming unconscious.<br>• Give water to rinse out mouth, then provide liquid slowly and as much as casualty can comfortably drink.<br>• Transport to hospital or doctor without delay. |

### Indication of any immediate medical attention and special treatment needed

Treat symptomatically.

Figure 34: PMMA Lucitone 199 Powder Composition and safety data sheet taken from the Company website (51).

# Appendix D

## FURIER TRANSFORM INFRARED SPECTROSCOPY ON COATED AND NON COATED PMMA SAMPLES

FTIR is a common technique used to detect the functional groups and the types of bonding inside the samples (57). In this study, Nicolet Magna IR 560 Spectrometer E.S.P. was used, in the "Specular Reflectance" mode. 128 scans were averaged to obtained the final set of data. The environment is rich in $CO_2$, so the 2200 $cm^{-1}$ peak will be the strongest one. Ez Omic FTIR Software was used to process the data obtained. Then the data were processed with Excel Software. The command "auto baseline" was used to get the data on the same line to have a more readable graph, the sensitivity was also set in order to get the most intense peaks and shadow the less intense ones that would confuse the picture. The peaks were analyzed and recognized based on different studies in literature (Fig. 35). Three samples were tested: an uncoated PMMA and two coated samples, with 30 nm thick titania and zirconia layers on top.

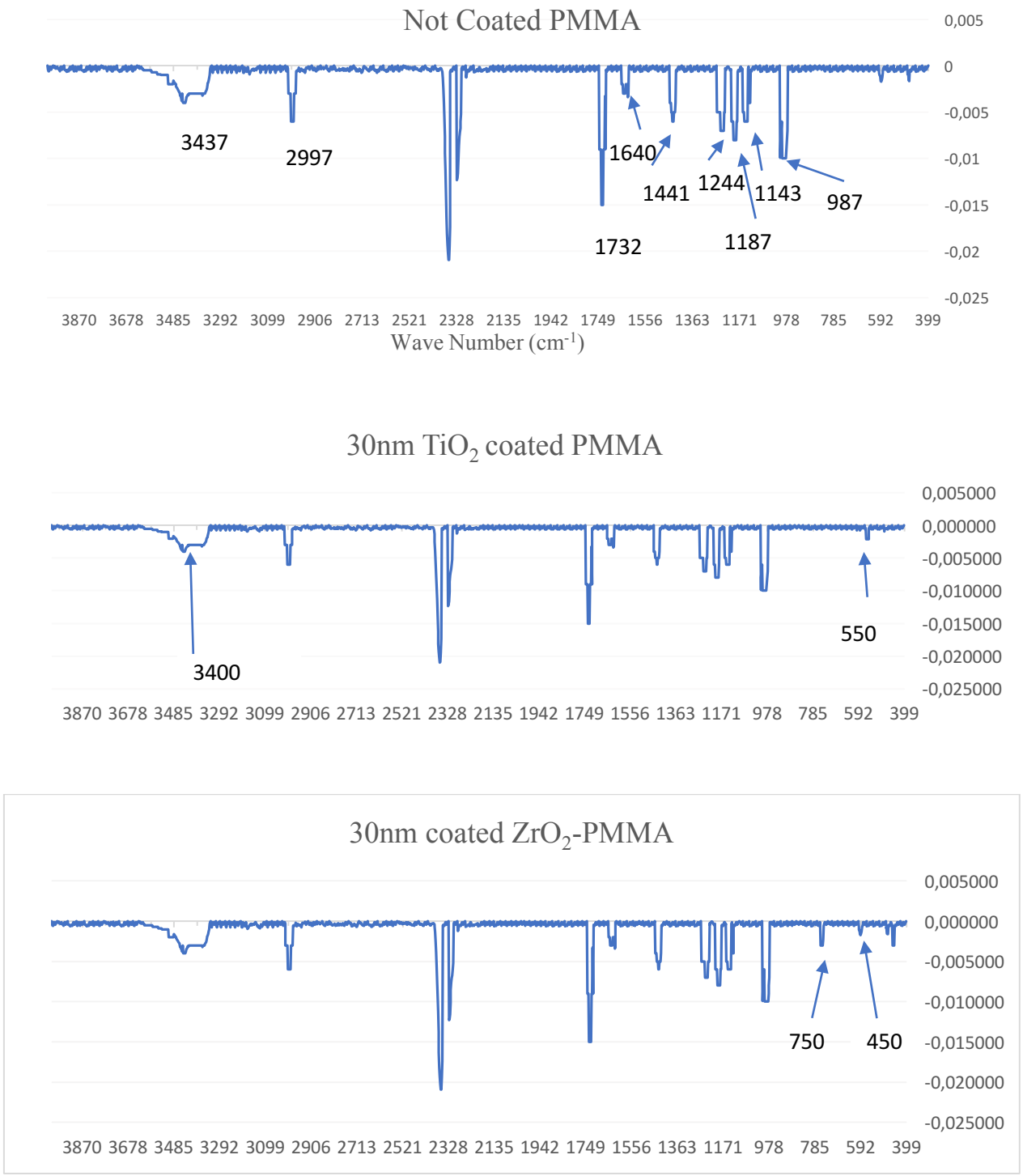


Figure 35: FTIR spectra of uncoated PMMA and 30nm $TiO_2$/ 30nm $ZrO_2$ coated PMMA stored in DI water for 3 weeks.

As you can see from Fig. 35 the characteristics peaks for PMMA are present: 987 $cm^{-1}$ is typical absorption of PMMA, 1143 $cm^{-1}$ , 1187 $cm^{-1}$ and 1244 $cm^{-1}$ from the vibration of the ester group, 1441 $cm^{-1}$ ($\nu O\text{-}CH_3$ ), 1732 $cm^{-1}$ ($\nu C{=}O$), 2997 $cm^{-1}$ which can be attributed to the stretching

vibration of $CH_3$ , the broad 3437 $cm^{-1}$ peak and the weaker 1640 $cm^{-1}$ should correspond to the absorption of δ(-OH) and δ(-O-H) functional groups that may come from water bound to the surface, due to the long storage in DI water (58).

The coated graphs look quite similar to the uncoated one: the $TiO_2$ coated spectrum presents the 550 $cm^{-1}$ vibration, which is typical of titanium oxide while the while the vibrations of the Zr-O groups are around 450-750 $cm^{-1}$ (57, 59).

The results were as expected, both titania and zirconia were detected and also the water bond on the surface due to the long DI water storage. As a future work, more samples with different thicknesses might be tested and samples freshly coated just after the deposition, to see if the peaks and the bonds detected are the same as after 3 weeks of storage.

# CITED LITERATURE


1. Johnson, R.W., Hultqvist, A., and Bent, S.F.: A brief review of atomic layer deposition: from fundamentals to applications. Materials today 17, 2014.

2. George, S.M.: Atomic layer deposition: an Overview. Chemical Reviews 110, pages 111-131, 2010.

3. Christensen, S. T., and Elam, J. W.: Atomic Layer Deposition of Ir-Pt Alloy films. Chemistry of Materials 22 (8), pages 2517-2525, 2010.

4. Chang, S., and Takoudis, C.G.: Growth behavior and structural analysis of atomic layer deposited $Sn_xTi_{1-x}O_y$ films. Journal of Vacuum Science & Technology A: Vacuum, Surfaces, and Films 36, 2018.

5. Jarvis, K.L., and Evans, P.J.: Growth of thin barrier films on flexible polymer substrates by atomic layer deposition. Thin Solid Films 624, pages 111-135, 2017.

6. Knohl, S., Roy, A.K., Goedel, W.A., Schulze, S., and Hietschold, M.: Atomic layer deposition onto carbon fiber: From single layer deposition via multilayer structure to metal oxide microtubes. Journal of Vacuum Science & Technology A: Vacuum, Surfaces, and Films 31, pages 01A1391-7, 2013.

7. Yin, Z.F., Wu, W.L., Yang, H.G., and Su, Y.H.: Recent progress in biomedical applications of titanium dioxide. Physical Chemistry Chemical Physics 15, pages 4844-4858, 2013.

8. Das, L., Dutta, M., and Jayanta, K.B.: Photocatalytic degradation of phenol from industrial effluent using titania-zirconia nanocomposite catalyst. International journal of environmental science 4, 2013.

9. Hisbergues, M., Vendeville, S., and Vendeville, P.: Zirconia: Established Facts and Perspectives for a Biomaterial in Dental Implantology. Wiley InterScience, pages 519-529, 2008.

10. Si, J., Zhang, J., Liu, S., Zhang, W., Yu, D., Wang, X., Guo, L., and Shen, S.G.F.: Characterization of a micro-roughened TiO2/ZrO2 coating: mechanical properties and HBMSC responses *in vitro*. Acta Biochim Biophys Sin 46, pages 572-581, 2014.

11. Scarano, A., Piattelli, M., Caputi, S., Favero, G.A., and Piattelli, A.: Bacterial adhesion on commercially pure titanium and zirconium oxide disks: an in vivo human study. J Periodontol 75, pages 292–296, 2004.

12. Rimondini, L., Cerroni, L., Carrassi, A., and Torricelli, P.: Bacterial colonization of zirconia ceramic surfaces: an in vitro and in vivo study. The International Journal of Oral & Maxillofacial Implants 17(6), 2002.

13. Gad, M.M., Fouda, S.M., Al-Harbi, F.A., Näpänkangas, R., and Raustia, A.: PMMA denture base material enhancement: a review of fiber, filler, and nanofiller addition. International Journal of Nanomedicine 12, pages 3801–3812, 2017.

**CITED LITERATURE (continued)**


14. Yang, Q., Yuan, W., Liu, X., Zheng, Y., Cui, Z., Yang, X., Pan, H., and Wu, S.: Atomic layer deposited ZrO2 nanofilm on Mg-Sr alloy for enhanced corrosion resistance and biocompatibility. Acta Biomaterialia 58, pages 515–526, 2017.

15. Elshereksi, N.W., Mohamed, S.H., Arifin, A., and Ishak, Z.A.M.: Thermal Characterisation of Poly(Methyl Methacrylate) Filled with Barium Titanate as Denture Base Material. Journal of Physical Science 25 (2), pages 15–27, 2014.

16. Lopez, J., Martinez, J., Abundiz, N., Dominguez, D., Murillo, E., Castillon, F.F, Machorro, R., Farias, M.H., and Tiznado, H.: Thickness effect on the optical and morphological properties in $Al_2O_3$/ZnO nanolaminate thin films prepared by atomic layer deposition. Superlattices and Microstructures 90, pages 265-273, 2016.

17. Lin, K. Y., Young, L.B., Cheng, C.K., Lin, Y.H., Wan, H.W., Cai, R.F., Lo, S.C., Li, M.Y., Kwo, J., and Hong, M.: Enhancement of effective dielectric constant using high-temperature mixed and sub-nano laminated atomic layer deposited Y2O3/Al2O3 on GaAs(001). Microelectronic engineering 178, pages 271-274, 2017.

18. Choi, J. H., Zhang, F., Perng, Y., and Chang, J.P.: Tailoring the composition of lead zirconate titanate by atomic layer deposition. J. Vac. Sci. Technol. B 31(1), 2013.

19. Benner, F., Jordan, P.M., Richter, C., Simon, D.K., Dirnstorfer, I., Knaut, M., Bartha, J.W., and Mikolajick, T.: Atomic layer deposited high-k nanolaminate for silicon surface passivation. J. Vac. Sci. Technol. B 32(3), 2014

20. Mitchell, D.R.G., Triani, G., Attard, D.J., Finnie, K.S., Evans, P.J., Barbe, C.J. and Bartlett, J.R.: Atomic layer deposition of TiO2 and Al2O3 thin films and nanolaminates. Smart Mater. Struct. 15, S57-S64, 2006

21. Kemell, M., Färm E., Ritala, M., and Leskelä, M.: Surface modification of thermoplastics by atomic layer deposition of Al2O3 and TiO2 thin films. European Polymer Journal 44, pages 3564–3570, 2008.

22. Wilson, C.A, Grubbs, R.K., and George, S.M.: Nucleation and Growth during ALD Al2O3 on polymers. Chem. Mater. 17, pages 5625-5634, 2005.

23. Kaariainen, T. O., Cameron, D.C, and Tanttari, M.: Adhesion of Ti and TiC Coatings on PMMA Subject to Plasma Treatment: Effect of Intermediate Layers of Al2O3 and TiO2 Deposited by Atomic Layer Deposition. Plasma Process. Polym. 6, pages 631–64, 2009.

24. Ahmed, M.A., and Ebrahim, M.I.: Effect of Zirconium Oxide Nano-Fillers Addition on the Flexural Strength, Fracture Toughness, and Hardness of Heat-Polymerized Acrylic Resin. World Journal of Nano Science and Engineering 4, pages 50-57, 2014.

25. Fuchs, B., Schlenkrich, F., Seyffarth, S., Meschede, A., Rotzoll, R., Vana, P., Großmann, P., Mann, K., and Krebs, H.: Hardening of smooth pulsed laser deposited PMMA films by heating. Appl Phys A 98, pages 711–715, 2010.

26. Yu, J., Tao, X., Tam, H., and Demokan, M.S.: Modulation of refractive index and thickness of Polymethyl methacrylate thin films with UV irradiation and heat treatment. Applied Surface Science 252, pages 1283–1292, 2005.

**CITED LITERATURE (continued)**


27. Jin, C., Liu, B., Lei, Z., Sun, J.: Structure and photoluminescence of the TiO2 films grown by atomic layer deposition using tetrakis-dimethylamino titanium and ozone. Nanoscale Research Letters, 2015.

28. Hilfiker, J.N., Pietz, B., Dodge, B., Sun, J., Hong, N., and Schoeche, S.: Spectroscopic ellipsometry characterization of coatings on biaxially anisotropic polymeric substrates. Applied Surface Science 421, pages 500–507, 2017

29. El-Nasser, H.M.: Morphology and spectroscopic ellipsometry of PMMA thin films. Applied Physics Research 9 (2), 2017.

30. Synowicki, R. A.: Suppression of backside reflections from transparent substrates. Phys. stat. sol. 5, pages 1085 – 1088, 2008.

31. Bernardin, J.D., Mudawar I., Walsh C.B., and Frances E.I.: Contact angle temperature dependence for water droplets on practical aluminum surfaces. Int. J. Heat mass transfer 40, pages 1017-1033, 1997

32. Seah, M.P.: A review of the analysis of surfaces and thin films by AES and XPS. Vacuum 34, pages 463-476, 1984.

33. https://caf.ua.edu/kratos-axis-165-xpsauger/, 2018 [Online; accessed 04/12/2018].

34. Sturm, H., Schartel, B., Weiß, A., and Braun, U.: SEM/EDX: Advanced investigation of structured fire residues and residue formation. Polymer Testing 31, pages 606–619, 2012.

35. Hansma, P., Elings, V., Marti, O. and Bracker, C.: Scanning tunneling microscopy and atomic force microscopy: application to biology and technology. Science 242, pages 209-216, 1988.

36. Alhareb, A. O., Akil, H. M., and Ahmad, Z. A.: Impact strength, fracture toughness and hardness improvement of PMMA denture base through addition of nitrile rubber/ceramic fillers. The Saudi Journal for Dental Research 8, pages 26–34, 2017.

37. Mathew, M., Shenoy, K., and Ravishankar, K.S.: Vickers hardness and Specific wear resistance of E glass reinforced poly methyl methacrylate. International Journal of Scientific & Engineering Research 5, pages 652-656, 2014.

38. Zeng, X., Wen, S., Li, M., and Xie, G.: Estimating Young's Modulus of Materials by a New Three-Point Bending Method. Advances in Materials Science and Engineering, 2014.

39. Arioli Filho, J.N., Butignon, I.E., Pereira, R., Lucas, M.G., and Mollo, J. F.: Flexural strength of acrylic resin repairs processed by different methods: water bath, microwave energy and chemical polymerization. J Appl Oral Sci. 9, pages 249-253, 2011.

40. http://www.polident.com/en_ca/denture-products/denture-cleansers/polident-overnight.html, 2018 [Online; accessed 04/13/2018].

**CITED LITERATURE (continued)**


41. Ferguson, J. D., Weimer, A. W., and George, S. M.: Atomic Layer Deposition of Al2O3 Films on Polyethylene Particles, Chem. Mater. 16, pages 5602-5609, 2004.

42. Mori, K., Tsuji, M., Ueda, T., and Sakurai, K.: color and gloss evaluation of titanium dioxide coating for acrylic resin denture base material. Journal of prosthodontic research 59, pages 249–253, 2015

43. Lu, H., Liu, Y., Huang, W.M., Wang, C., Hui, D., and Fu, Y.Q.: Controlled evolution of surface patterns for ZnO coated on stretched PMMA upon thermal and solvent treatments. Composites Part B 132, pages 1-9, 2018

44. Bora, M.O.: The influence of heat treatment on scratch behavior of Polymethylmethacrylate(PMMA). Tribology International 78, pages 75-83, 2014.

45. Coban, O.: Heat treatment effect on erosion behavior of Polymethylmethacrylate for optical transmittance efficiency. Applied Surface Science 317, pages 405-413, 2014

46. Huang, S.: Improving polymethyl methacrylate resin using a novel nano-ceramic coating. Master's thesis, University of Illinois at Chicago, Chicago, 2017.

47. Kim, Y., and Kim, D.: Atomic Layer deposition of TiO2 from tetrakis-dimethylamido-titanium and ozone. Korean J. Chem. Eng., 29(7), pages 969-973, 2012.

48. Shim, J.H., Chao, C., Huang, H., Fritz, B., and Prinz, F.B.: Atomic Layer Deposition of Yttria-Stabilized Zirconia for Solid Oxide Fuel Cells. Chem. Mater. 19, pages 3850-3854, 2007.

49. Kashiwagi, T., Inaba, A., and Brown, J.E.: Differences in PMMA degradation characteristics and their effects on its fire properties. Fire Safety science- Proceedings of the first international symposium

50. Stevens, N., Priest, C.I., Sedev, R, and Ralston, J.: Wettability of Photoresponsive Titanium Dioxide Surfaces. Langmuir 19, pages 3272-3275, 2003.

51. Gonzalez-Martin, M.L., Labajos-Broncano, L., Janczuk, B., and Bruque, J.M.: Wettability and surface free energy of zirconia ceramics and their constituents. Journal of materials science 34, pages 5923– 5926, 1999.

52. Azuma, Akinobu, N. A. and Minakuchi., S.: Hydrophilic surface modification of acrylic denture base material by silica coating and its influence on candida albicans adherence. Journal of medical and dental sciences, pages 1–7, 2012.

53. https://xpssimplified.com/elements/zirconium.php, 2018 [Online; accessed 04/12/2018].

54. https://xpssimplified.com/elements/titanium.php, 2018 [Online; accessed 04/12/2018].

55. Barreca, D., Giovanni, A., Battiston, G.A., Gerbasi, R., Tondello, E., and Zanella P.: Zirconium Dioxide Thin Films Characterized by XPS. Surface Science Spectra 7 (4), pages 303-309, 2000.

**CITED LITERATURE (continued)**

56. http://www.dentsplyestore.com.au/secure/downloadfile.asp?fileid=1002341, 2018 [Online; accessed 05/10/2018]

57. Reyes-Acosta, M.A., Torres-Huerta, A.M., Domínguez-Crespo, M.A., Flores-Vela, A.I., Dorantes-Rosales, H.J., and Ramírez-Meneses, E.: Influence of $ZrO_2$ nanoparticles and thermal treatment on the properties of PMMA/$ZrO_2$ hybrid coatings. Journal of Alloys and Compounds 643, pages 150–158, 2015.

58. Wang, Q., Wang, X., Li, X., Cai, Y., and Wei, Q.: Surface modification of PMMA/O-MMT composite microfibers by $TiO_2$ coating. Applied Surface Science 258, pages 98–102, 2011.

59. Murashkevich A.N, Lavitskaya A. S., Barannikova T. I. and Zharskii I. M.: Infrared absorption spectra and structure of $TiO_2$–$SiO_2$ composites. Journal of Applied Spectroscopy 75, 2008.

# VITA

NAME: Eleonora Pensa

EDUCATION:

- Bachelor of Engineering in Biomedical Engineer, Politecnico di Milano, 2016, Italy

LANGUAGE SKILLS:

- Italian native speaker
- English Full working proficiency
- Spanish elementary proficiency

SCOLARSHIPS:

- Fall 2018: First-class scholarship among exchange Italian biomedical engineers, Politecnico di Milano, Italy

RESEARCH EXPERIENCES:

- Mar. 2016-Sept. 2016: Characterization of a deoxygenator for *ex vivo* cell culture systems. Mentor: M. Soncini
- Aug. 2017-May 2018: Enhanced Properties of Polymethyl Methacrylate Coated with Atomic Layer Deposited Ceramic Nanofilm. Mentors: C.G. Takoudis, B. Yang

Ceramic coating ($TiO_2$ -$ZrO_2$ ) on acrylic resin denture material (PMMA) with ALD technique. Surface characterization via wettability, XPS, SEM, Ellipsometry, AFM, bending test, hardness test.

WORK EXPERIENCE:

- Jan. 2018-May 2018: Research Assistant in Bioengineering Department and Department of Restorative Dentistry (Implant and Innovations Center) at the University of Illinois at Chicago

TECHNICAL SKILLS:

- Proficient in MATLAB, ImageJ
- Skilled in Microsoft Office, Solidworks, AutoCAD, SPSS Statistics